CHARACTERIZATION OF SINGLE AND MULTI SIZES SPHERE PACKING

A Thesis

Submitted to the College of Engineering

of Nahrain University in Partial Fulfillment

of the Requirements for the Degree of

Master of Science
in
Chemical Engineering

by

Wekar Abd Al-Wahed Abd Al-Nabi

(B. Sc. In Chemical Engineering 2004)

Jamadi Al-thani 1428

June 2007

Certification

I certify that this thesis entitled **"Characterization of Single and Multi Sizes Sphere Packing"** was prepared by **Wekar Abd Al-Wahed Abd Al-Nabi** under my supervision at Nahrain University/College of Engineering in partial fulfillment of the requirements for the degree of Master of Science in Chemical Engineering.

Signature: Latif

Name: **Dr. Mohammed N. Latif**

(Supervisor)

Date: 24/6/2007

Signature:

Name: **Prof. Dr. Qasim J. Slaiman**

(Head of Department)

Date: 1/7/2007

Certificate

We certify, as an examining committee, that we have read this thesis entitled **"Characterization of Single and Multi Sizes Sphere Packing"**, examined the student **Wekar Abd Al-Wahed Abd Al-Nabi** in its content and found it meets the standard of thesis for the degree of Master of Science in Chemical Engineering.

Signature: Latif	Signature:
Name: **Dr. Mohammed N. Latif** (Supervisor)	Name: **Dr. Malek M. Mohammed** (Member)
Date: 24/6/ 2007	Date: 1 /7/ 2007
Signature: Naseer Al-Habobi	Signature: A. Sula
Name: **Dr. Naseer A. Al-Habobi** (Member)	Name: **Prof. Dr. Abbas H. Sulaymon** (Chairman)
Date: 1 /7/ 2007	Date: 24/6/ 2007

Approval of the College of Engineering

Signature: M. J. Jweeg

Name: **Prof. Dr. Muhsin J. Jweeg**

(Acting Dean)

Date: 15 /7 2007

Abstract

This work presents the study of fluid flow through a packed bed, where two fluids were used separately (air and water). The packed bed contains spherical glass particles distributed randomly.

The packed bed was 7.62 cm in diameter and 57 cm long. The glass particles were 0.42, 0.50, 0.61, 0.79 and 1.01 cm in diameter. Different flow rates of fluid were used which expressed by modified Reynolds number. The experiments were carried out at laboratory temperatures ($32^{\circ}C$) for air flow and at tap water temperature ($25^{\circ}C$) for water flow. Many variables were studied in this work such as fluid type (air or water), flow rate and the packing porosity (mono, binary, and multi-size mixture), in order to study the effect of these variables on the pressure drop and friction factor.

The results showed that the pressure drop through a packed bed is highly sensitive to the packing porosity which has a significant effect on the friction factor. It was found that as the bed porosity increases from 0.3455 to 0.4359 the friction factor values decrease from 0.808 to 0.366, and the pressure drop values decrease from 33.8 to 7.1 Pa.

The air flow Reynolds number was ranged from 8.42 to 265.63 which lead to decrease in the friction factor values from 0.992 to 0.374. For water flow the Reynolds number range from 38.47 to 1504.22 which lead to decrease in the friction factor values from 0.456 to 0.284.

It was studied the effect of working fluid (air and water) on the pressure drop and friction factor through the packed bed. It was found that for the same packing porosity and fluid flow rate the pressure drop of air flow was less than the pressure drop of water flow.

Empirical correlations for friction factor as a function of Reynolds number for air and water flow through packed of multi-sizes particles are:

a. For air flow

$$f = 4.72\,\mathrm{Re}_1^{-1} + 0.59\,\mathrm{Re}_1^{-0.1}$$

The correlation coefficient was 0.9662 and percentage of average errors was 3.79%.

b. For water flow through packed bed

$$f = 3.73\,\mathrm{Re}_1^{-1} + 0.56\,\mathrm{Re}_1^{-0.1}$$

The correlation coefficient was 0.8994 and percentage of average errors was 4.16%.

List of Contents

Notations

Symbols		Notations
A	=	The bed cross-sectional area (m^2)
a	=	Representation of packing and fluid characteristics at laminar flow
b	=	Representation of packing and fluid characteristics at turbulent flow
D	=	Diameter of cylinder (m)
d_m	=	Equivalent diameter of the pore channels (m)
d_p	=	Diameter of the particle (m)
d_{pav}	=	Average particles size (m)
d_{pi}	=	Diameter of particle i in mixture (m)
d_t	=	Diameter of tube (m)
e	=	Porosity of the bed
f	=	Modified friction factor
f_w	=	Correction factor
K'	=	Is a dimensionless constant whose value depends on the structure of the bed
K''	=	Kozeny constant
L	=	The height of packing in the bed (m)
L′	=	Length of channel (m)
Δp	=	Pressure drop through packed bed ($kg/m.s^2$)
Q	=	Flow rate (m^3/h)
q	=	Number of components in the mixture
$\frac{R_1}{\rho u_1^2}$	=	Modified friction factor
Re_1	=	Modified Reynolds number

S	=	Specific surface area of the particles (m^2/m^3)
S_B	=	Specific surface area of the bed (m^2/m^3)
S_c	=	Surface of the container per unit volume of bed (m^2/m^3)
u	=	Superficial velocity (m/s)
u_1	=	Average velocity through the pore channels (m/s).
Xi	=	The proportion of the component i in the mixture
x_i	=	The weight fraction of particle i

Greek Symbols

ε	=	Porosity of the bed
ρ	=	Density of fluid (kg/m^3)
ρ_b	=	Bulk density (kg/m^3)
ρ_t	=	True density (kg/m^3)
ρ_{ti}	=	True density of component i (kg/m^3)
ρ_{tm}	=	True density of mixture (kg/m^3)
μ	=	Fluid viscosity (kg/m.s)
$Ø_s$	=	Sphericity
δ	=	orientation factor
θ	=	Angle of the solid liquid interface with the stream direction

List of Tables

List of Figures

Chapter One

Introduction

Fluid flow through packed bed has many important applications in chemical and other process engineering fields such as fixed-catalytic reactor, adsorption of a solute, gas absorption, combustion, drying, filter bed, wastewater treatment and the flow of crude oil in petroleum reservoir [1].

A typical packed bed is a cylindrical column that is filled with a suitable packing material. The packing material may be spheres, cylinders, irregular particles or various kinds of commercial packing. It should have a large void volume to allow flow of fluid without excessive pressure drop and be chemically inert to fluids being processed [2, 3, 4].

One of the problems concerning the flow of fluids through beds of particles is the manner in which the particles are packed and the distribution of voids within the packed bed [5].

The particles packed together to form a structure which depends on a large number of parameters many of them are difficult to measure, or even to define. These include the shape and size distribution of particles, the way the packing has put together and the various forces exerted on it afterward [6].

The advantage of using packed column rather than just tank or other reaction vessel is that the packing affords a large contacting surface area for fluids [7].

Usually increased surface area provides a high degree of turbulence in the fluids which are achieved at the expense of increased capital cost and/ or pressure drop, and a balance must be made between these factors when arriving at an economic design [8].

The aim of the work is to:

1. Study the effect of particles size and size distribution on the bed porosity.
2. Study the effect of bed porosity on the pressure drop and friction factor through packed bed.
3. Study the effect of working fluid (air or water) on the pressure drop and friction factor through packed bed.
4. Study the effect of superficial velocity of fluid on the pressure drop and friction factor through packed bed.
5. Find empirical correlations between friction factor and Reynolds number for air and water flow through packed bed, and compare them with other correlations exist.

Chapter Two

Literature Survey and Theoretical Background

2.1 The flow of fluid through granular beds

The flow of fluids through beds composed either of irregularly shaped materials, or of packing of regular geometrical form has attracted considerable attention from many investigators [9]. **Kozeny in 1927 [10]**, **Carman in 1938 [11]**, **Blank in 1962 [12]**, **Green and Ampts in 1962 [13]**, studied the flow of air through columns packed with spherical materials.

Schoenborn and Dougherty in 1944 [14], studied the flow of air, water, and oil through beds of various commercial ring and saddle packing.

The flow of one or two fluids through packed beds have many important engineering applications such as adsorption (one phase flow through the bed), distillation (flow of two countercurrent fluids), and/or trickle bed reactor (flow of two co-current fluids) [15, 16].

The fluid path is made of many parallel and interconnecting channels. The channels are not of fixed diameter but widen and narrow repeatedly, and even twist and turn in varying directions as the particles obstruct the passageway. The channels do not even have the same average cross section or total length. The fluid phase is accelerated and/or decelerated and kinetic-energy losses are repeated. The rough surfaces of the particles produce the usual drag and skin friction, and the resistance to the fluid flows through the bed is the resultant of the total drag of all particles in the bed [4, 16].

Owing to the complicated nature of the flow channels in granular bed, there should not be a sharp transition from laminar to turbulent flow as occurs in pipe flow. Rather there should be a smooth transition from laminar flow throughout - to laminar flow in parts of the granular bed and turbulent flow in other parts - to turbulent flow throughout [17].

2.2 Packing

The packing of particles is of great interest in a variety of scientific and technological areas. These include production of concrete, coal technology, packed columns [18].

Many types of packing materials have been used, ranging from simple, readily available solids such as stones or broken bottles to expensive complex geometric shapes. In general, the packing material should have the following characteristics [4]:

1. It should have a large void volume to allow reasonable throughput of phase without excessive pressure drop.
2. It should be corrosion resistant.
3. It should be relatively inexpensive (represent low cost).
4. It should be chemically inert to fluids being processed.
5. It should have structural strength to permit easy handling and installation [19].

Actually, no one packing possesses all the above desirable qualities and so compromises must be made. Although the packing material may be designed to give excellent phase contacting, the method of packing must be considered because, if the phases do not contact everywhere within the tower, the packing is not completely effective [4].

The packing is built under gravity, particle by particle. Each particle is dropped at a randomly chosen position above the already placed particles, and rolls down over them until it reaches a stable position with respect to gravity [20].

The packing of solid particles has been studied more or less continuously for a number of years [21]. The first study of the modes of packing of spheres appears to have been undertaken by **Sticker in 1899**.

Furnas in 1931 [22], Westman and Hugill in 1930 [23], studied the packing of a bed of different sizes solid particles [24]. **Graton and Fraser in 1985 [25]** studied the packing of spheres led to the much-quoted limits of porosity for regular packing of single-size spheres.

An attempt has been made by **Yu and Standish in 1989 [26]** to establish general theory of the random packing of particles. They developed an analytical model based on the experimental results of binary mixtures.

2.3 The packing of beds

The problem of packing particles has received considerable attention from many investigators such as **Graton and Fraser in 1967 [27]**, and **Slichter in 1987 [28]**. It has been shown that the same value of porosity may be obtained with different arrangements of particles which may lead to different hydraulic resistances. If the particles are dropped into the column from a short distance above the packing, a reproducible packing is obtained which may be called the normal packing for that material. To obtain beds with porosity less than normal, the particles may be dropped into the column from greater heights above the bed. To obtain beds with porosity greater than normal, the particles may be allowed to fall to a measured depth of oil in the column. An indication of the effect of the height of fall on the porosity is given in Table 2.1.

Table 2.1 Effect of height of fall on porosity [9]

Material		Porosity for depth of fall in Air (inches)			
Shape	Size	96	72	24	2
Plate	1/16 in	0.33	0.34	0.37	0.46
Plate	5/22 in	0.41	0.42	0.45	0.53
Cube	1/4 in	0.29	0.31	0.32	0.38
Cylinder	1/8 in	0.34	0.34	0.36	0.40
Cylinder	1/4 in	0.33	0.33	0.35	0.38

The shape of the particle has a pronounced influence on the range of porosity that can be obtained, thus cubes and plates have a wide range of porosity while with cylinders it is difficult to cover more than a very small range in particle [9].

2.4 Granular bed

The flow of fluid through bed composed of stationary granular particles is a frequent occurrence in the chemical industry and therefore expressions are needed to predict pressure drop across beds due to the resistance caused by the presence of the particles [8].

Packed system in industry may be divided into the following classes:

1. Fixed beds
   a. Solid-gas system.
   b. Solid-liquid systems.
2. Moving beds.
3. Solid-liquid-gas system.

Typical example of solid-gas fixed-bed systems are the catalytic reactors which were used by the Germans in the Frischer-Tropsch synthesis retorting of Oil Shale, roasting of ores, combustion of coal and coke in fuel beds, and blast furnace operations.

The most important solid-liquid fixed-bed applications are water filtration, flow of oil through sand strata, coal washing, and leaching.

Moving beds are employed in the FCC (fluidized catalytic cracking) process.

The solid-liquid-gas system comprises fractionating towers, absorbers, scrubbers, and many other kinds of chemical engineering equipment [29].

2.5 Variables affecting flow through granular bed

The variables affecting resistance to flow through a granular bed can be classified into two basic categories [30]:

- Variables related to the fluid flowing through the bed such as viscosity, density, and rate of fluid flow.
- Variables related to the nature of the bed are numerous and to be considered as shape and size of the particles, container walls effects, porosity of the bed, surface roughness of the particle, and orientation of particles.

2.5.1 The shape and size of the particles

To define regular particles such as cube, cylinder or sphere, the width, length, thickness or diameter are usually used. However the problem becomes difficult when the particles are irregular. In this case the equivalent particle size is normally used, i.e., the size of the sphere having the same volume as the actual particle has. It is further assumed that the size of the particle is small in comparison with the column size in which the packing is contained; the ratio of the column diameter to the particle diameter should be a minimum of 8:1 to 10:1 to attain uniform voids distribution and to reduce wall effects [3, 31]. Figure 2.1 shows the relationship between bed porosity and the ratio of particles to column sizes for different types of packing materials.

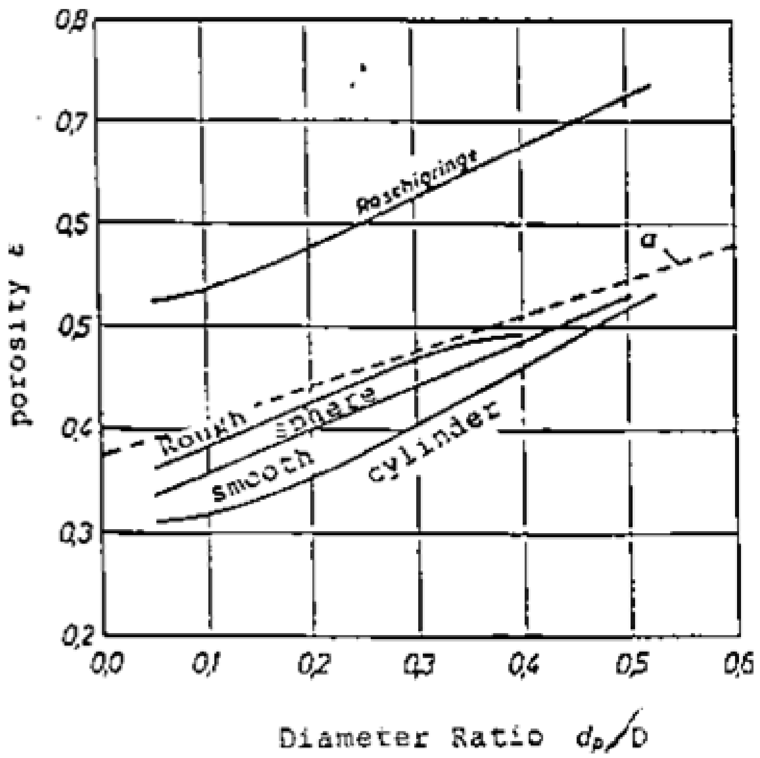

Figure 2.1 The relationship between bed porosity and diameter ratio [32]

Particle shape is usually measured by a factor called the shape factor. This factor is difficult to ascertain, particularly when dealing with small irregular shapes. The particle shape affects the packed bed resistance in two ways [30]:

i) The fluid paths in beds of irregular particles are more tortuous than those in similar beds of spheres (Fig.2.2)

ii) It have voids differing in both size and shape from those of similar beds consisting of spheres.

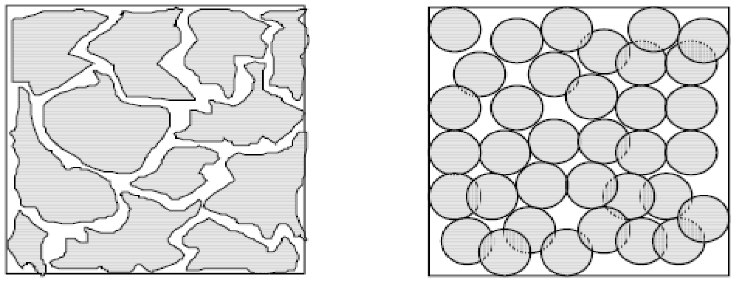

a. irregular particles b. regular particles

Figure 2.2 Different shapes of particles [33]

The sphericity shape factor ($\O_s$) of a particle is the ratio of the surface area of a sphere having the same volume as the particle to the actual surface area of the particle [3].

$$\O_s = \frac{\pi \, d_p^2}{S} \qquad \text{... (2.1)}$$

where :

d_p is the diameter (equivalent diameter) of the sphere having the same volume as the particle.

S is the actual surface area of the particle.

Table 2.2 Shape factor for different particles [3]

Material	Shape Factor
Spheres	1.0
Cubes	0.81
Cylinders, d_p=L (length)	0.87
Berl saddles	0.3
Rasching rings	0.3
Sands, average	0.75
Crushed glass	0.65

Table 2.2 summarized values of shape factor for different shapes of particles. The particles shapes affect the bed porosity, the lower the particle sphericity the more open is the bed [4].

2.5.2 Container walls effects

The walls retaining a granular packed bed affect the resistance of the bed in two ways [30]:

i) The particles adjacent to the walls pack more loosely than those more remote from them thus increasing the porosity of the zone near the walls. Figure 2.3 shows the fluctuation of porosity in a bed of spheres and cylinders.

ii) They create an additional surface area providing additional resistance to flow.

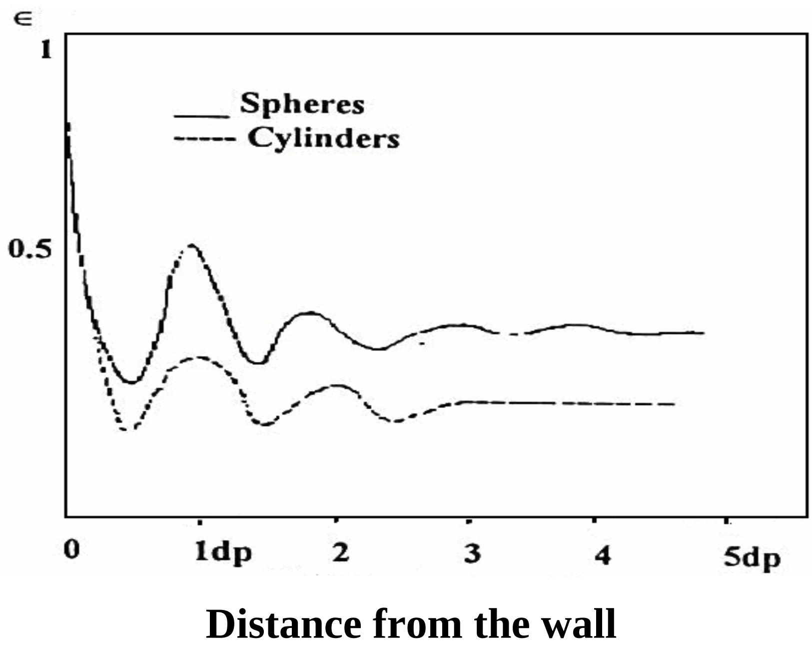

Figure 2.3 The Fluctuation of porosity in a bed of spheres and cylinders [34]

To decrease wall effects, the particle diameter should be small in comparison with the column diameter in which the packing is contained [31]. **In 1931, Furnas [22]** studied the wall effect and found that when the ratio of the column diameter to the particle diameter is greater than 10:1, the wall effect can be neglected.

Graton and Fraser in 1953 [35] showed that the porosity of the bed is greater in the layers next to the wall, which lead to increase the fluid permeability there.

Carman in 1937 [36] and Coulson in 1949 [37] made no correction for the change in porosity near to the wall. They used the mean porosity and for low rates added half the area of the walls to the surface area of the particles. A wall effect correction factor *fw* for velocity though packed bed has been determined experimentally by Coulson as [8].

$$f_w = \left(1 + \frac{1}{2}\frac{S_c}{S}\right)^2 \qquad \ldots (2.2)$$

where:

S_c is the surface of the container per unit volume of bed.

S is the specific surface area of the particles.

Numerous investigators including **Carman in 1937, Sullivan and Hertel in 1940, Coulson in 1949,** and **Leva in 1949** have stated that at high flow rates the wall effect is negligible. On the contrary, **Dudgeon in 1964** believed that the wall effect was independent of the flow rate, but his work has been subjected to considerable criticism by **Franzini in 1967** [30].

2.5.3 The porosity of the bed

The porosity of the bed (ε) is defined as the ratio of the void volume to the total volume of the bed, or the volume fraction occupied by the fluid phase, i.e.

$$e = \frac{Volume\ of\ voids\ in\ a\ bed}{total\ volume\ of\ the\ bed} \quad \text{... (2.3)}$$

Other names given the porosity include void fraction, fractional voidage, or simply voidage [38].

One of the problems concerning the flow of fluids through beds of particles is the manner in which the particles are packed and the distribution of voids within the packed bed [5].

Particles stacked directly on top of each other (cubic packing) have higher porosity (e=0.476) than the particles in a pyramid shape sitting on top of two other particles (e=0.259) (rhombohedra packing). When smaller particles are mixed with larger particles, the smaller particles could fill the void spaces between the larger particles (Cubic packing with smaller grains filling the void space); this would result in a lower porosity as shown in Fig. 2.4 [39].

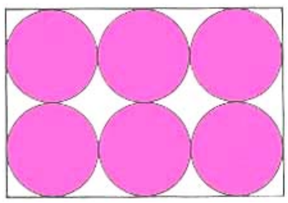

Cubic packing

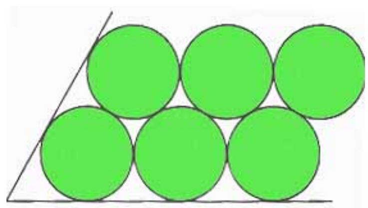

Rhombohedral packing

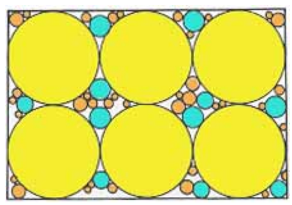

Cubic packing with smaller grains filling the void space

Figure 2.4 Different types of packing [39]

The porosity has a great effect on the properties of granular media. There is no doubt that any small change in porosity of the bed leads to a big change in pressure drop across the bed. **Leva in 1951** found that a 1% decrease in the porosity of the bed produced about an 8% increase in the pressure drop, whilst **Carman in 1956** reported a higher value, 10% increase in the pressure drop for every 1% decrease in porosity [30].

2.5.4 The surface roughness of the particles

Surface roughness has major effects on flow of fluid through packed bed [30]:

i) it increases the porosity of the bed.

ii) it increases the resistance of the bed .

The surface roughness of particles in contact with the moving fluid has a considerable effect upon the friction in the transition and turbulent region. Roughness does not affect the friction in the laminar region because the laminar boundary layer completely covers the roughness elements and no eddies are generated [29, 30].

2.5.5 The orientation of the particles

The orientation of the particles composing the bed with respect to the direction of flow has a significant effect which depends on the shape and the arrangement of the particles. **Coulson and Gupta in 1949** found that for the same porosity the resistance to flow changed with the arrangement of the particles relative to each other [30].

Sullivan and Hertel in 1940 have suggested a factor for the orientation and their equation for flow through a packed bed is denoted by:

$$\delta = \left(Sin^2\,\theta\right)_{avg} \qquad \text{... (2.4)}$$

where:

δ is the orientation factor

θ is the angle which the normal to the solid-liquid interface makes with the stream direction.

They have presented data for three specific packings. Table 2.3 shows values of the orientation factor for different materials.

Table 2.3 Orientation factors for different packing [30]

Material	Orientation Factor, δ
Spheres	$\frac{2}{3}$
Cylinder perpendicular to flow direction	$\frac{1}{2}$
Cylinder parallel to flow direction	1

2.6 Velocity measurement

The precise measurement of velocities within the packing of bed would be virtually impossible. Therefore, the flow rate was studied in the column just downstream from the packing. This meant that the velocities so obtained were superficial values, which based upon the total void and non-void area. The objective was to determine the average velocity that would exist in the bed at a given radial position based upon the total area rather than the actual void area. Such a measurement is an average velocity because the void fraction varies with distance along the axis of the pipe. In order to attain this objective, the effect of distance of the measuring device from the packing must be examined. If this distance is too large, the observed velocity profiles may be more descriptive of empty column conditions than those existing within the packed bed. If the distance is too small, velocity components perpendicular to the direction of flow may be significant [24].

2.7 Prediction of voidage distribution

The characteristics of the flow through packed bed are important in filter design and an understanding of the relationship between void fraction and the flow distribution is essential. Figure 2.5 shows a typical radial voidage distribution (in a bed of 98 mm in diameter packed with 4 mm spherical beads). It has been shown that, for flow through a fixed bed of uniform particles that there is a maximum velocity approximately one particle diameter from the outer wall of the bed, which decrease sharply toward the wall and more gradually away from it.

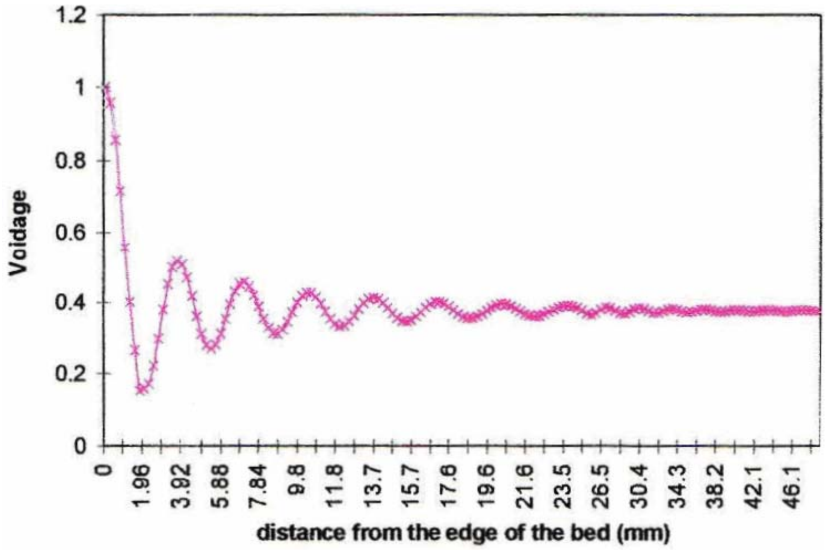

Figure 2.5 Typical radial voidage distribution [40]

Simple geometrical considerations indicate that near the wall of the bed the flow are larger and smaller resistances than near the center of the column. The fraction of the bed influenced by this velocity profile depends on the ratio of particle to bed diameters [24, 40].

The voidage is found to be a minimum about half a particle diameter from the wall of the bed and then follow a dumped oscillatory function until it reaches a constant value about 5 particle diameters from the wall, where the packing is random [40].

Large randomly packed beds of uniform spheres tend to pack with an average void fraction of 39% since locally the voidage varies from point to point. Near the wall of the containing vessel the void fraction will be larger than near the center of the bed. Immediately adjacent to the wall the void fraction approach unity and in the center of the bed a minimum voidage observed (0.215) [41].

2.8 Specific surface area

The general structure of a bed of particles can often be characterized by the specific surface area of the bed (S_B). S_B is the surface area presented to the fluid per unit volume of bed when the particles are packed in a bed. Its units are $(\text{length})^{-1}$. S the specific surface area of the particles is the surface area of particle divided by its volume. Its units are $(\text{length})^{-1}$. For sphere:

$$S = \frac{\pi {d_p}^2}{\pi\left({d_p}^3/6\right)} = \frac{6}{d_p} \qquad \text{... (2.5)}$$

It can be seen that S and S_B are not equal due to the porosity occurring when the particles are packed into a bed. If point contact occurs between particles so that only a very small fraction of surface area is lost by overlapping, then:

$$S_B = S(1-e) \quad \text{... (2.6)}$$

where S_B is the specific surface area of packing exposed to fluid flow.

For a given shape of particle S increases as the particle size is reduced [8, 42].

When mixtures of sizes are studied the value of S for spheres of mixed sizes is given by [43].

$$S = 6(1-e)\sum\left(\frac{x_i}{d_{pi}}\right) \quad \text{... (2.7)}$$

Where x_i is fractional weight for particle of size d_{pi}

2.9 Friction factor

The friction factor is determined for the entire Reynolds number. For Re<10 the flow through packed bed is laminar, the range 10<Re<100 is commonly referred to as transitional whereas flows characterized by Re>100 are considered turbulent [44].

Amount of work has been done in correlating data for packed columns at higher fluid velocities where the pressure drop appears to vary with some power of the velocity, the exponent ranging between 1 and 2. **Blanke in 1962 [12]** suggested that this change of relationship between pressure drop and velocity is entirely analogous to that which occurs in ordinary pipes and proposed a friction factor plot similar to that of commonly friction factor of

Stanton. The equation used was that for kinetic effect modified by a friction factor, which is a function of Reynolds number [45].

$$\Delta p = 2f\,(\rho u^2 / d_p) \qquad \ldots (2.8)$$

$$f = \phi\,(Re_1) \qquad \ldots (2.9)$$

Some workers have included the effect of void fraction by the addition of another factor in equation 2.8. It is usually given in the form $(1-\varepsilon)^m/\varepsilon^3$ where m is either 1 or 2.

Carman and Kozeny in 1938 [11] suggested that the change of relationship between void fraction, pressure drop and velocity, and proposed a friction factor for entire Reynolds number by plotting on a logarithmic basis [46].

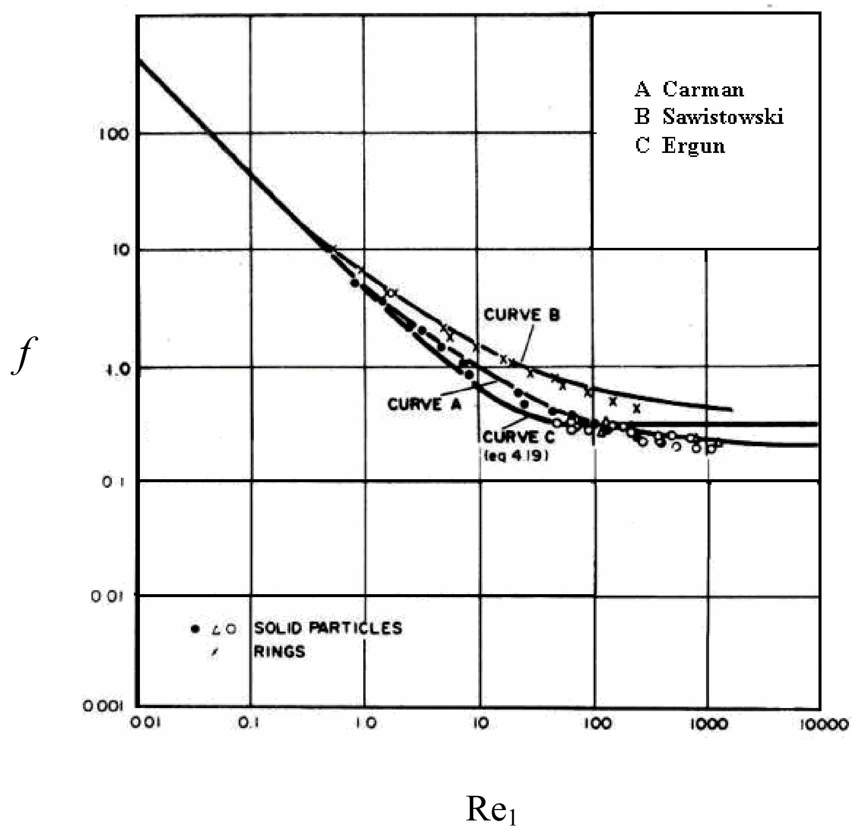

Figure 2.6 Friction factor versus Reynolds number [8]

Figure 2.6 is a correlation of the friction factor as a function of the Reynolds number for condition of fixed bed operation. This figure was found to work satisfactorily for constant diameter fractions of the glass spheres.

Carman in 1938 correlated data for flow through randomly packed beds of solid particles by a single curve (curve A, Fig. 2.6), whose general equation was:

$$f = 5\,\mathrm{Re}_1^{-1} + 0.4\,\mathrm{Re}_1^{-0.1} \qquad \text{... (2.10)}$$

where Re_1 is the modified Reynolds number.

$$\mathrm{Re}_1 = \frac{\rho u}{S(1-e)\mu} \qquad \text{... (2.11)}$$

As where ρ, u, S , e and μ are the density of the fluid, fluid velocity, surface area of particles, porosity of the bed, and the fluid viscosity respectively.

Sawistowski in 1957 has compared the results obtained for flow of fluids through beds of hollow packing and has noted that equation 2.10 gives lower values of friction factor for hollow packing. Thus, Sawistowski modified equation 2.10 as:

$$f = 5\,\mathrm{Re}_1^{-1} + \mathrm{Re}_1^{-0.1} \qquad \text{... (2.12)}$$

Equation 2.12 is represented as curve B in Fig. 2.6.

Ergun in 1952 suggested equation for flow through ring packings as:

$$f = 4.17\,\mathrm{Re}_1^{-1} + 0.29 \qquad \text{... (2.13)}$$

Equation 2.13 is plotted as curve C in Fig. 2.6.

As shown in Fig. 2.6, the first term of equations 2.10, 2.12 and 2.13 predominates at low rates of flow (Re < 10) where the losses are mainly skin friction and the second term is small. At high flow rates (2< Re <100), the second term becomes more significant and the slope of the plot gradually changes from -1.0 to about $-\frac{1}{4}$. At higher flow rates (Re >100) the plot is approximately straight. The change from complete streamline flow to complete turbulent flow is very gradual because flow conditions are not the same in all the pores [8].

2.10 The surface roughness effect on the friction factor

Attempts to study the effect of surface roughness on the friction factor have shown that the variable has a significant effect but no quantitative method of evaluating the effect has been formulated.

Leva in 1949 carried out important experiments using three different groups of materials. He used glass and porcelain as smooth particles, clay and Alundum as rough materials, Aloxite and MgO granules as rougher materials. The degree of the materials roughness was described qualitatively (as a result of his tests). This method of description does not help in the development of a quantitative correlation between the relative roughness (ε/d) and the friction factor.

Leva expressed equations for the friction factor as a function of Reynolds number which range from 130 to 7000 for these materials as follow. For smooth materials the expression was:

$$f = \frac{1.75}{{Re_1}^{0.1}} \qquad \text{... (2.14)}$$

For rough materials the expression was:

$$f = \frac{2.625}{{Re_1}^{0.1}} \qquad \text{... (2.15)}$$

Whilst for rougher materials the expression was:

$$f = \frac{4.0}{{Re_1}^{0.1}} \qquad \text{... (2.16)}$$

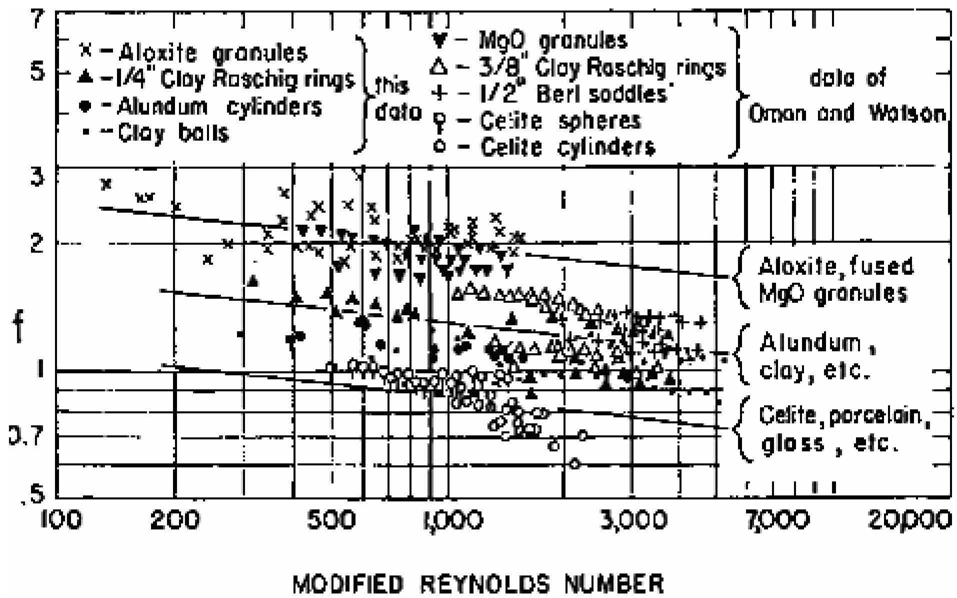

Figure 2.7 Friction factor for various materials [14]

Figure 2.7 shows that the friction factor through packed beds is approximately doubled when the degree of surface roughness was increased from that represented by porcelain to the roughness of Aloxite granules [14].

These expressions do not include the relative roughness (ε/d) and can only therefore be used for the materials that were used. Leva concluded (from previous expressions) that the degree of surface roughness had no effect on the slope of the log f –log Re curve between the limits of Re from 130 to 7000 which covered the range was used [30].

2.11 Pressure drop

The pressure drop of fluid flow through the packed bed is an important issue [2]. It is affected by several factors such as fluid flow rate, fluid viscosity and density, bed geometry, particle size and size distributions. A partial relationship was found between these variables and the pressure drop which was proportional to fluid velocity at low rates, and proportional to the square of the velocity at high flow rates. Reynolds was the first to formulate the resistance by friction on the motion of fluid as the sum of these two conditions [47]:

$$\frac{\Delta p}{L} = a u + b \rho u^2 \qquad \text{... (2.17)}$$

where a and b are representative of packing and fluid properties

Carman and Kozeny derived an expression for pressure drop under viscous flow as:

$$\frac{\Delta p}{L} = \frac{150\,(1-e)^2\, u\, \mu}{e^3\, \text{Ø}_s^2\, d_p^2} \qquad \text{... (2.18)}$$

Burke and Plummer derived an expression for change in pressure at turbulent flow resulting from kinetic energy losses as [47]:

$$\frac{\Delta p}{L} = \frac{1.75(1-e)\rho u^2}{e^3 \O_s \, d_p} \qquad \text{... (2.19)}$$

Ergun found that the total pressure drop is the sum of the viscous and kinetic forces, and created a general relationship based on equations 2.18 and 2.19 as [15]:

$$\frac{\Delta p}{L} = \frac{150(1-e)^2 u \mu}{e^3 \O_s^2 d_p^2} + \frac{1.75(1-e)\rho u^2}{e^3 \O_s d_p} \qquad \text{... (2.20)}$$

where ΔP, e, ρ, d_p, $\O_s$, u, L, and μ are the pressure drop, void fraction of the bed, density of the fluid, particle diameter, sphericity of the particle, fluid velocity, height of the bed, and the fluid viscosity respectively.

Ergun equation is unique among many equations because it covers any flow type and condition (laminar, transitional and turbulent) [7].

For beds consisting of a mixture of different particle diameters, the average particle diameter ($d_{p\,av}$) can be used instead of d_p (in equation 2.20) as [16, 48].

$$d_{p\,av} = \frac{1}{\sum_{i=1}^{n} \frac{x_i}{d_{pi}}} \qquad \text{… (2.21)}$$

where x_i is the weight fraction for particle of size d_{pi}.

2.12 The relation between depth of bed and pressure drop

From the reading of the manometers, **Coulson in 1949 [9]** found that the difference in pressure over varying thicknesses of the packing was obtained directly.

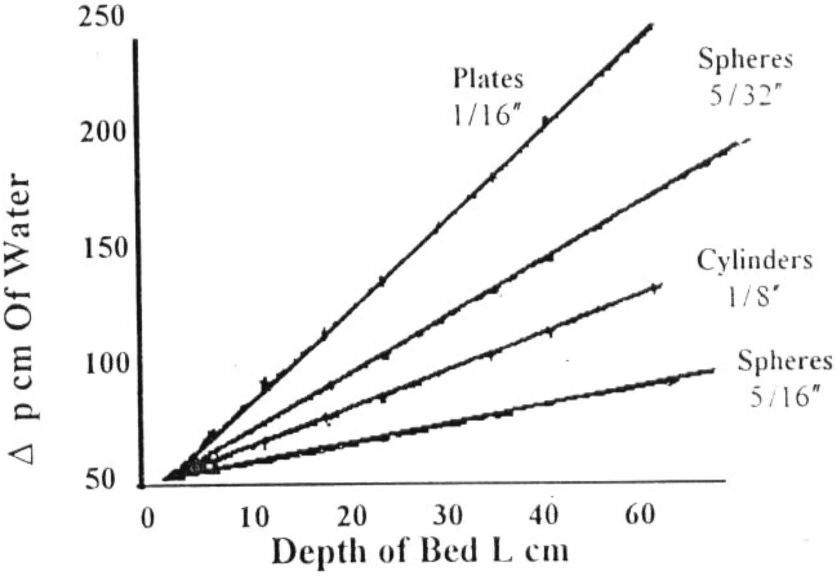

Figure 2.8 Relation between depth of bed and pressure drop [9]

Some results for bed of spherical particles are shown graphically in Fig 2.8. The experimental points are seen to lie on straight lines indicating a linear relation between Δp and L. Figure 2.8 also shows similar results for beds of other material.

2.13 Theory

The porosity of any mixture in a given particulate system depends on the proportions of the components present, but not on the total amount of the mixture. Let q be the number of components and X_i the proportion of the ith component in the mixture, so that

$X_i \geq 0 \qquad (i=1,2,\ldots\ldots,q)$

$X_1 + X_2 + \ldots\ldots\ldots\ldots + X_q = 1 \qquad \ldots (2.22)$

In the simplex- centroid design, $2^q - 1$ measurements are taken one on each of the following. The q pure components, the $\binom{q}{2}$ binary mixtures with equal proportions, the $\binom{q}{3}$ ternary mixtures with equal proportions, and the q-nary mixture with equal proportions. This corresponds to the points (X_1, X_2,..., …, X_q) of the simplex Equation 2.22 by making the following permutations:

$\binom{q}{1}$ of (1, 0, ……….. , 0)

$\binom{q}{2}$ of (1/2, 1/2, 0, ………. , 0)

$\binom{q}{3}$ of (1/3, 1/3, 1/3, 0,………., 0)

$\binom{q}{4}$ of (1/4, 1/4, 1/4, 1/4,0,………., 0)

$\binom{q}{5}$ of (1/5, 1/5, 1/5, 1/5, 1/5,0,………., 0)

$\binom{q}{q}$ of (1/q, 1/q,........, 1/q)

Table 2.4 gives the simplex- centroid design for quinary mixture [49].

Table 2.4 Experimental design of quinary mixture [49]

No.	X_1	X_2	X_3	X_4	X_5
1	1	0	0	0	0
2	0	1	0	0	0
3	0	0	1	0	0
4	0	0	0	1	0

5	0	0	0	0	1
6	1/2	1/2	0	0	0
7	1/2	0	1/2	0	0
8	1/2	0	0	1/2	0
9	1/2	0	0	0	1/2
10	0	1/2	1/2	0	0
11	0	1/2	0	1/2	0
12	0	1/2	0	0	1/2
13	0	0	1/2	1/2	0
14	0	0	1/2	0	1/2
15	0	0	0	1/2	1/2
16	1/3	1/3	1/3	0	0
17	1/3	1/3	0	1/3	0
18	1/3	1/3	0	0	1/3
19	1/3	0	1/3	0	1/3
20	1/3	0	0	1/3	1/3
21	1/3	0	1/3	1/3	0
22	0	1/3	1/3	1/3	0
23	0	1/3	1/3	0	1/3
24	0	1/3	0	1/3	1/3
25	0	0	1/3	1/3	1/3
26	1/4	1/4	1/4	1/4	0
27	1/4	1/4	1/4	0	1/4
28	1/4	1/4	0	1/4	1/4
29	1/4	0	1/4	1/4	1/4
30	0	1/4	1/4	1/4	1/4
31	1/5	1/5	1/5	1/5	1/5

2.14 Fluid flow through randomly packed columns

Many attempts have been made to obtain general expressions for pressure drop and mean velocity for flow through packing in terms of voidage and specific surface, as these quantities are often known or can be measured.

A horizontal pipe with a concentric element marked ABCD is shown in Fig. 2.9.

The forces acting are the normal pressures over the ends and shear forces over the curved sides.

Force over AB= $p\pi s^2$

Force over CD= $-\left(p+\frac{dp}{dl}\delta l\right)\pi s^2$

Force over curved surface $= 2\pi s\,\delta l\, R_y$

Where the shear stress R_y is given by:

$$R_y = \mu\frac{du_x}{ds} = -\mu\left(\frac{du_x}{dy}\right) \qquad \text{... (2.23)}$$

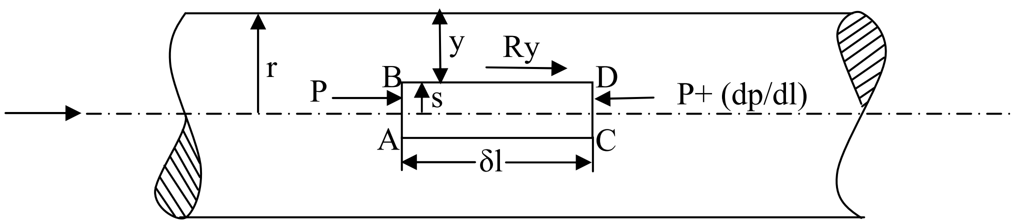

Figure 2.9 Flow through pipe [50]

Taking force balance:

$$p\pi s^2 - \left(p+\frac{dp}{dl}\delta l\right)\pi s^2 + 2\pi s\delta l\mu\frac{du_x}{ds} = 0$$

$$\left(-\frac{dp}{dl}\right)s + 2\mu\left(\frac{du_x}{ds}\right) = 0 \qquad \text{... (2.24)}$$

From equation 2.23

$$\frac{du_x}{dy} = -\frac{du_x}{ds}$$

and hence in equation 2.24

$$\frac{du_x}{dy} = \left(-\frac{dp}{dl}\right)\frac{s}{2\mu}$$

and the shear stress at the wall is given by

$$\left(\frac{du_x}{dy}\right)_{y=o} = \left(-\frac{dp}{dl}\right)\frac{r}{2\mu} = \left(-\frac{dp}{dl}\right)\frac{d}{4\mu} \qquad \text{... (2.25)}$$

The velocity at any distances s from the axis of the pipe can now be found by integrating equation 2.24

Thus:

$$u_x = \frac{1}{2\mu}\frac{dp}{dl}\frac{s^2}{2} + \text{Constant}$$

At the wall of the pipe (where s=r) the velocity u_x must be zero to satisfy the condition of zero wall slip. Substituting the value $u_x=0$ when s=r we get

$$\text{Constant} = \frac{1}{2\mu}\left(-\frac{dp}{dl}\right)\frac{r^2}{2}$$

and therefore

$$u_x = \frac{1}{4\mu}\left(-\frac{dp}{dl}\right)\left(r^2 - s^2\right)$$

Thus the velocity over the cross-section varies in parabolic manner with distance from the axis of the pipe. The velocity of the flow is seem to be a maximum when s=0. Thus, the maximum velocity at the pipe axis, is given by u_{cl} where [50].

$$u_{max} = u_{cl} = \frac{1}{4\mu}\left(-\frac{dp}{dl}\right)r^2 = \left(-\frac{dp}{dl}\right)\frac{d^2}{16\mu} \quad \text{... (2.26)}$$

Where $u = \frac{u_{max}}{2}$ for laminar flow

Hagen-Poiseuille equation for laminar flow through pipe was:

$$u = \frac{-\Delta p\, d_t^2}{32\, L\, \mu} \quad \text{... (2.27)}$$

If the free space in the bed is assumed to consist of a series of tortuous channels, equation (2.27) for flow through a bed may be rewritten as:

$$u_1 = \frac{d_m^2(-\Delta p)}{K'\, \mu L'} \quad \text{... (2.28)}$$

In a cube of side x, the volume of free space is ex^3 so that the mean cross- sectional area for flow is the free volume divided by the height, or ex^2. The volume flow rate thought this cube is ux^2, so that the average linear velocity through the porous u_1, is given by Depuit as:

$$u_1 = \frac{u\,x^2}{e\,x^2} = \frac{u}{e} \quad \text{... (2.29)}$$

Although equation 2.29 is reasonably true for random packing, it does not apply to all regular packing.

The equivalent diameter of pore space (d_m) could be taken as:

$$d_m = \frac{e}{S_B} = \frac{e}{S(1-e)} \qquad \text{... (2.30)}$$

Then taking $u_1 = \frac{u}{e}$ and L' ∞L equation 2.28 becomes

$$u = \frac{e^3(-\Delta p)}{K'' S_B^2 \mu L} \qquad \text{... (2.31)}$$

Equation 2.31 (Kozeny equation) applies to stream flow condition, but Carman and others have extended the analogy with pipe flow to cover both streamline and turbulent flow conditions through packed bed. In this treatment a modified Reynolds number Re_1, is plotted against a modified friction factor $\frac{R_1}{\rho u_1^2}$.

The modified Reynolds number Re_1 is obtained by taking the same velocity and characteristic linear dimension d_m as were used in driving equation 2.31 thus:

$$Re_1 = \frac{u e \rho}{eS(1-e)\mu}$$

$$= \frac{\rho u}{S(1-e)\mu} \qquad \text{... (2.32)}$$

The friction factor, which is plotted against the modified Reynolds number is $\frac{R_1}{\rho u_1^2}$, where R_1 is the component of the drag force per unit area of particle surface in the direction of motion. R_1 can be related to the properties of the bed and pressure gradient as follows. Consider the force acting on the fluid in a bed of unit cross sectional area and thickness L. The volume of particle in the bed is L(1-e) and therefore the total surface is SL(1-e). Thus the resistance force = R_1SL(1-e). This force on the fluid must be equal to that produced by a pressure difference of Δp across the bed. Then, since the free cross- section of fluid is equal to e.

$$(-\Delta p)e = R_1 SL(1-e)$$

$$R_1 = \frac{e(-\Delta p)}{S(1-e)L} \qquad \text{... (2.33)}$$

Thus

$$\frac{R_1}{\rho u_1^2} = \frac{e^3(-\Delta p)}{S(1-e)L\rho u^2} \qquad \text{... (2.34)}$$

Carman in 1938 [8] plotted $\frac{R_1}{\rho u_1^2}$ against Re_1 using logarithmic coordinates, the general equation was:

$$\frac{R_1}{\rho u_1^2} = 5\,\mathrm{Re}_1^{-1} + 0.4\,\mathrm{Re}_1^{-0.1} \qquad \text{... (2.10)}$$

Sawistowski in 1957 [51] compared the result obtained for flow of fluids through beds of hollow packing and has noted that equation 2.10 gives as consistently low result for these materials. He proposed:

$$\frac{R_1}{\rho u_1^2} = 5\,\mathrm{Re}_1^{-1} + \mathrm{Re}_1^{-0.1} \qquad \text{... (2.12)}$$

Ergun in 1952 [52] obtained a good semi-empirical correlation for friction factor. He proposed [8]:

$$\frac{R_1}{\rho u_1^2} = 4.17\,\mathrm{Re}_1^{-1} + 0.29 \qquad \text{... (2.13)}$$

Chapter Three
Experimental Work

3.1 Aim of the work

This work represents the flow of single phase through a bed of spherical particles, where two fluids are used separately (either air or water). The aim of this work is to:

1. Study the effect of particles size and size distribution on the bed porosity.
2. Study the effect of bed porosity on the pressure drop and friction factor through the packed bed.
3. Study the effect of working fluids (air or water) on the pressure drop and friction factor through the packed bed.
4. Compare the experimental results with those of Carman, Ergun and Sawistowski correlations.

3.2 Description of materials

In this work five sizes of spherical glass particles were used. The spherical particles diameters were 0.42, 0.51, .61, 0.79 and 1.01cm.

The fluids used were air and water, and their properties were taken at laboratory temperature ($32^{\circ}C$) for air flow, and at tap water temperature ($25^{\circ}C$) for water flow. Table 3.1 shows the physical properties (density and viscosity) for air and water.

Table 3.1 The physical properties of fluids [53]

Type of fluid	Density, kg/m^3	Viscosity, kg/m.s
Air	1.1582	$1.88*10^{-5}$
Water	997.07	$0.89*10^{-3}$

3.3 Description of the apparatus used for packed bed

A schematic diagram of the apparatus used is shown in Fig. 3.1, and photographic pictures are shown in Figs. 3.2 and 3.3 respectively.

The packed bed column was made of glass tube (Q.V.F) 7.62 cm inside diameter and 57 cm height. The Q.V.F glass contains two pressure taps. The pressure taps were chosen to be small in diameter (2 mm) and inserted flush to the inside wall of the tube to avoid fluid turbulence and determine the static pressure accurately. The first tap was placed down stream at a distance of 1 cm from the sieve, and the second was placed at a distance of 1cm from the top of the packing. The distance between the inlet of the column and the sieve (packing rest) was 25 cm to avoid fluid turbulence at the bed inlet.

The fluids used were air and water, and each of them has its own apparatus as follows.

a. Air flow system

1. Air-flow is produced by a compressor to the packed column. The compressor contained a vane rotary type driven by AC motor. The compressor is used to supply the air to the packed bed at constant pressure.
2. A storage tank is used to receive air from the compressor and provide it to the rotameter. It is also used to regulate the flow of air and avoid disturbances.

3. A calibrated rotameter is used for measuring air flow rate with range up to 16 cubic meters per hour.

4. U-tube manometer (with ethanol) is used for measuring the pressure drop across the bed.

b. Water flow system

1. A glass (Q.V.F) storage tank with capacity of 100 liter is used to provide water for pumping.

2. A centrifugal pump with power of 1.5 kW is used for pumping water from the storage tank to the test section.

3. A calibrated rotameter is used for measuring water flow rate with range up to 5 cubic meters per hour.

4. U-tube manometer (with mercury) is used for measuring the pressure drop across the bed.

3.4 Experimental procedure

The particles were poured into the column and the bed porosity was determined using equation 3.1 [54].

$$e = 1 - \frac{\rho_b}{\rho_t} \qquad \text{... (3.1)}$$

where

ρ_t is the true density of the particles, (kg/m^3)

ρ_b is the apparent bulk density, (kg/m^3)

a. Air flow system

The fluid used was air provided by the compressor and its flow rates were up to 16 cubic meters per hour, and its flow was regulated by means of a regulating valve at the inlet of the rotameter. The average velocity of the fluid was obtained from the rotameter using equation 3.2.

$$u = \frac{Q}{A} \qquad \text{... (3.2)}$$

where:

Q is the volumetric flow rate of fluid, (m^3/h)

A is the bed cross-sectional area, (m^2)

The rotameter valve was opened for air flow. The rotameter float was ensured to achieve steady state, and the pressure drop across the bed was measured using U-tube manometer. The friction factor was obtained from the pressure drop using equation 2.34.

$$f = \frac{e^3(-\Delta p)}{S(1-e)L\rho u^2} \qquad \text{... (2.34)}$$

b. Water flow system

The fluid used was water provided by the pump and its flow rates were up to 5 cubic meters per hour, and its flow was regulated by means of a regulating valve at the inlet of the rotameter. The average velocity of the water flow was obtained from the rotameter using equation 3.2. The rotameter valve was opened until the bed was filled with water and the column became free from bubbles. The pressure drop across the bed was measured using U-tube manometer. The friction factor was obtained from the pressure drop using equation 2.34.

3.5 Test method

3.5.1 True density of particle

The true densities of particles (ρ_t) were determined using shifted water method. A known weight of particles was immersed in a graduated cylinder filled with water. The weight of the container was measured using a sensitive balance first when the container filled with water only and second when it contains the particles besides the water. In both cases, water level inside the container was carefully maintained at its permissible full mark level. Using the following equation, the true density of particles was determined as [32].

$$\rho_t = \frac{w_1 \times \rho_w}{w_2 - w_3 + w_1} \qquad \text{... (3.3)}$$

where:

ρ_w is the density of water at laboratory temperature, (kg/m^3).

w_1 is the weight of the particles, (kg)

w_2 is the weight of cylinder filled with water, (kg)

w_3 is the weight of cylinder with water and particles, (kg)

Table 3.2 The true densities of particles

Particle size, cm	True density, kg/m^3
1.01	2.5538
0.79	2.5289
0.61	2.5345
0.50	2.5411
0.42	2.4741

Table 3.2 shows the true densities of the particles. Each measurement was repeated three times for each tested particle to determine the true density value.

For mixture of particles, the true density of mixture (ρ_{tm}) was determined from the following equation [9].

$$\rho_{tm} = \frac{1}{\sum_{i=1}^{m} \frac{x_i}{\rho_{ti}}} \qquad \text{... (3.4)}$$

As where

x_i is the weight percent of component i

ρ_{ti} is the true density of component i

3.5.2 Bulk density

The bulk density (ρ_b) is defined by the following expression:

$$\rho_b = \frac{Weight\ of\ particles\ comping\ the\ bed}{Volume\ of\ bed} \qquad \text{... (3.5)}$$

For cylindrical bed

Volume = $\frac{\pi}{4} D^2 L$

where:

D is inside diameter of the bed, (m)

L is the level of particles in the bed, (m)

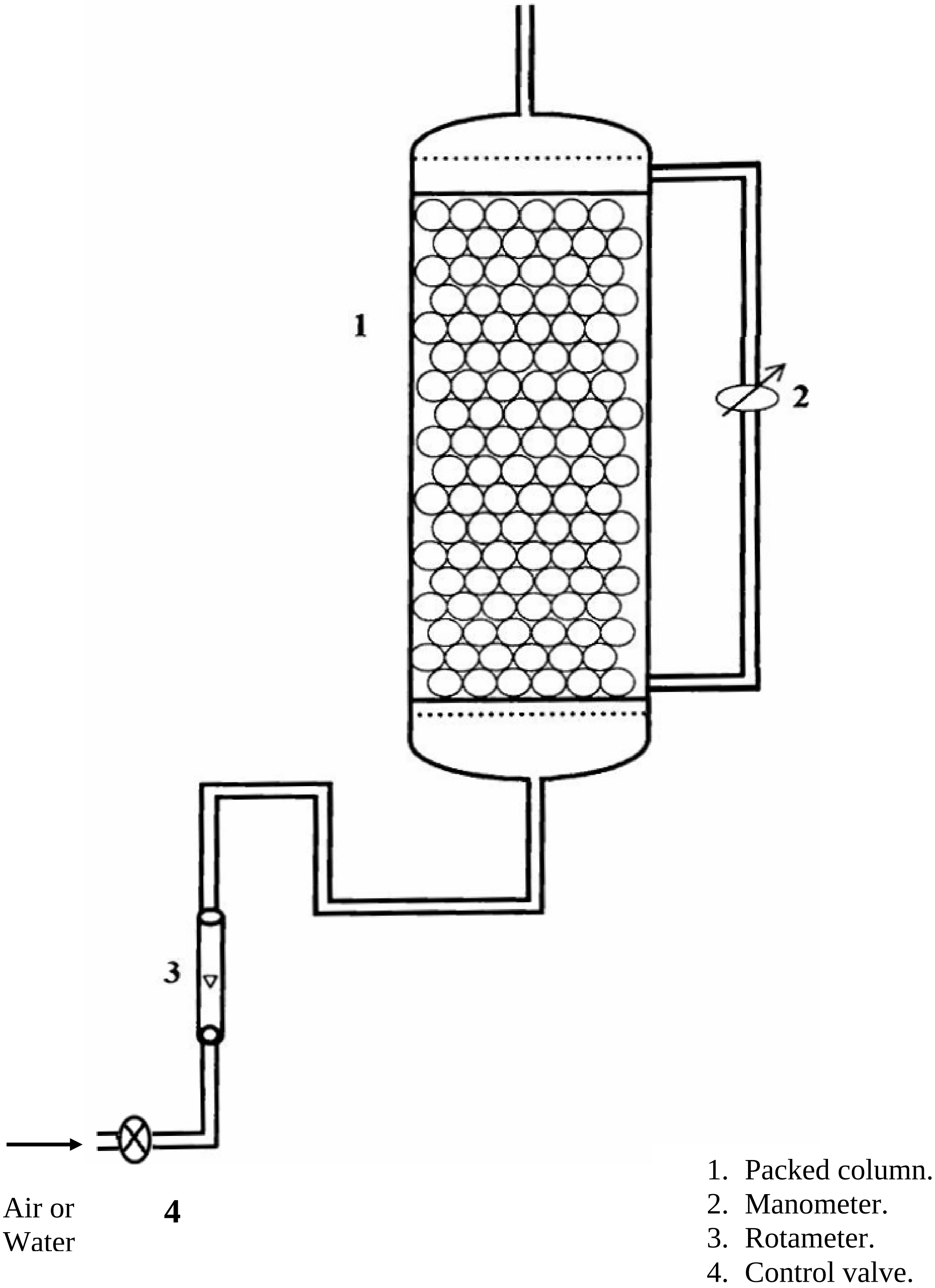

Figure 3.1 Apparatus diagram

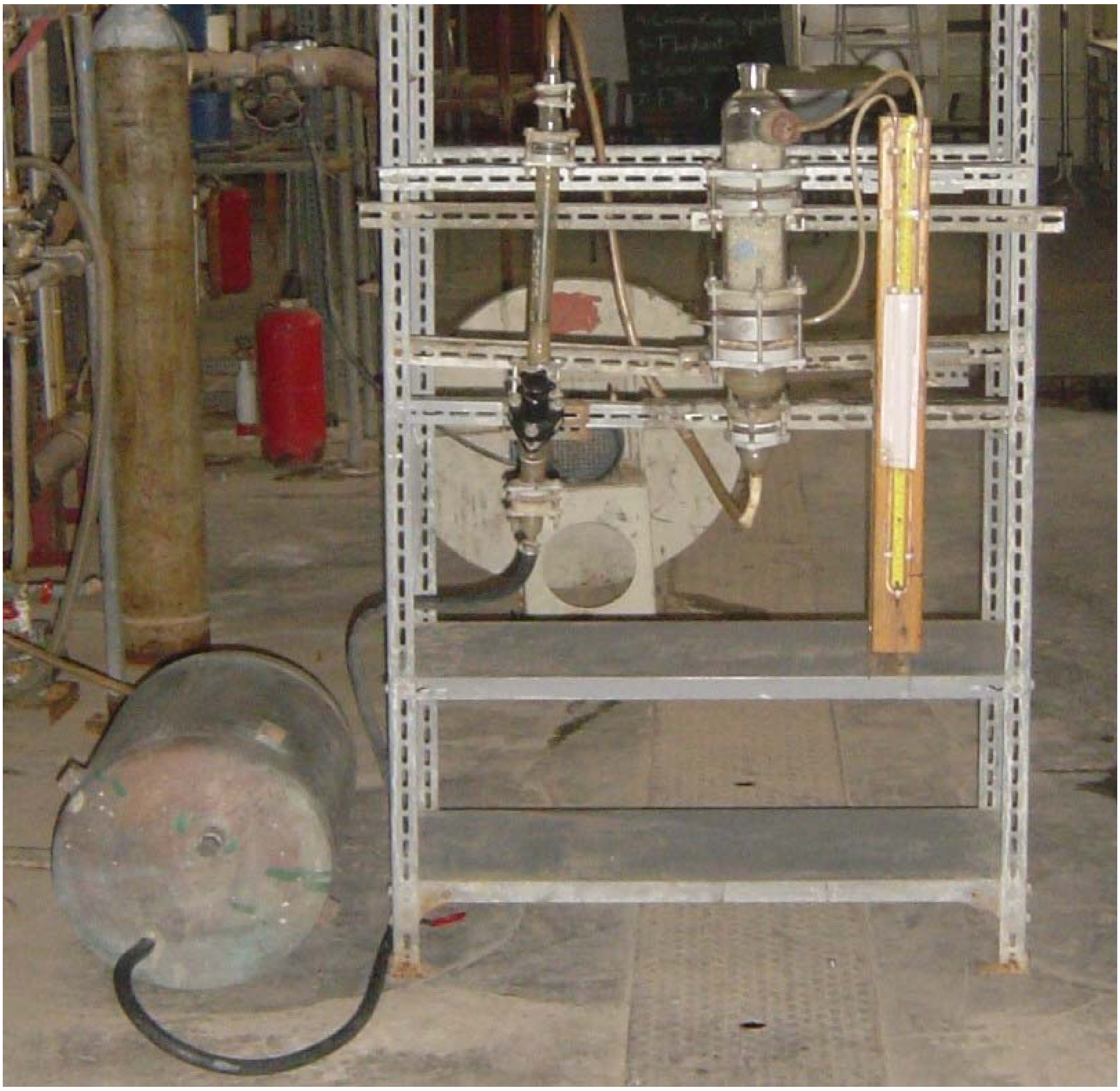

Figure 3.2 Photographic picture of air flow through packed bed

Figure 3.3 Photographic picture of water flow through packed bed

Chapter Four

Results and Discussion

4.1 Packing of mono sizes particles

4.1.1 Air flow

The values of friction factors for air flow through beds of mono sizes particles are plotted versus Reynolds numbers as shown in Figs. 4.1 to 4.5.

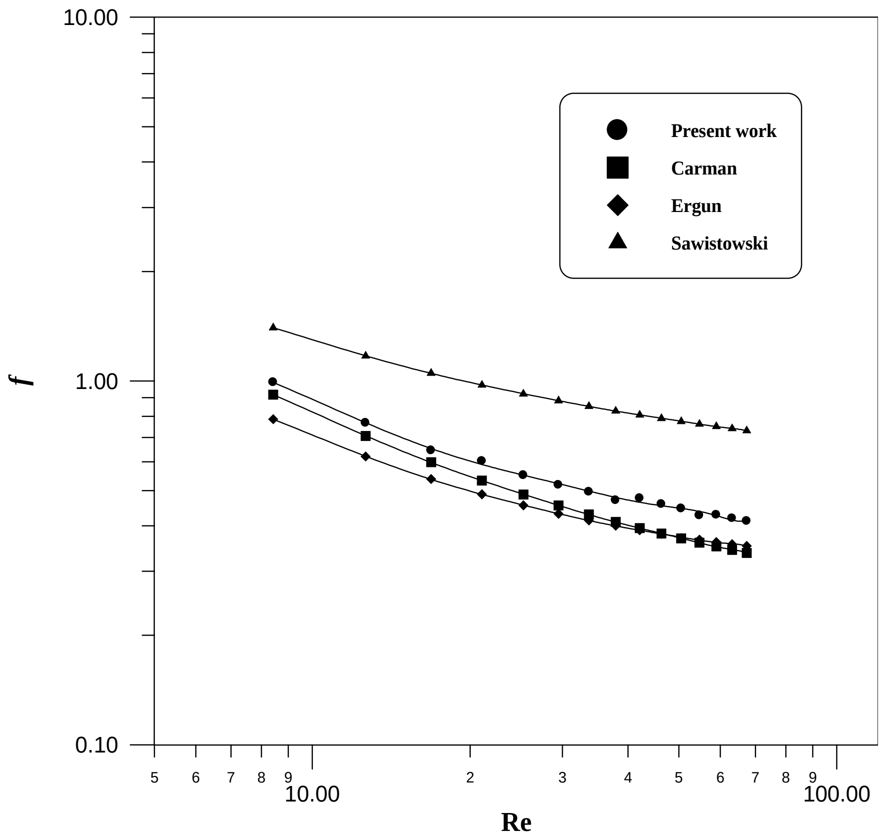

Figure 4.1 Friction factor versus Reynolds numbers for particles diameter of 0.42 cm and porosity of 0.3746 (Appendix A.1)

These Figs. show that the friction factor decreases as Reynolds number increases.

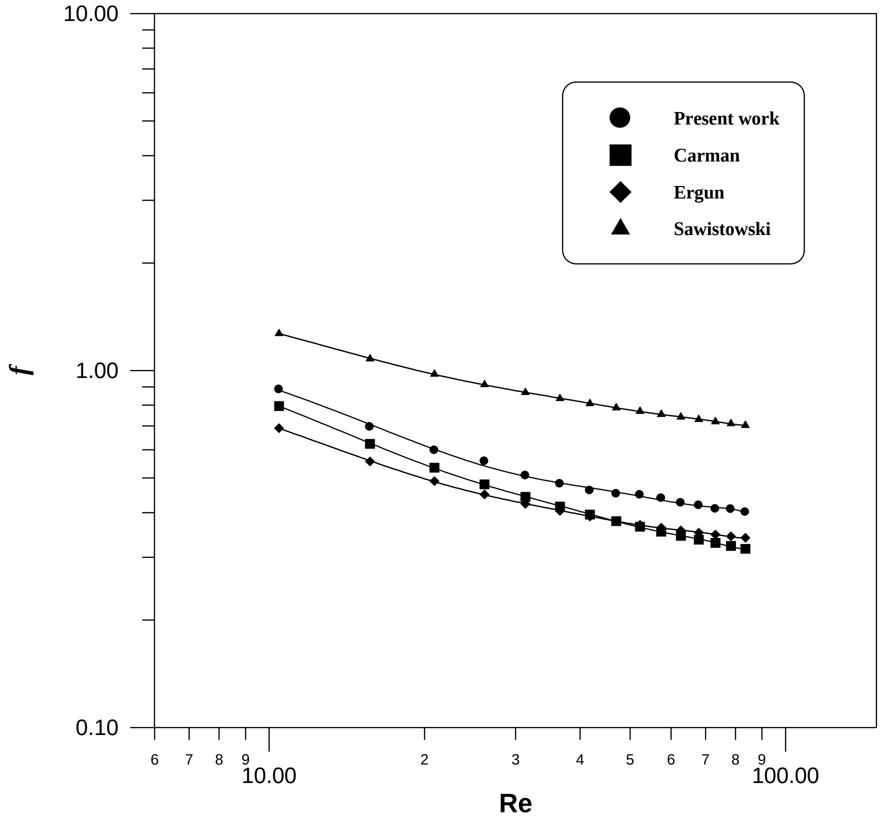

Figure 4.2 Friction factor versus Reynolds numbers for particles diameter of 0.51 cm and porosity of 0.3999 (Appendix A.2)

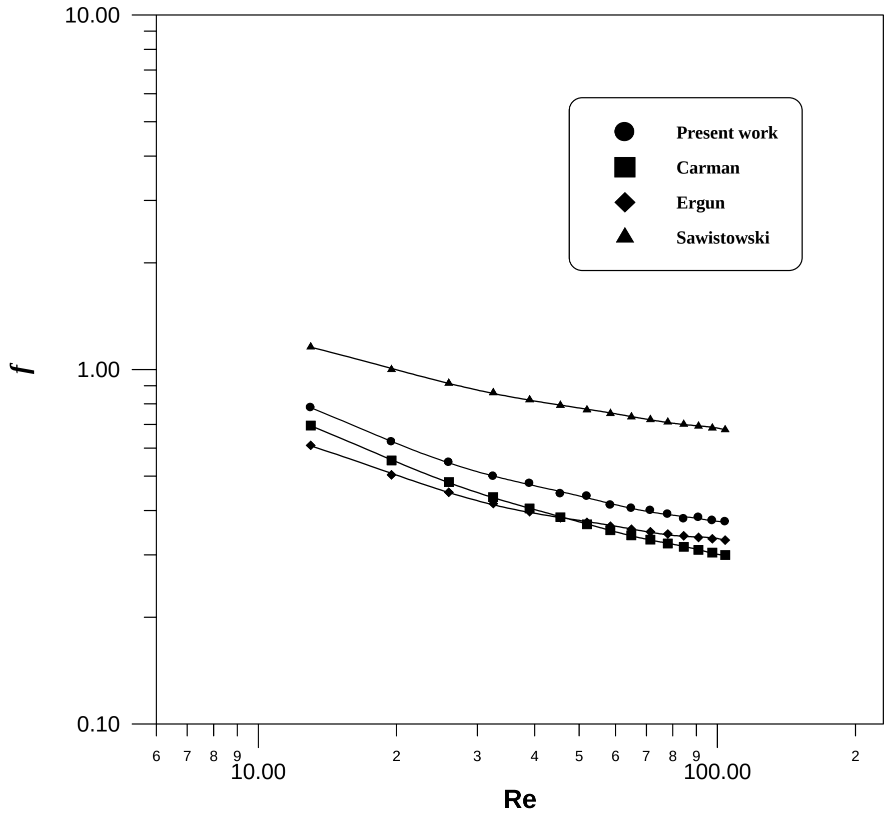

Figure 4.3 Friction factor versus Reynolds numbers for particles diameter of 0.61 cm and porosity of 0.4112 (Appendix A.3)

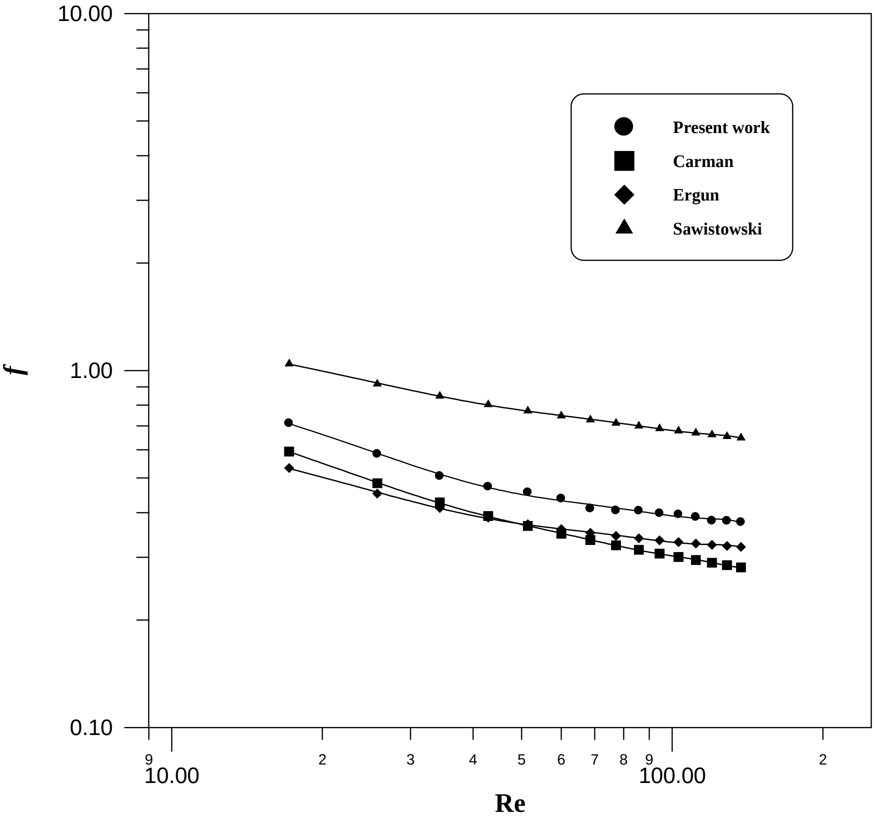

Figure 4.4 Friction factor versus Reynolds numbers for particles diameter of 0.79 cm and porosity of 0.4225 (Appendix A.4)

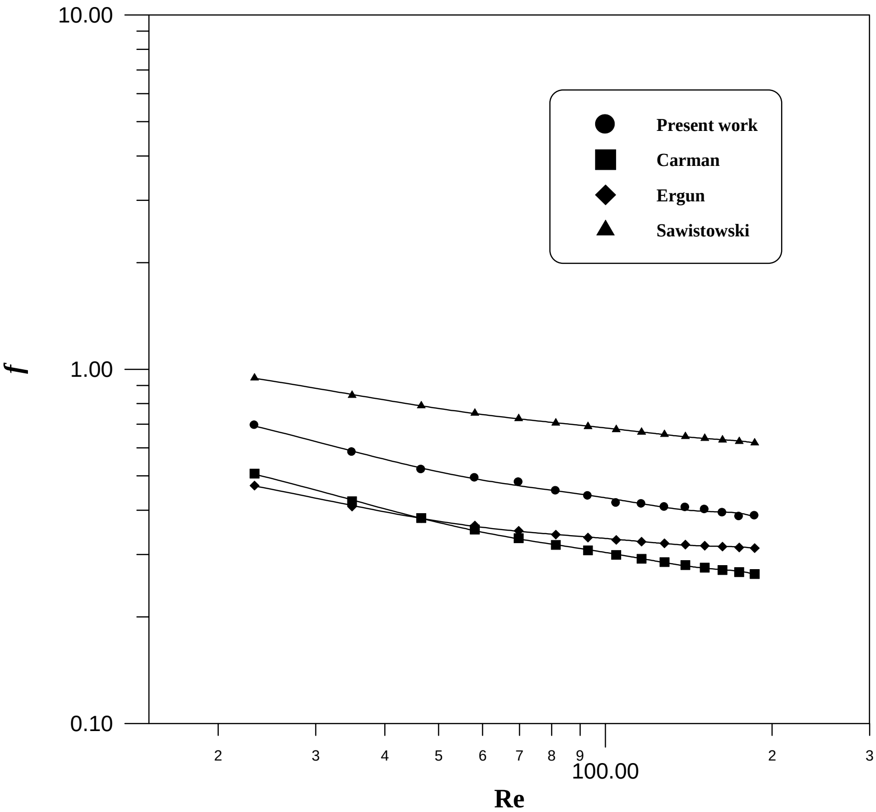

Figure 4.5 Friction factor versus Reynolds numbers for particles diameter of 1.01 cm and porosity of 0.4359 (Appendix A.5)

The wall affects the bed porosity and increases its value. This appears in Fig. 4.5 where the bed porosity increases to a value of 0.4359, this wall effect may be due to the ratio of bed diameter (7.62cm) to the particles diameter (1.01 cm) which is less than the supposed ratio (column diameter to the particle diameter should be greater than 10:1) [22].

Examining Figs. 4.1 to 4.5 show that the values of friction factor of Fig. 4.1 decrease sharply with increasing Reynolds numbers while that of Fig. 4.5 decrease slightly with increasing Reynolds number, because the fluid flow of Fig. 4.1 is at the laminar and transition regions (where the friction factor-Reynolds number curve is of slope of -1) while the fluid flow of Fig. 4.5 is at the transition and turbulent regions (where the friction factor-Reynolds number curve become straighter) [8].

The best fitting of the experimental results for air flow through beds of mono-sizes particles is represented by the following equation.

$$f = 4.43\,\mathrm{Re}_1^{-1} + 0.55\,\mathrm{Re}_1^{-0.1} \qquad \text{... (4.1)}$$

With the correlation coefficient is 0.9742 and percentage of average errors is 4.66 %.

4.1.2 Water flow

The friction factor values of water flow through beds of mono sizes particles are plotted versus Reynolds numbers in Figs. 4.6 to 4.10.

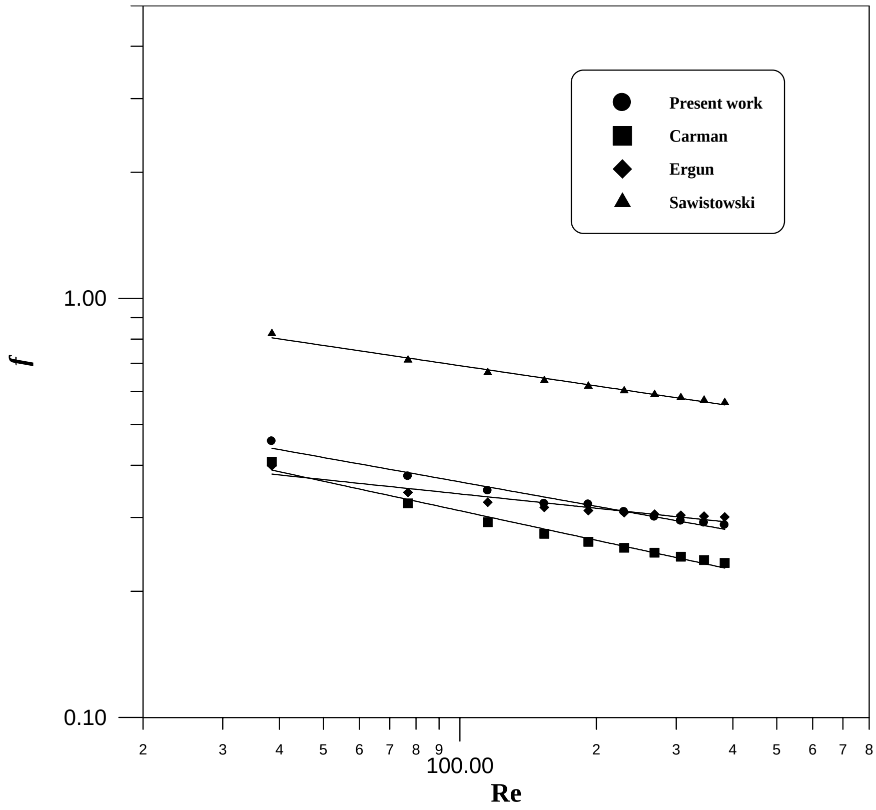

Figure 4.6 Friction factor versus Reynolds numbers for particles diameter of 0.42 cm and porosity of 0.3793 (Appendix B.1)

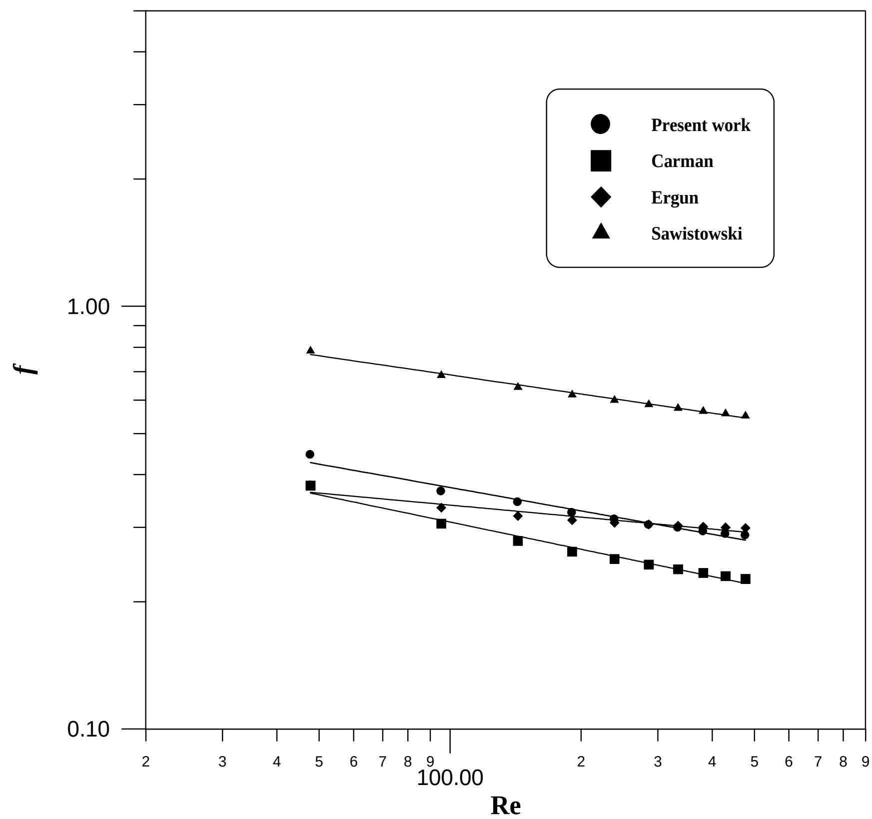

Figure 4.7 Friction factor versus Reynolds numbers for particles diameter of 0.51 cm and porosity of 0.4051 (Appendix B.2)

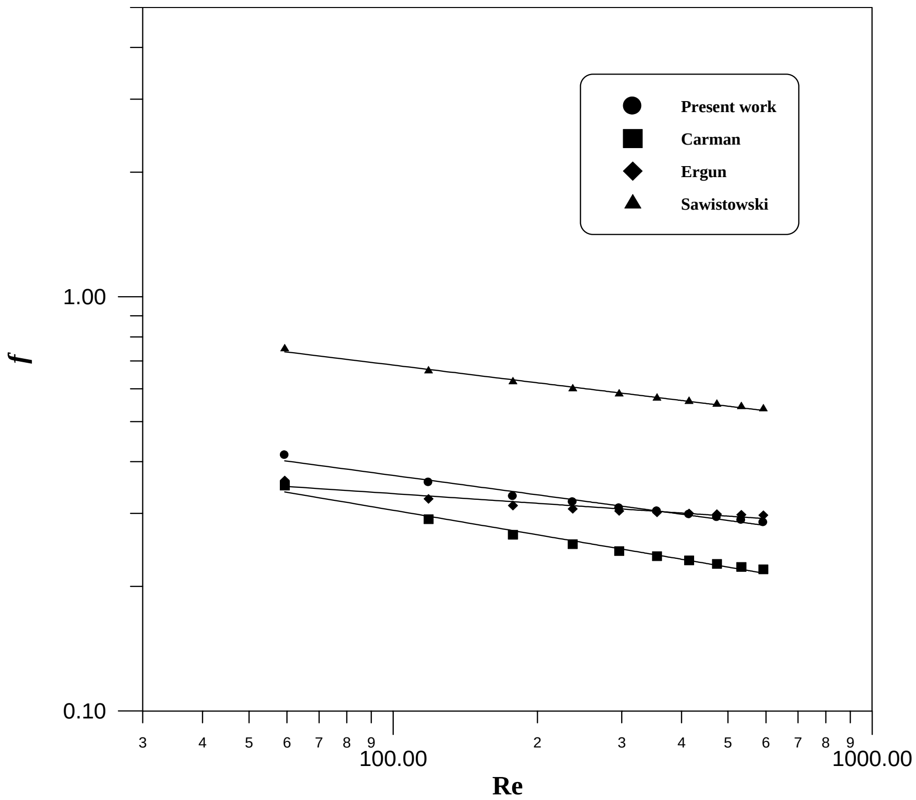

Figure 4.8 Friction factor versus Reynolds numbers for particles diameter of 0.61 cm and porosity of 0.4156 (Appendix B.3)

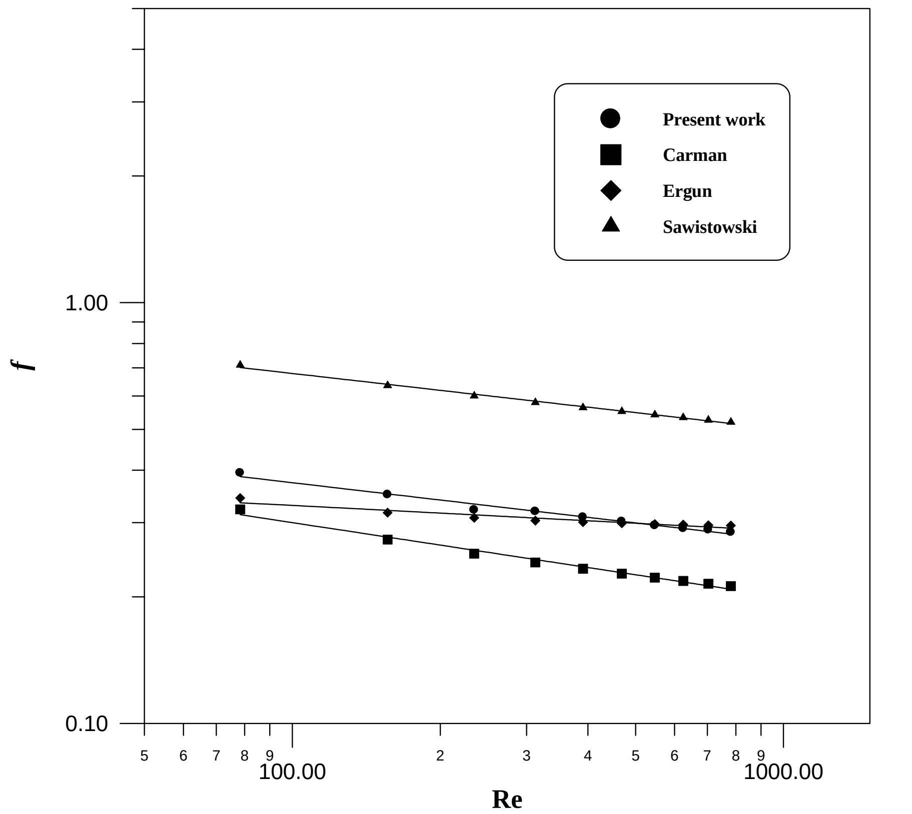

Figure 4.9 Friction factor versus Reynolds numbers for particles diameter of 0.79 cm and porosity of 0.4265 (Appendix B.4)

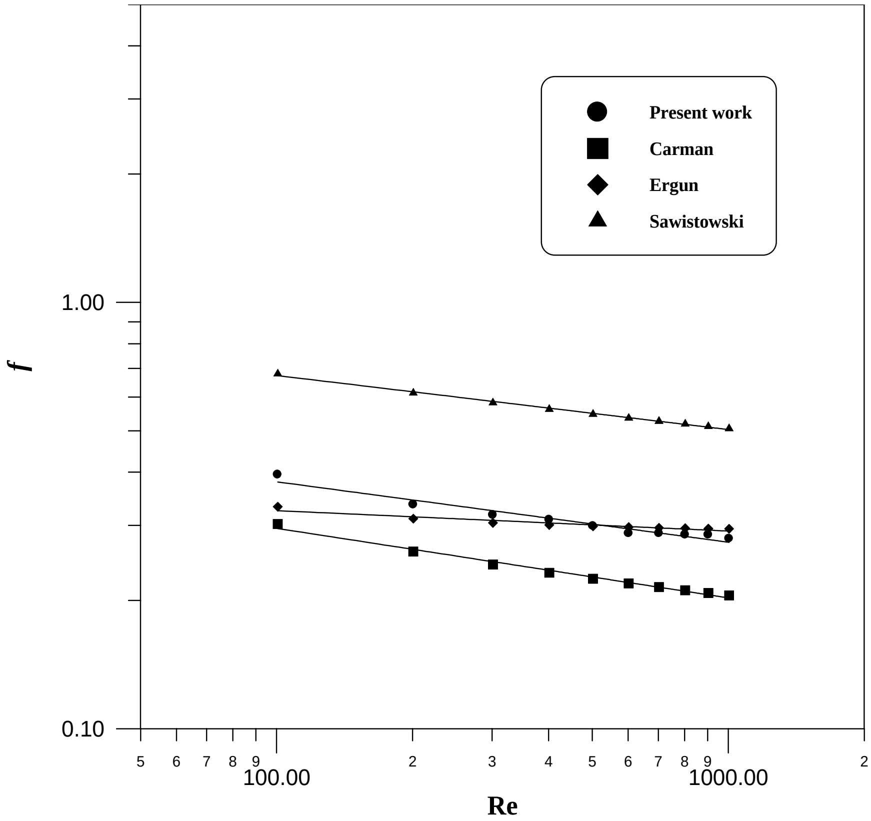

Figure 4.10 Friction factor versus Reynolds numbers for particles diameter of 1.01 cm and porosity of 0.4321 (Appendix B.5)

Figures 4.6 to 4.10 show that as the particle size increases from 0.42 to 1.01 cm, the bed porosity increase from 0.3793 to 0.4321 and the Reynolds number values increase from the range of 38.5- 384.2 (Fig. 4.6) to the range of 100.5-1004.0 (Fig. 4.10) which lead to decrease in the friction factor values from the range of 0.456-0.288 (Fig. 4.6) to the range of 0.394-0.279 (Fig. 4.10).

The best fitting of the experimental results for water flow through beds of mono-sizes particles is represented by the following equation.

$$f = 3.51 \mathrm{Re}_1^{-1} + 0.53 \mathrm{Re}_1^{-0.1} \qquad \text{... (4.2)}$$

With the correlation coefficient is 0.97406 and percentage of average errors is 2.44%.

Comparison the results of air and water flow shows that the values of water flow friction factor are close to those of air flow for approximately near values of Reynolds numbers and bed porosities, e.g., at near values of Reynolds number 38.5 (Fig. 4.6) and 37.9 (Fig. 4.1), the friction factor values are 0.456 (Fig. 4.6) and 0.470 (Fig. 4.1) approximately close to each other.

4.2 Packing of binary sizes particles

4.2.1 Air flow

The values of air flow friction factors through beds of binary sizes particles are plotted versus Reynolds numbers as shown in Figs 4.11 to 4.20.

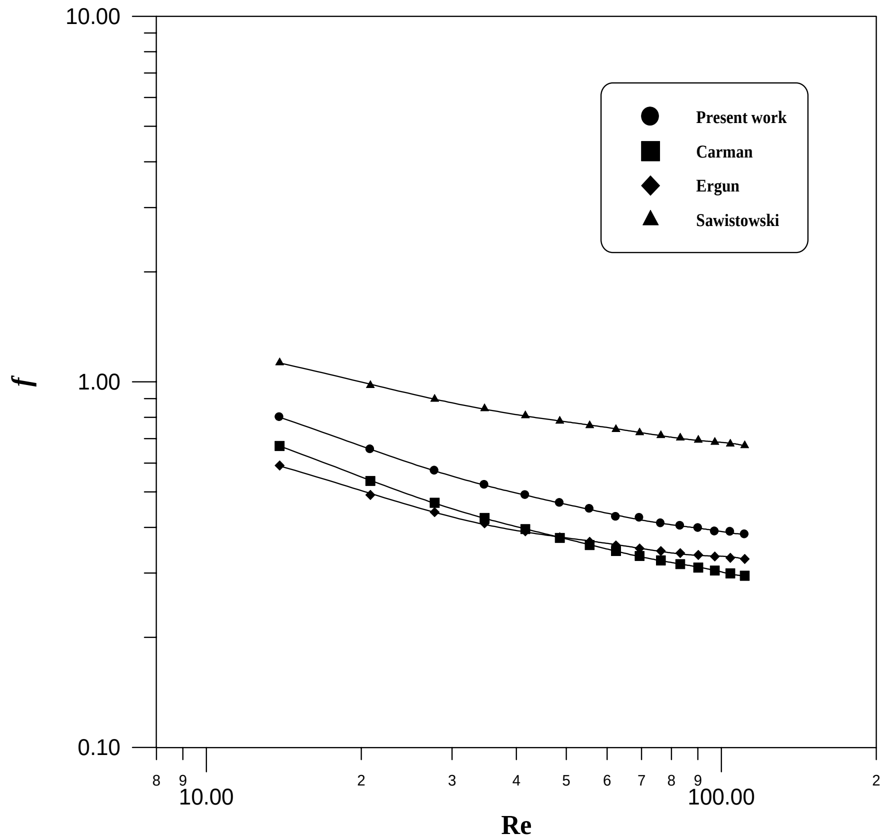

Figure 4.11 Friction factor versus Reynolds numbers for bed with particles diameters of 0.42 and 0.51 cm and porosity of 0.3577 (Appendix A.6)

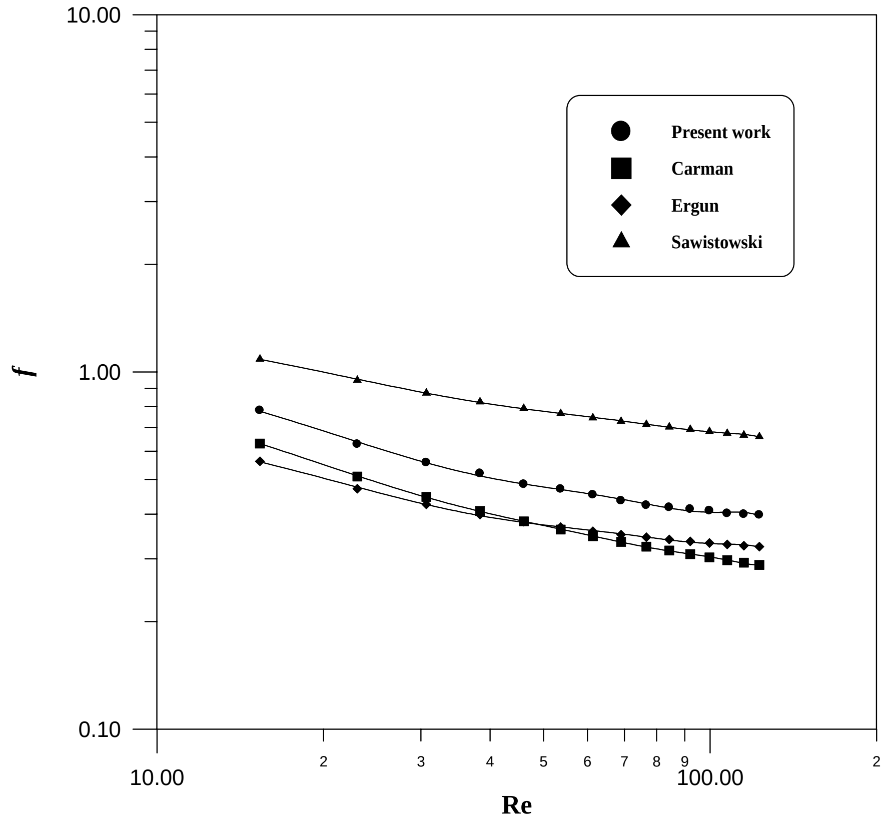

Figure 4.12 Friction factor versus Reynolds numbers for bed with particles diameters of 0.42 and 0.61 cm and porosity of 0.3622 (Appendix A.7)

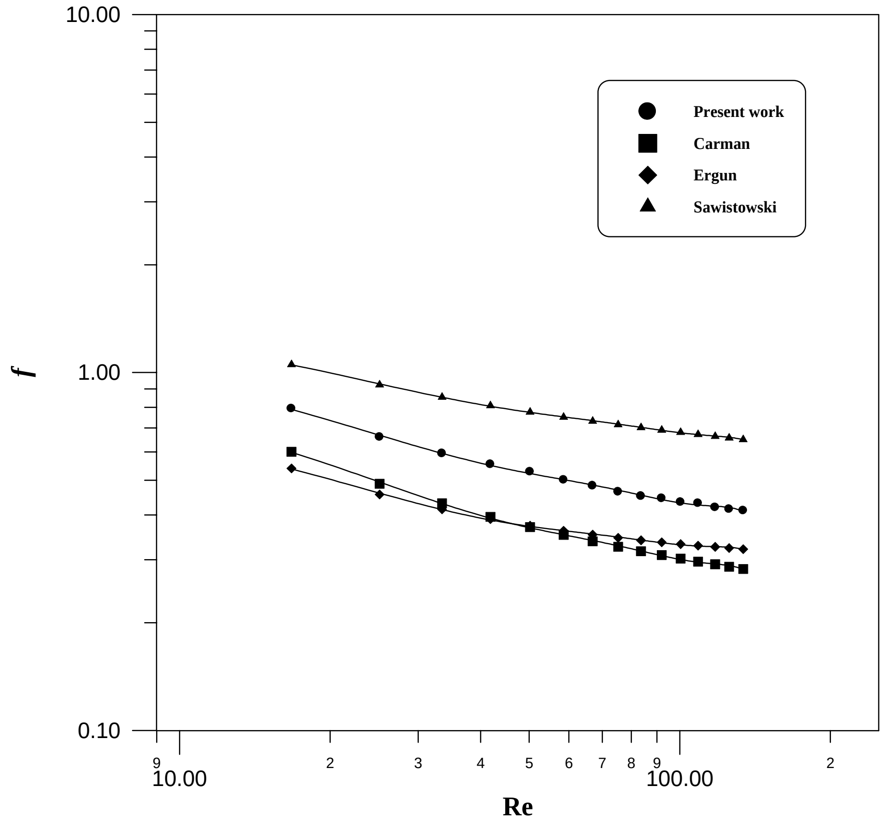

Figure 4.13 Friction factor versus Reynolds numbers for bed with particles

diameters of 0.42 and 0.79 cm and porosity of 0.3589 (Appendix A.8)

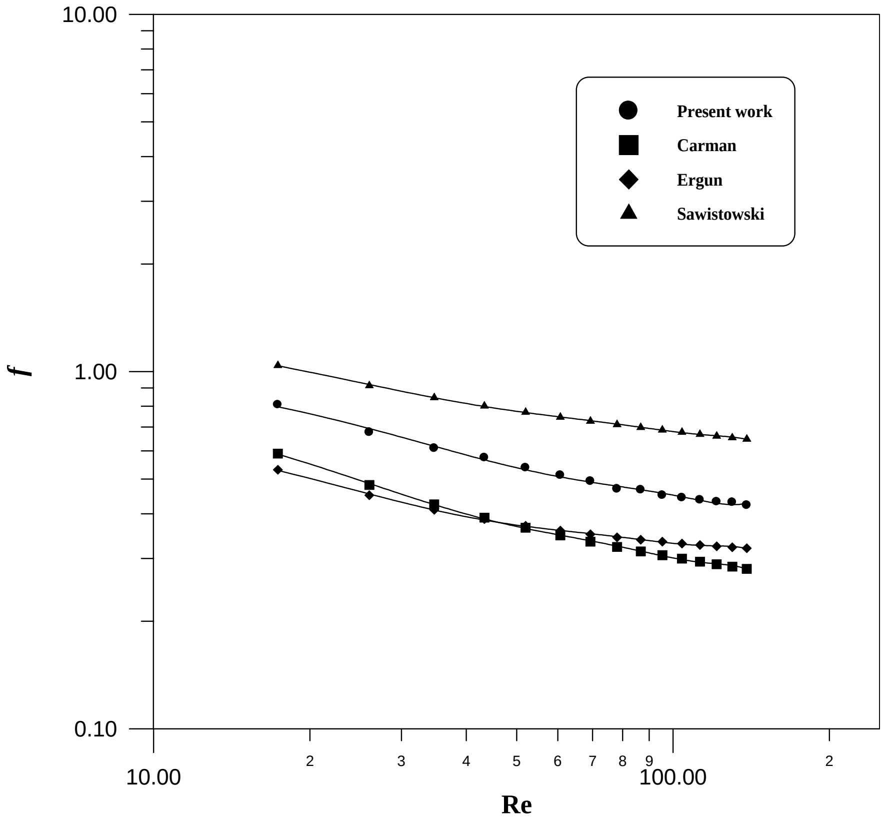

Figure 4.14 Friction factor versus Reynolds numbers for bed with particles diameters of 0.42 and 1.01 cm and porosity of 0.3455 (Appendix A.9)

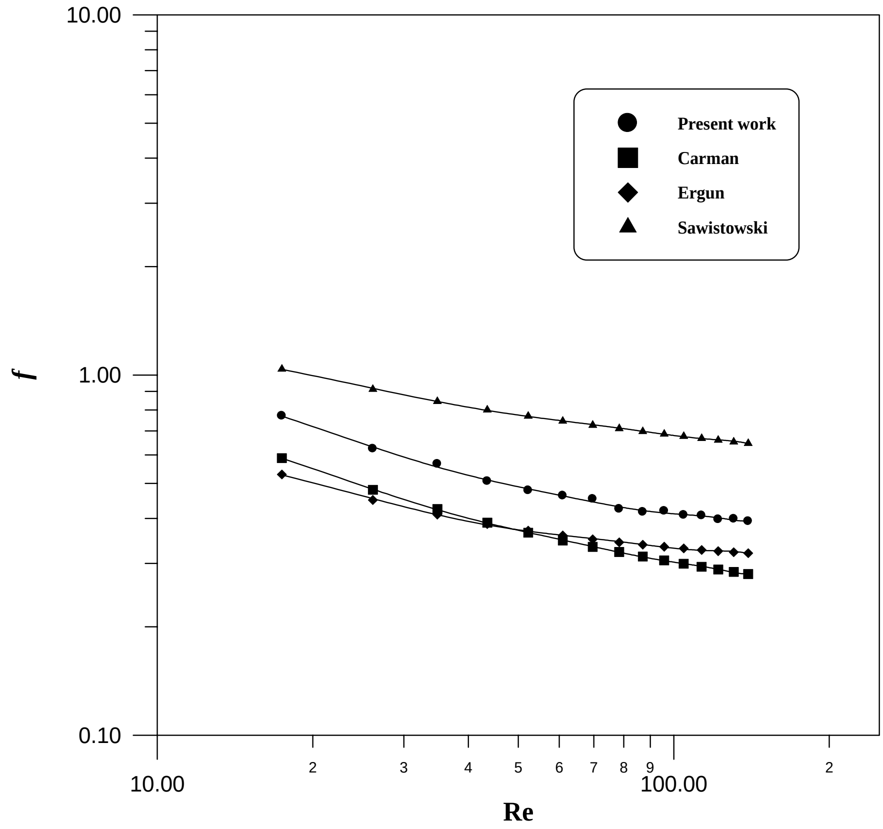

Figure 4.15 Friction factor versus Reynolds numbers for bed with particles diameters of 0.51 and 0.61 cm and porosity of 0.3709 (Appendix A.10)

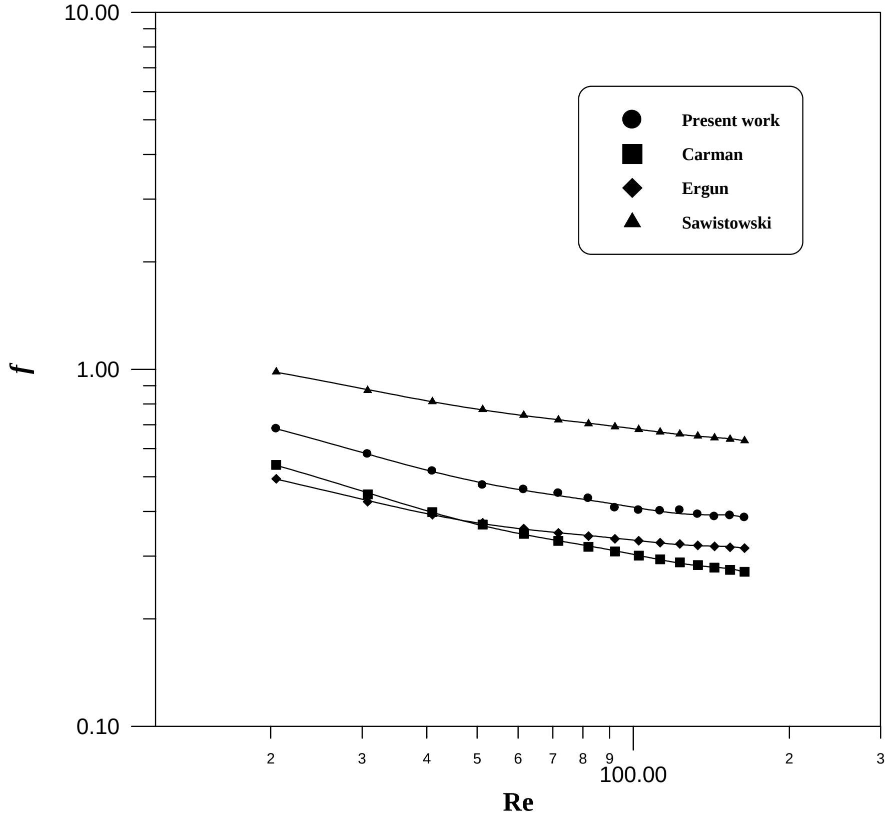

Figure 4.16 Friction factor versus Reynolds numbers for bed with particles diameters of 0.51 and 0.79 cm and porosity of 0.3879 (Appendix A.11)

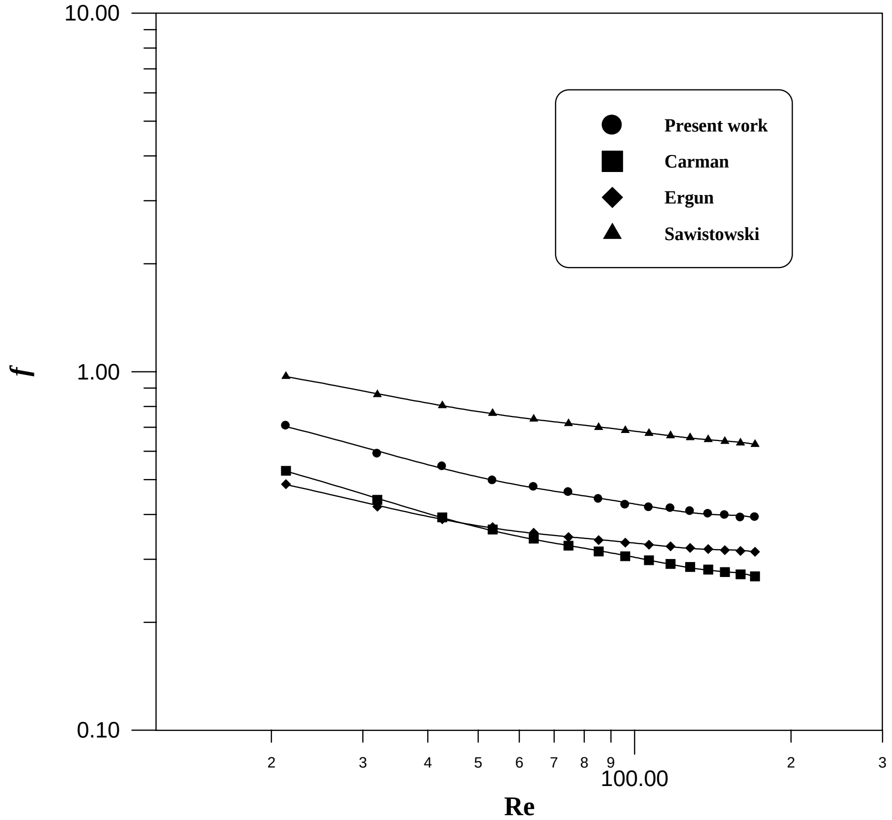

Figure 4.17 Friction factor versus Reynolds numbers for bed with particles diameters of 0.51 and 1.01 cm and porosity of 0.3733 (Appendix A.12)

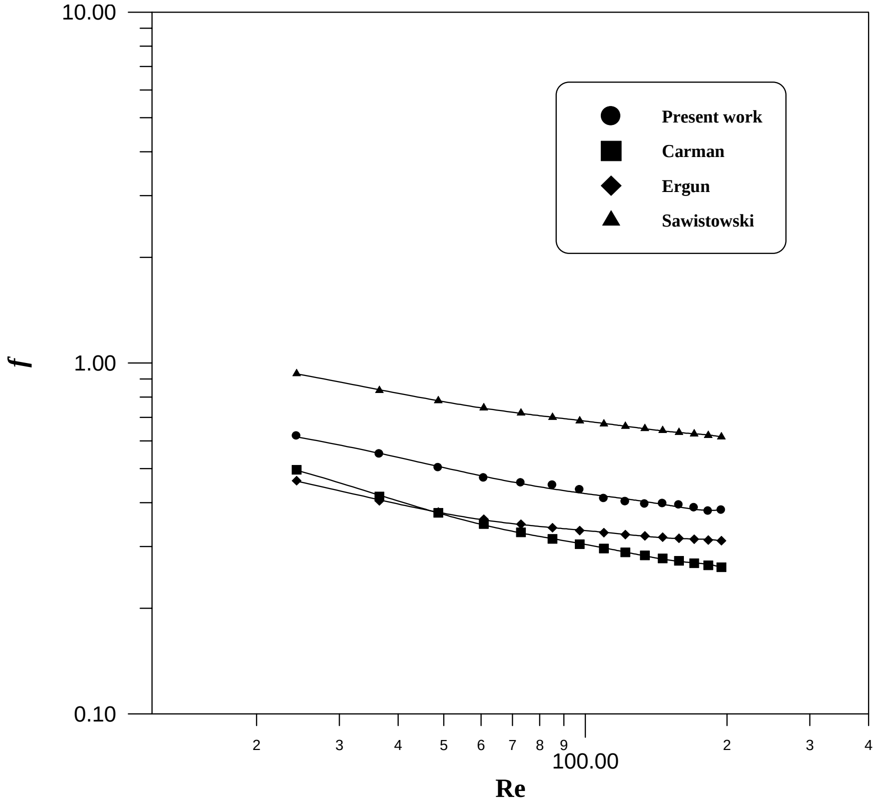

Figure 4.18 Friction factor versus Reynolds numbers for bed with particles diameters of 0.61 and 0.79 cm and porosity of 0.4042 (Appendix A.13)

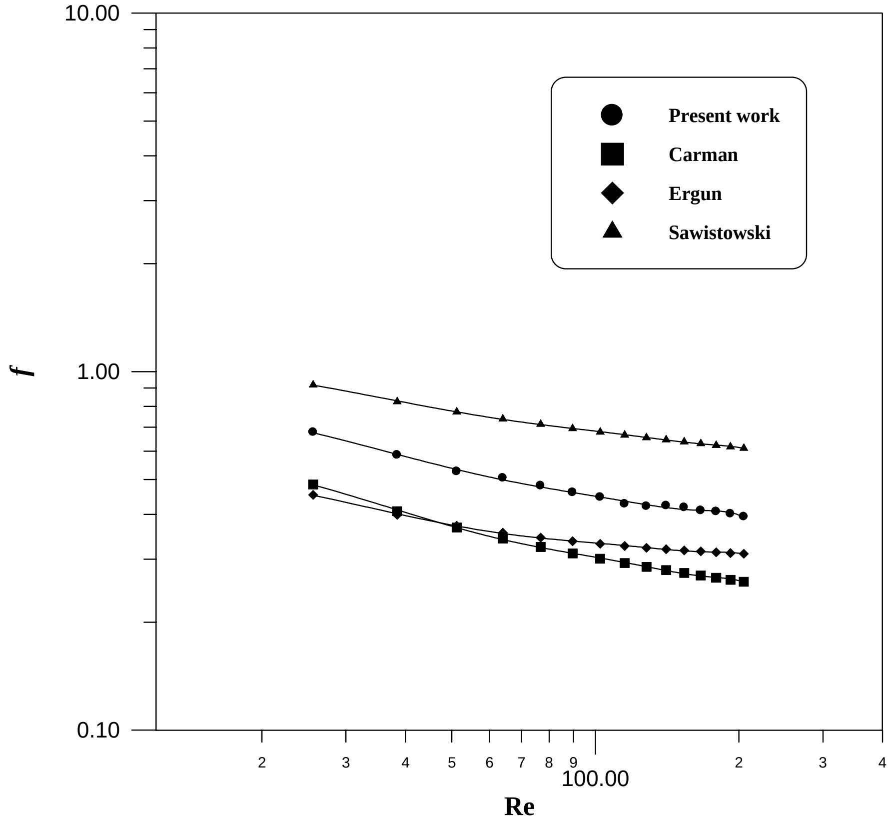

Figure 4.19 Friction factor versus Reynolds numbers for bed with particles diameters of 0.61 and 1.01cm and porosity of 0.3901 (Appendix A.14)

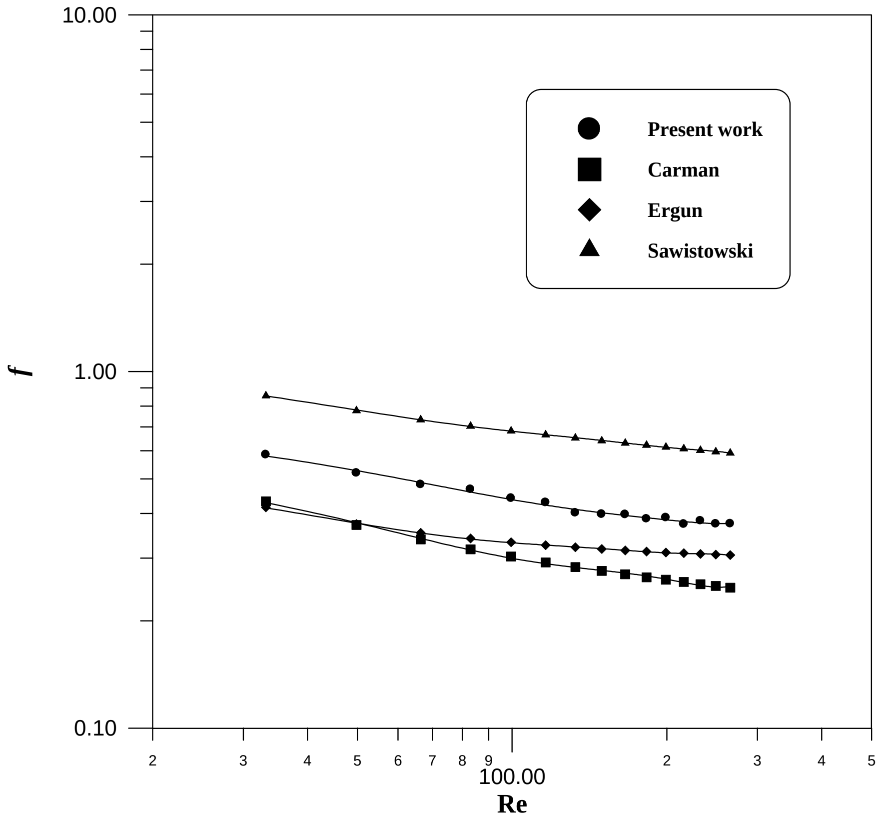

Figure 4.20 Friction factor versus Reynolds numbers for bed with particles diameters of 0.79 and 1.01cm and porosity of 0.4220 (Appendix A.15)

It can be noticed that the values of friction factor of binary sizes system are less than those of mono sizes system for approximately near values of bed porosity. For example, Fig. 4.17 (binary system) shows that the values of friction factor range from 0.707 to 0.393 are less than those of Fig. 4.1 (mono system) which range from 0.992 to 0.412, because the values of Reynolds number of this binary size system which range from 21.3 to 170.6 are greater than those of mono size system which range from 8.4 to 67.4 (at the same volumetric flow from 2 to 16 m^3/hr). This is due to the fact that the contacting surface area of this binary size system (561.95 m^{-1}) is less than it of mono size system (1425.178 m^{-1}).

As the flow rate of fluid increases the pressure drop across the bed increases, e.g., table A.6 shows that the pressure drop values increase from 38.5 to 1178.7 Pa with increasing the fluid rate from 2 to 16m^3/h [19].

The best fitting of the experimental results for air flow through beds of binary-sizes particles is represented by the following equation.

$$f = 5.22\,\mathrm{Re}_1^{-1} + 0.59\,\mathrm{Re}_1^{-0.1} \qquad \text{... (4.3)}$$

With the correlation coefficient is 0.9710 and percentage of average errors is 3.89%.

4.2.2 Water flow

The values of water flow friction factors are plotted versus Reynolds numbers as shown in Figs. 4.21 to 4.30.

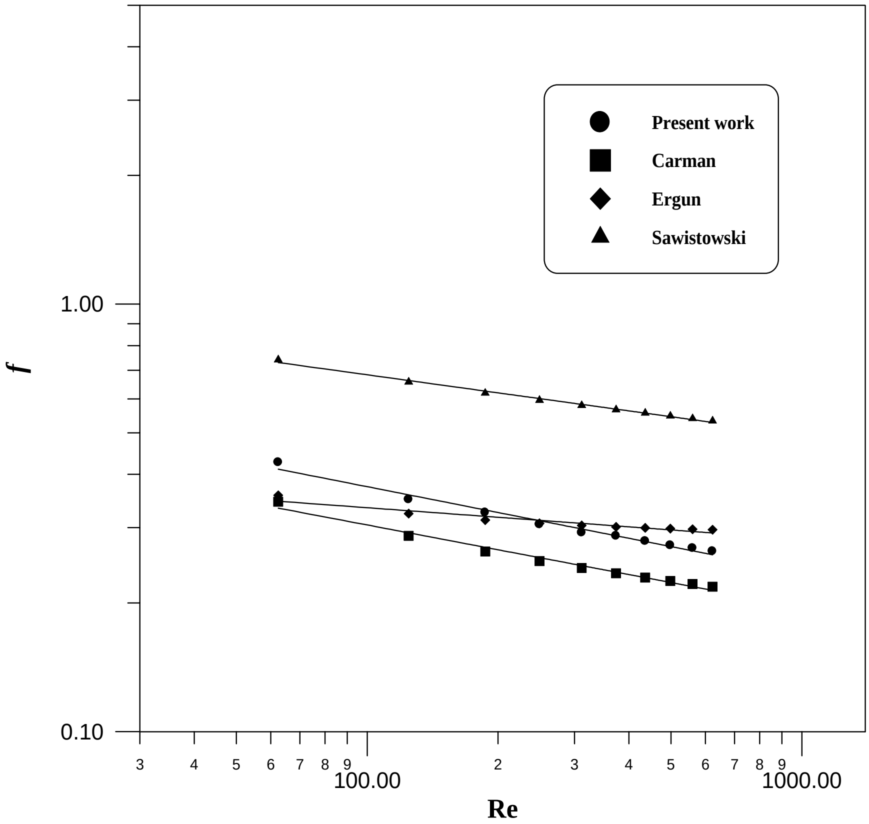

Figure 4.21 Friction factor versus Reynolds numbers for bed with particles diameters of 0.42 and 0.51 cm and porosity of 0.3551 (Appendix B.6)

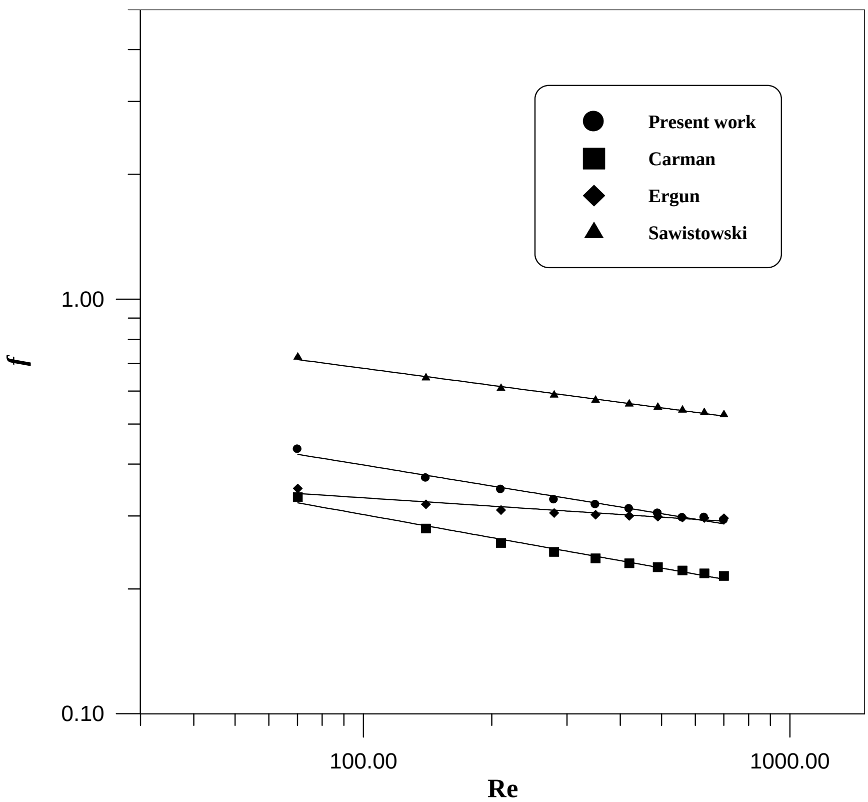

Figure 4.22 Friction factor versus Reynolds numbers for bed with particles

diameters of 0.42 and 0.61 cm and porosity of 0.3650 (Appendix B.7)

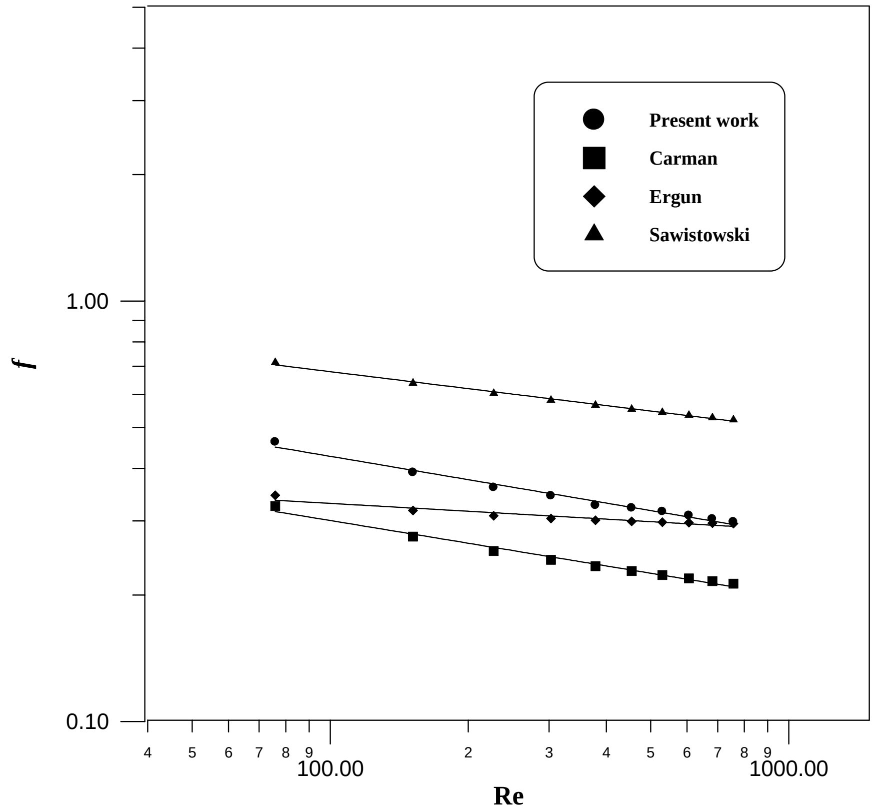

Figure 4.23 Friction factor versus Reynolds numbers for bed with particles diameters of 0.42 and 0.79 cm and porosity of 0.3590 (Appendix B.8)

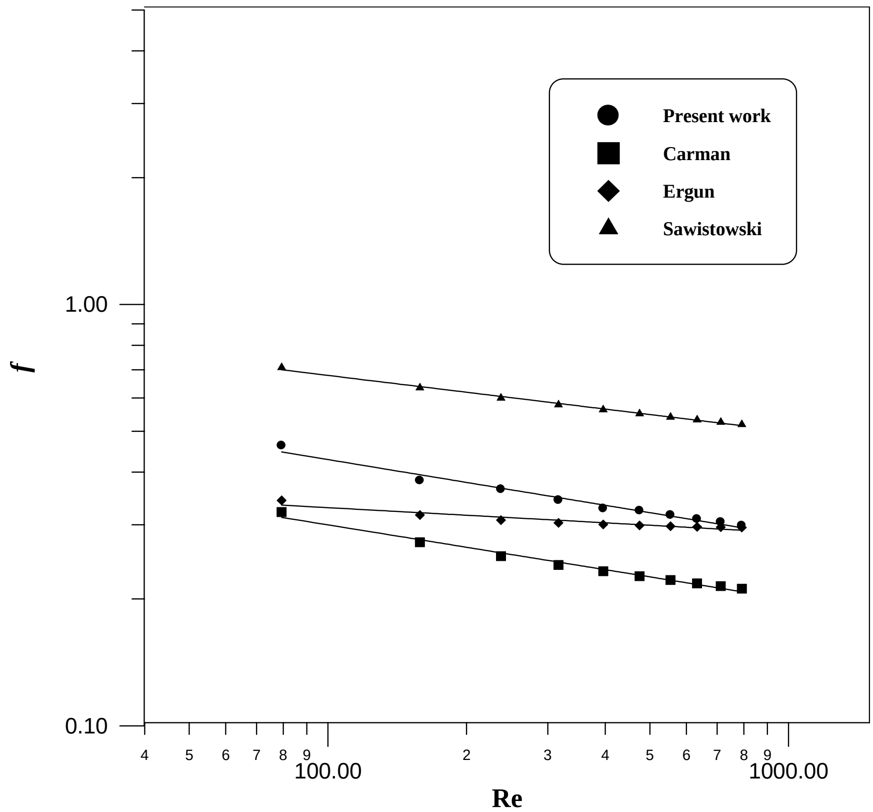

Figure 4.24 Friction factor versus Reynolds numbers for bed with particles

diameters of 0.42 and 1.01 cm and porosity of 0.3484 (Appendix B.9)

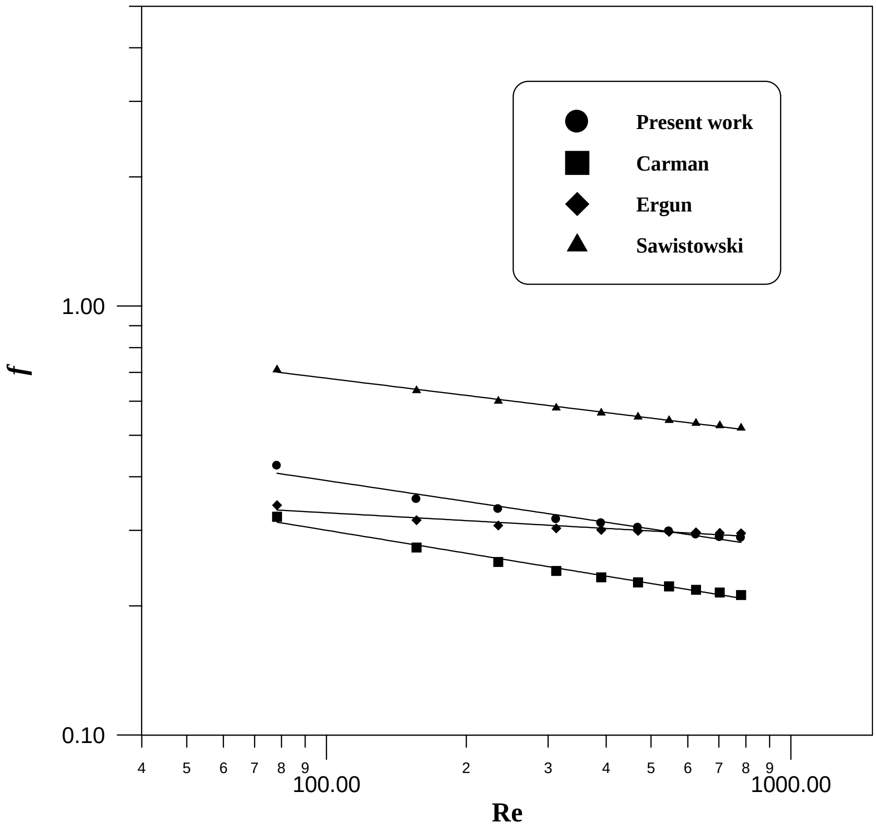

Figure 4.25 Friction factor versus Reynolds numbers for bed with particles diameters of 0.51 and 0.61 cm and porosity of 0.3681 (Appendix B.10)

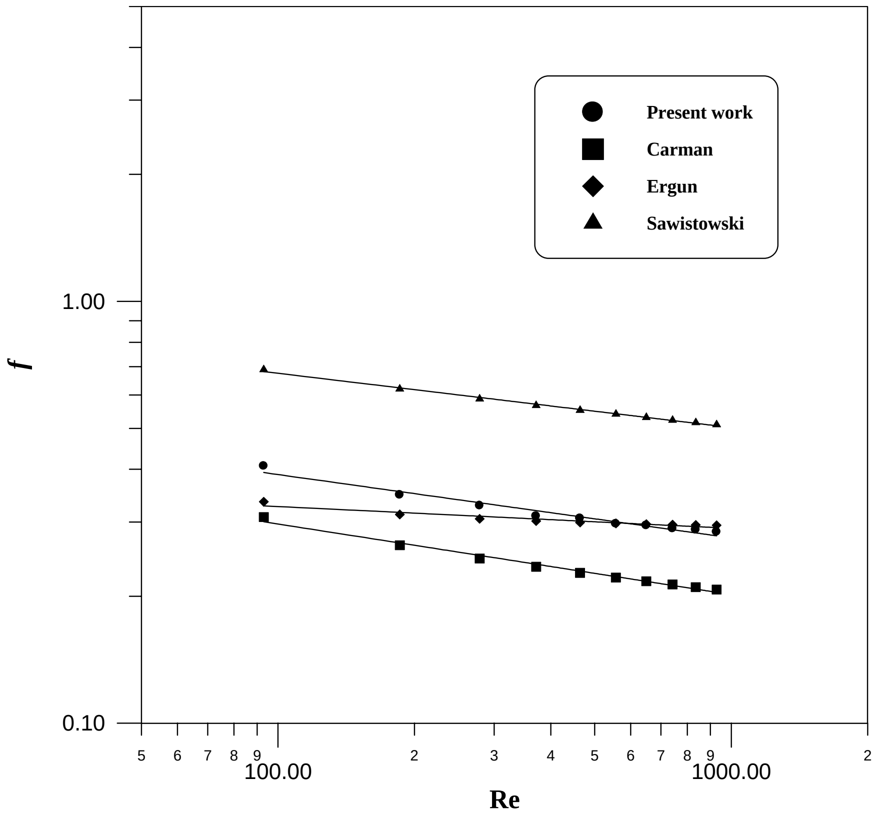

Figure 4.26 Friction factor versus Reynolds numbers for bed with particles diameters of 0.51 and 0.79 cm and porosity of 0.3882 (Appendix B.11)

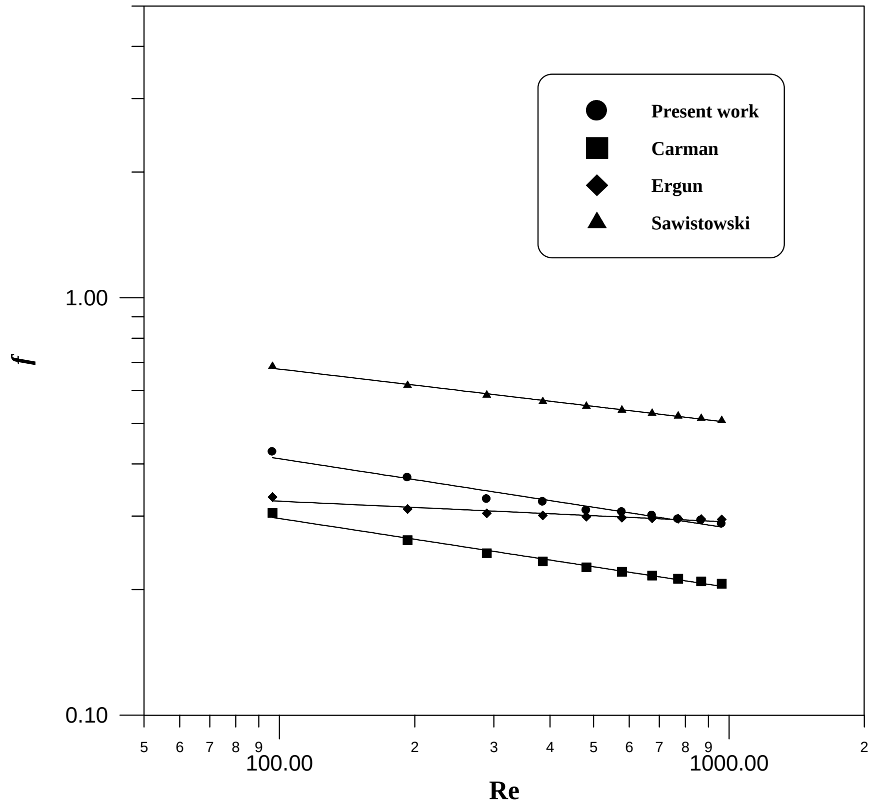

Figure 4.27 Friction factor versus Reynolds numbers for bed with particles diameters of 0.51 and 1.01 cm and porosity of 0.3730 (Appendix B.12)

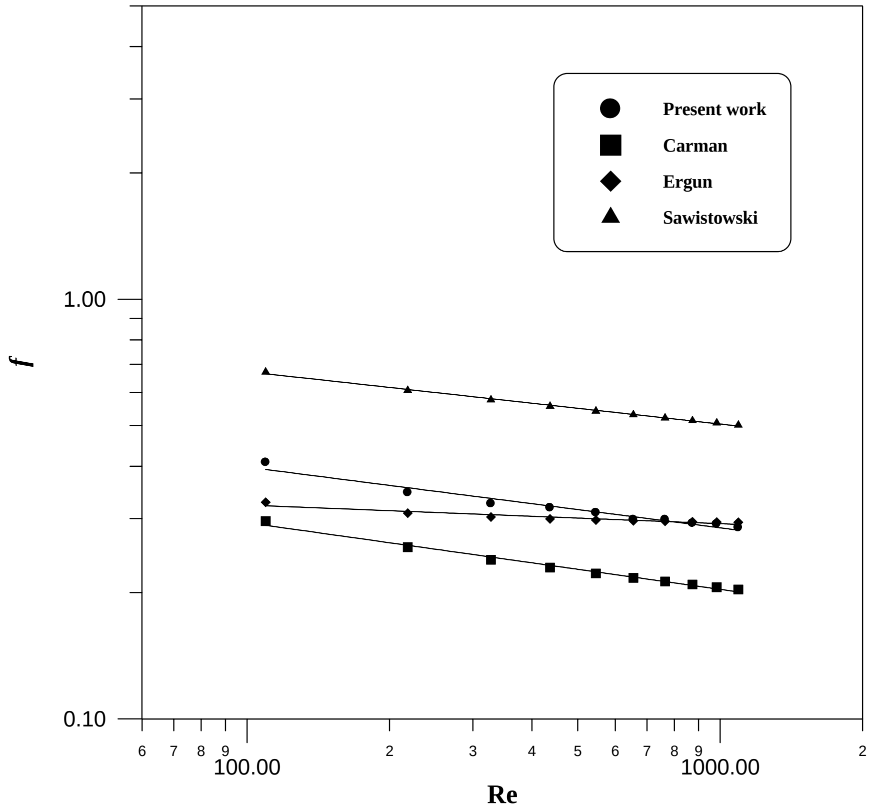

Figure 4.28 Friction factor versus Reynolds numbers for bed with particles diameters of 0.61 and 0.79 cm and porosity of 0.4019 (Appendix B.13)

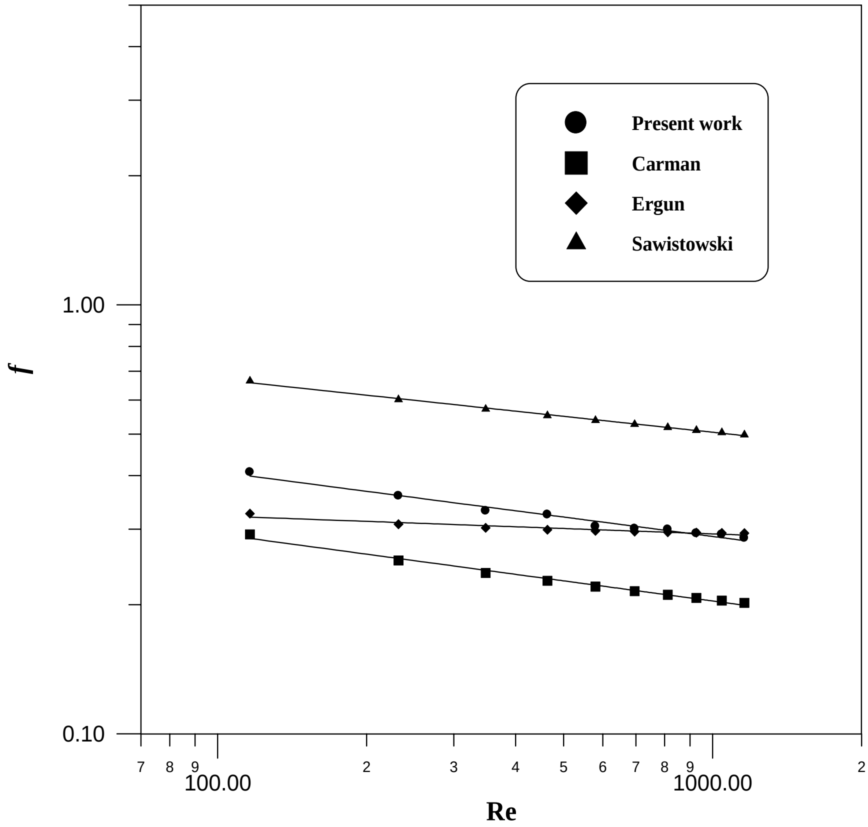

Figure 4.29 Friction factor versus Reynolds numbers for bed with particles diameters of 0.61 and 1.01cm and porosity of 0.3904 (Appendix B.14)

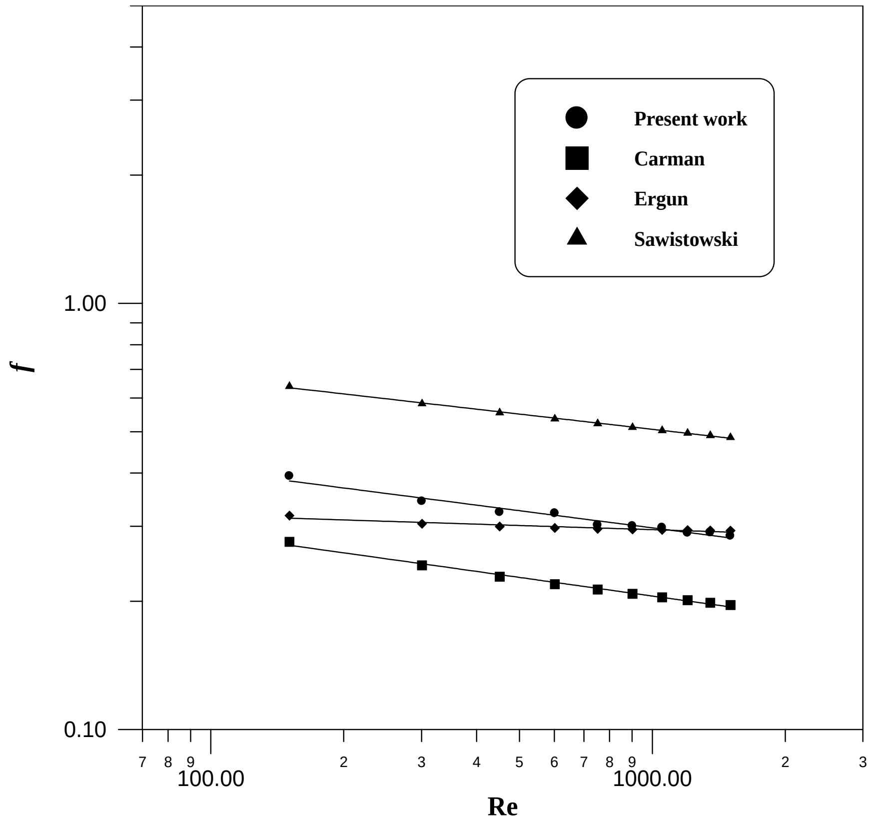

Figure 4.30 Friction factor versus Reynolds numbers for bed with particles diameters of 0.79 and 1.01cm and porosity of 0.4223 (Appendix B.15)

The porosities of binary size systems are less than those of mono size systems, because for binary system the particles with smaller sizes tend to fill the void spaces between the larger sizes particles [5].

Comparison of the results of air and water flow show that the values of water flow pressure drop are greater than those of air flow, because the physical properties of water (density and viscosity) are greater than those of air, e.g., the pressure drop values of table B.13 (water flow) which range from 5.69 to 31.9kPa are greater than those of table A.13 (air flow) which range from 12.6 to 59.7 Pa at the same fluid velocity (0.1218-.3046 m/s).

The best fitting of the experimental results for water flow through beds of binary-sizes particles is represented by the following equation.

$$f = 5.56\,\mathrm{Re}_1^{-1} + 0.55\,\mathrm{Re}_1^{-0.1} \qquad \text{... (4.4)}$$

With the correlation coefficient is 0.9351 and percentage of average errors is 3.46%.

4.3 Packing of ternary sizes particles

4.3.1 Air flow

The values of air flow friction factors through beds of ternary sizes particles are plotted versus Reynolds numbers as shown in Figs 4.31 to 4.40.

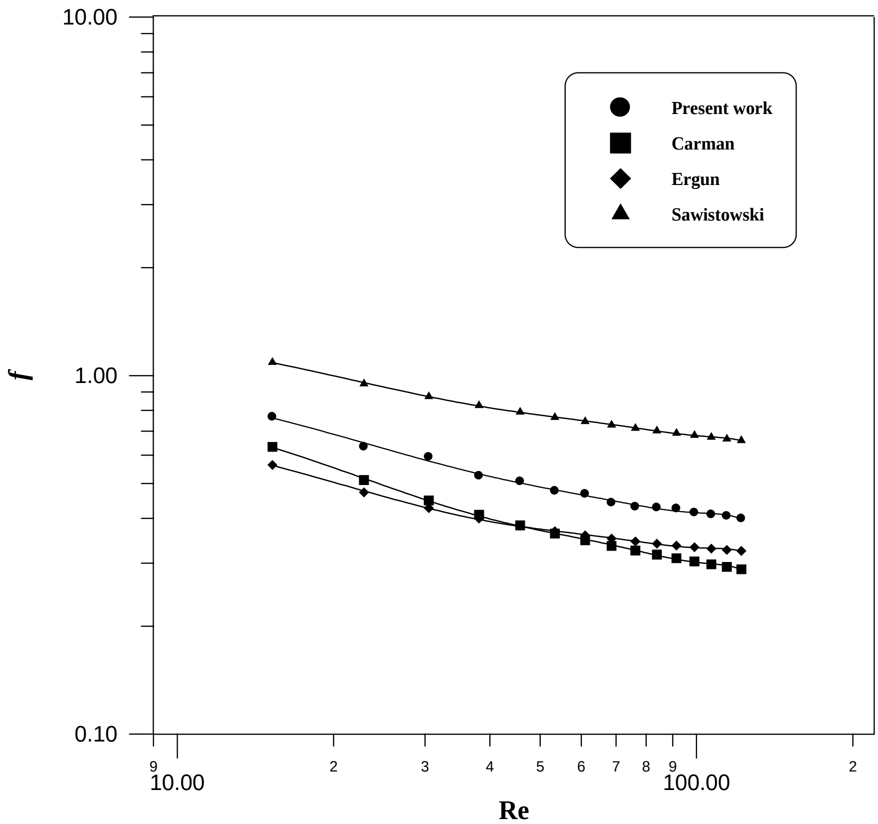

Figure 4.31 Friction factor versus Reynolds numbers for bed with particles diameters of 0.42, 0.51 and 0.61cm and porosity of 0.3598 (Appendix A.16)

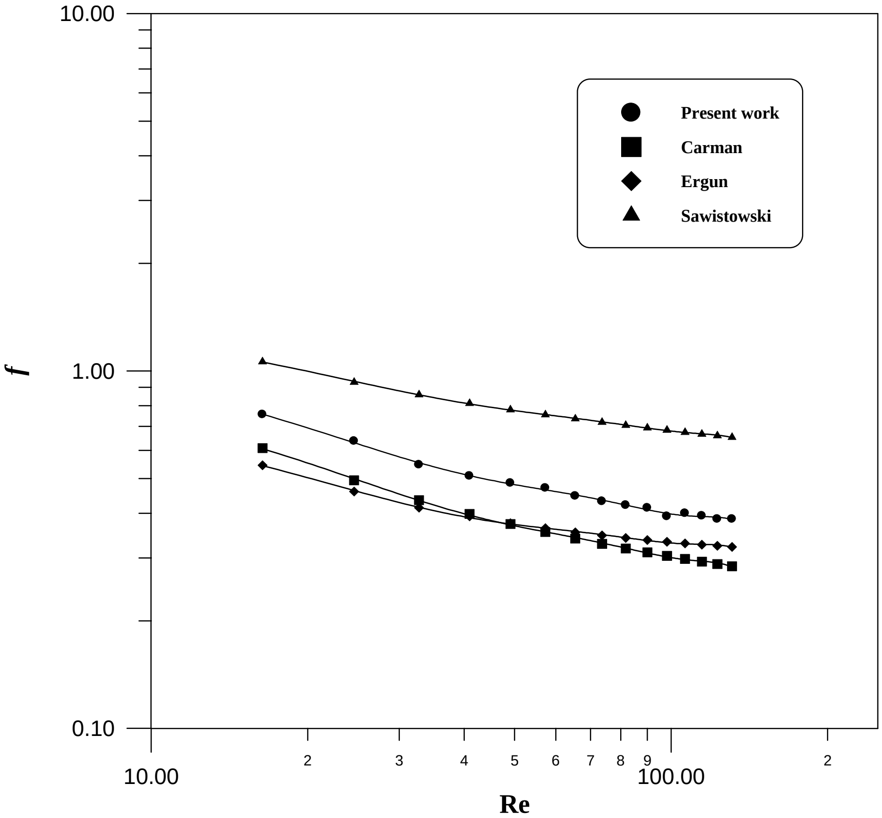

Figure 4.32 Friction factor versus Reynolds numbers for bed with particles diameters of 0.42, 0.51 and 0.79cm and porosity of 0.3620 (Appendix A.17)

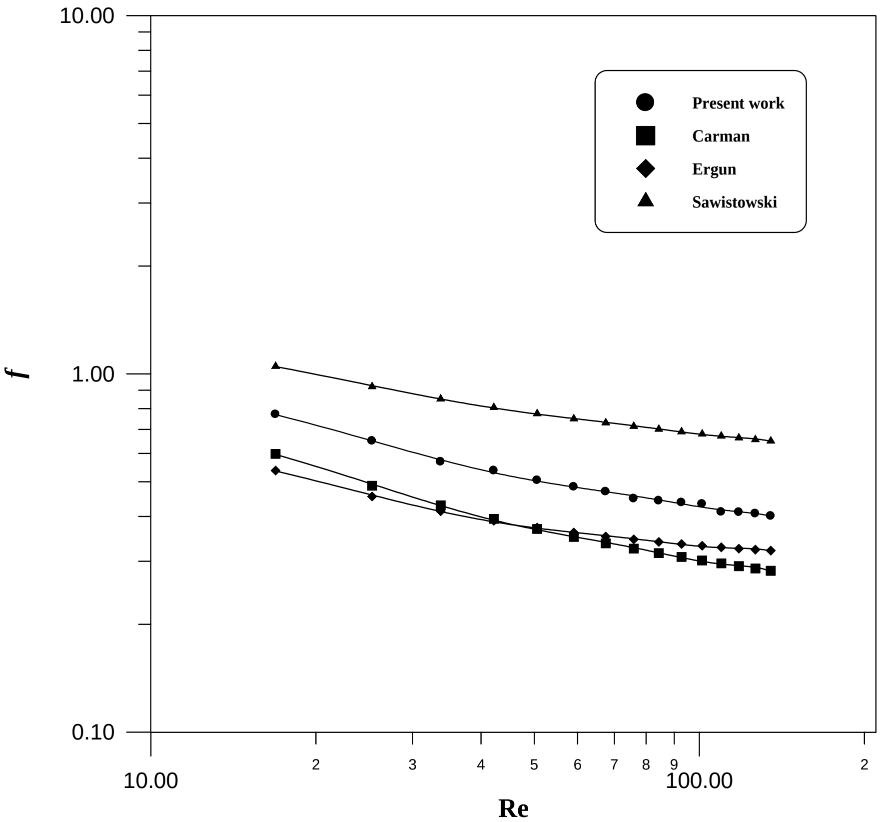

Figure 4.33 Friction factor versus Reynolds numbers for bed with particles diameters of 0.42, 0.51 and 1.01cm and porosity of 0.3561 (Appendix A.18)

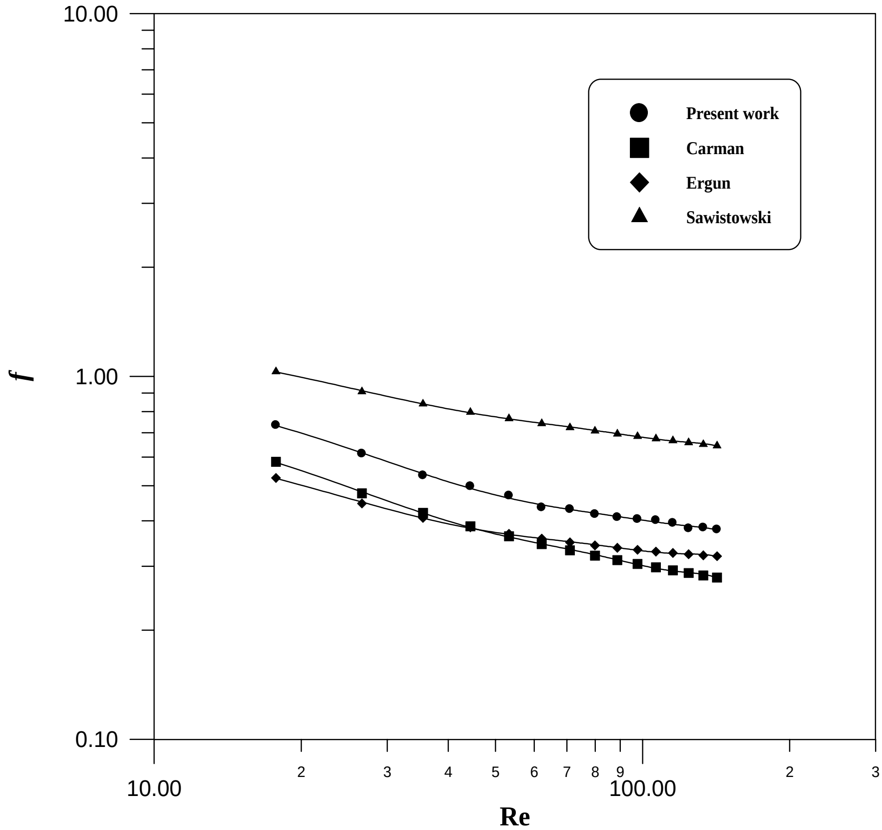

Figure 4.34 Friction factor versus Reynolds numbers for bed with particles diameters of 0.42, 0.61 and 0.79cm and porosity of 0.3668 (Appendix A.19)

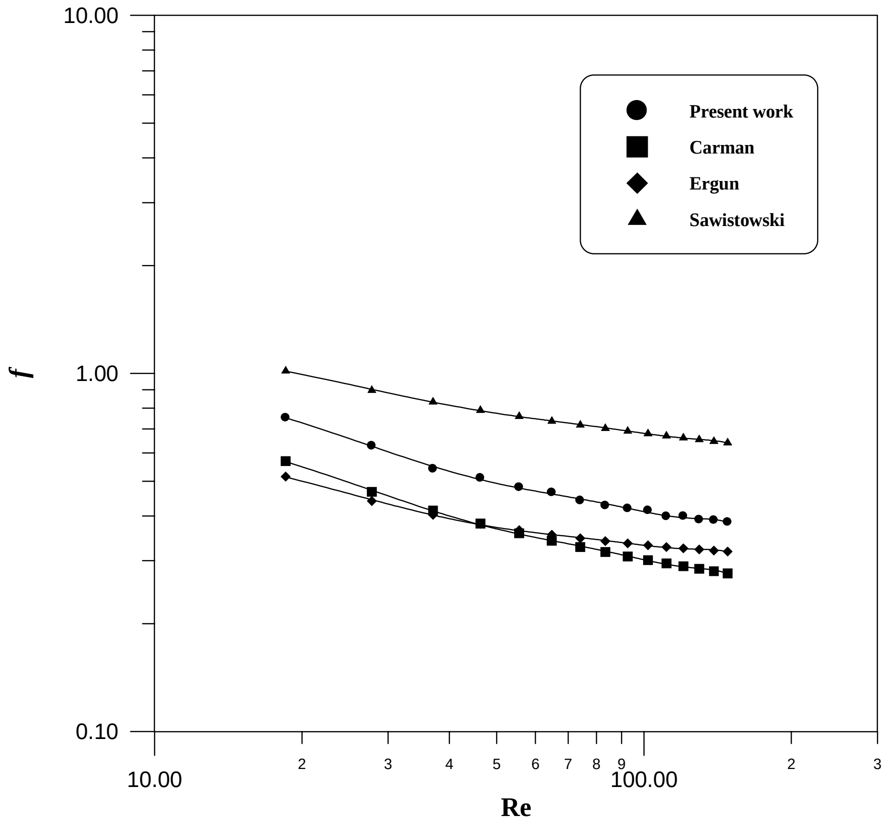

Figure 4.35 Friction factor versus Reynolds numbers for bed with particles diameters of 0.42, 0.61 and 1.01cm and porosity of 0.3636 (Appendix A.20)

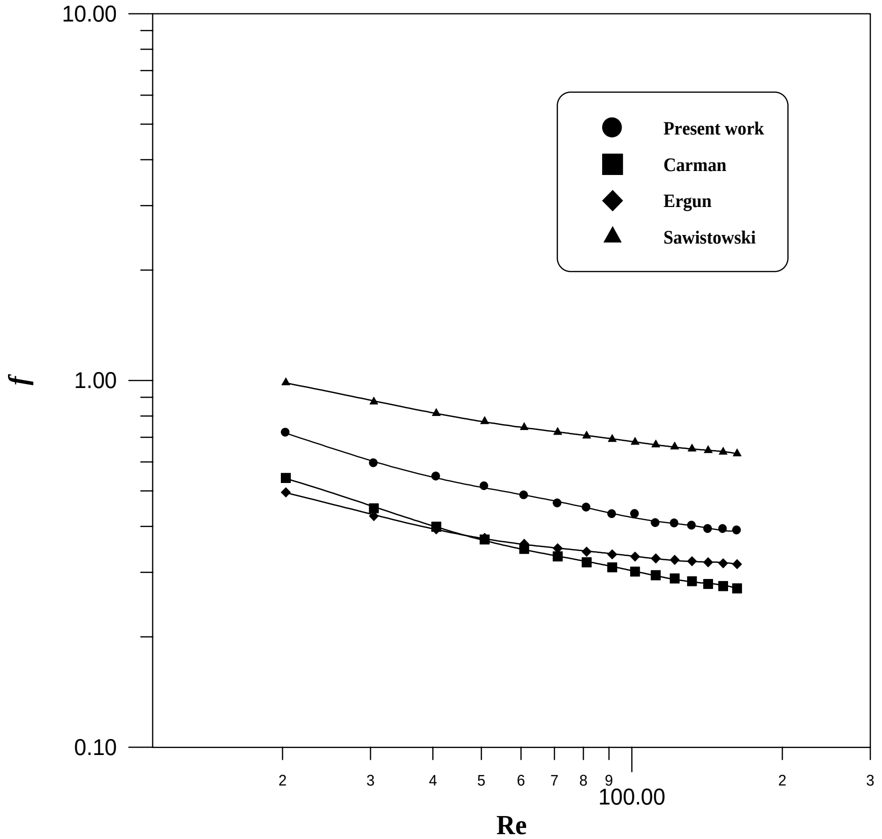

Figure 4.36 Friction factor versus Reynolds numbers for bed with particles diameters of 0.42, 0.79 and 1.01 cm and porosity of 0.3682 (Appendix A.21)

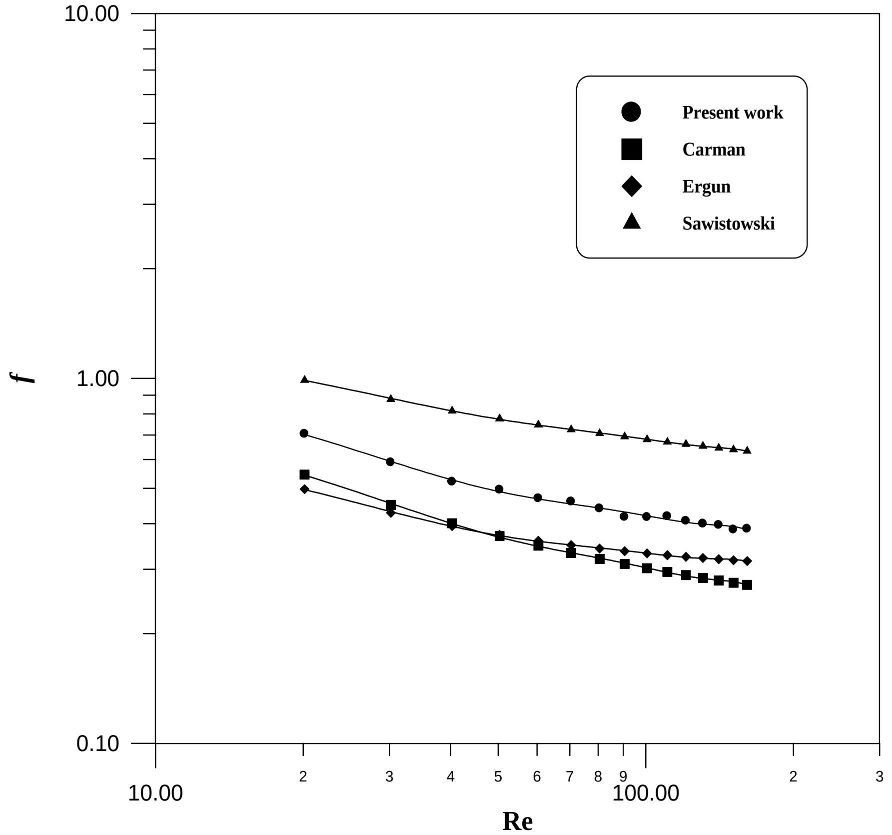

Figure 4.37 Friction factor versus Reynolds numbers for bed with particles diameters of 0.51, 0.61 and 0.79cm and porosity of 0.3827 (Appendix A.22)

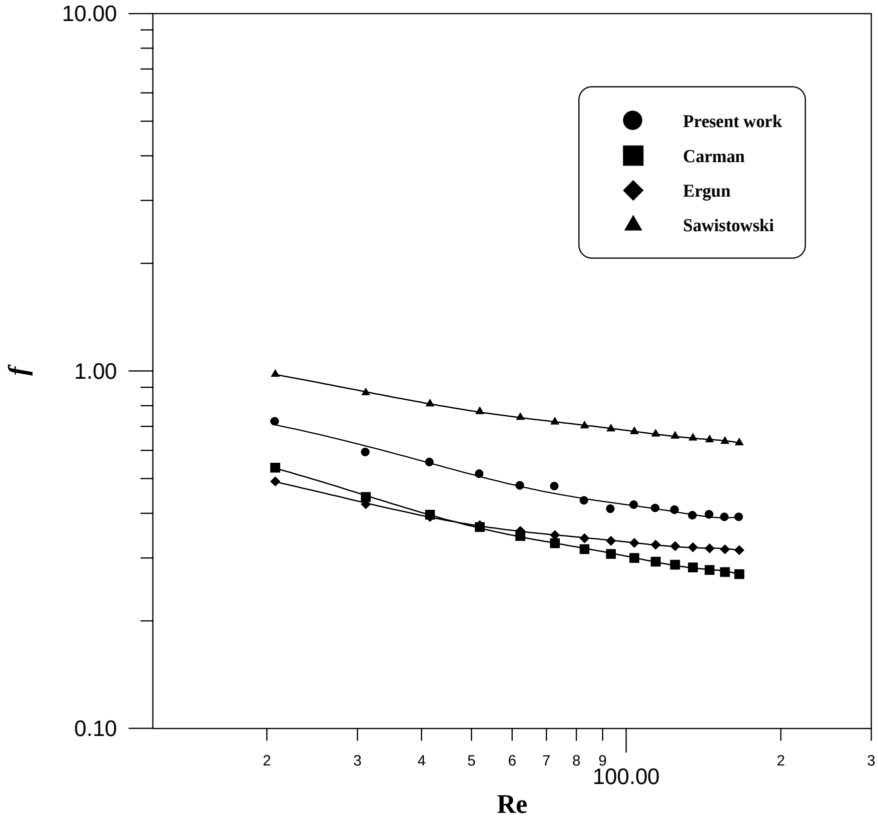

Figure 4.38 Friction factor versus Reynolds numbers for bed with particles diameters of 0.51, 0.61 and 1.01cm and porosity of 0.3746 (Appendix A.23)

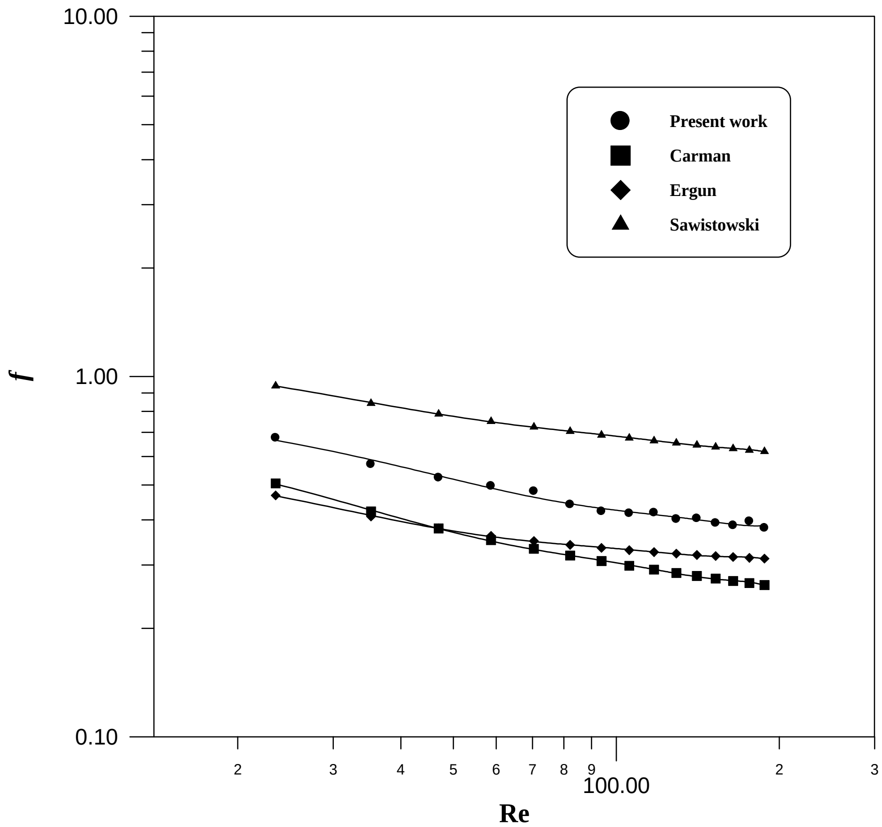

Figure 4.39 Friction factor versus Reynolds numbers for bed with particles diameters of 0.51, 0.79 and 1.01cm and porosity of 0.3868 (Appendix A.24)

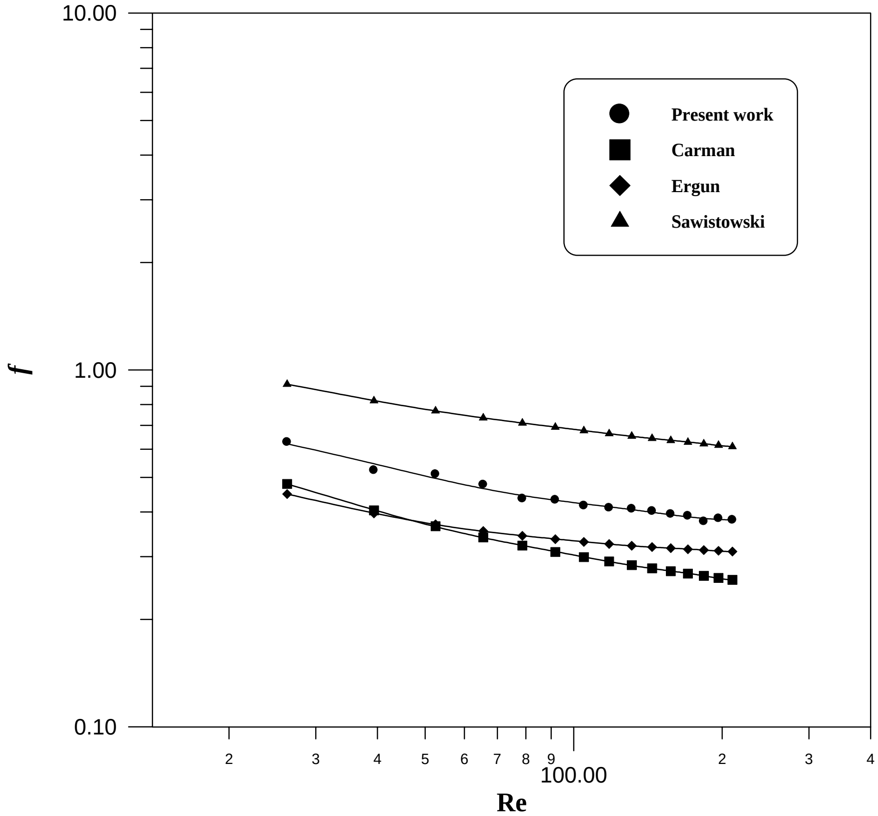

Figure 4.40 Friction factor versus Reynolds numbers for bed with particles diameters of 0.61, 0.79 and 1.01cm and porosity of 0.3935 (Appendix A.25)

Although the bed porosity highly affects the pressure drop and inversely proportional to it, but table A.18 shows that for bed porosity of 0.3561 the pressure drop values which range from 30.7 to 1021.5 Pa are less than those of table A.16 which for larger value of bed porosity of 0.3598 the pressure drop values range from 33.0 to 1100.0 Pa, this is may be due to that the average particles diameter (d_{pavg}) of table A.18 (0.499 cm) is less than of table A.16 (0.559 cm) (the pressure drop inversely proportional to particles diameters) [16].

Figures 4.31 to 4.40 show that as the bed porosity increase from 0.3561 (Fig. 4.33) to 0.3935 (Fig. 4.40) the Reynolds number values increase from the range of 16.9-135. 1 (Fig. 4.33) to the range of 26.2-209.8 (Fig. 4.40), which lead to decrease in the friction factor values from the range of 0.770-0.401 to the range of 0.628-0.380.

The best fitting of the experimental results for air flow through beds of ternary-sizes particles is represented by the following equation.

$$f = 5.45\,\mathrm{Re}_1^{-1} + 0.58\,\mathrm{Re}_1^{-0.1} \qquad \text{... (4.5)}$$

With the correlation coefficient is 0.9898 and percentage of average errors is 2.30%.

4.3.2 Water flow

The values of water flow friction factors through beds of ternary sizes particles are plotted versus Reynolds numbers as shown in Figs 4.41 to 4.50.

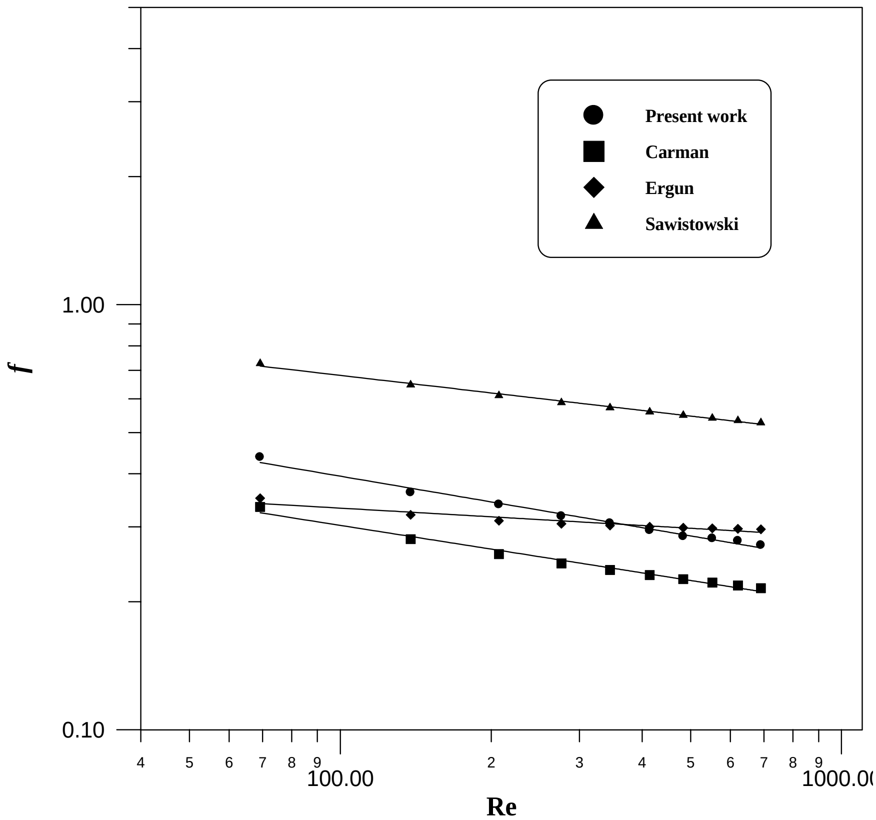

Figure 4.41 Friction factor versus Reynolds numbers for bed with particles diameters of 0.42, 0.51 and 0.61cm and porosity of 0.3600 (Appendix B.16)

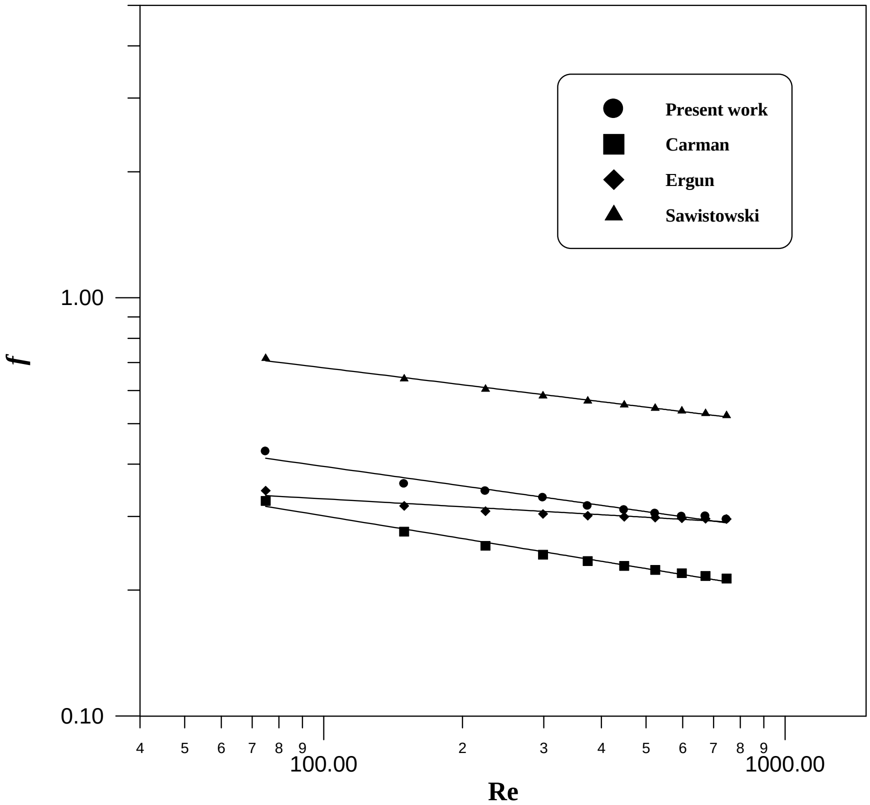

Figure 4.42 Friction factor versus Reynolds numbers for bed with particles diameters of 0.42, 0.51 and 0.79cm and porosity of 0.3648 (Appendix B.17)

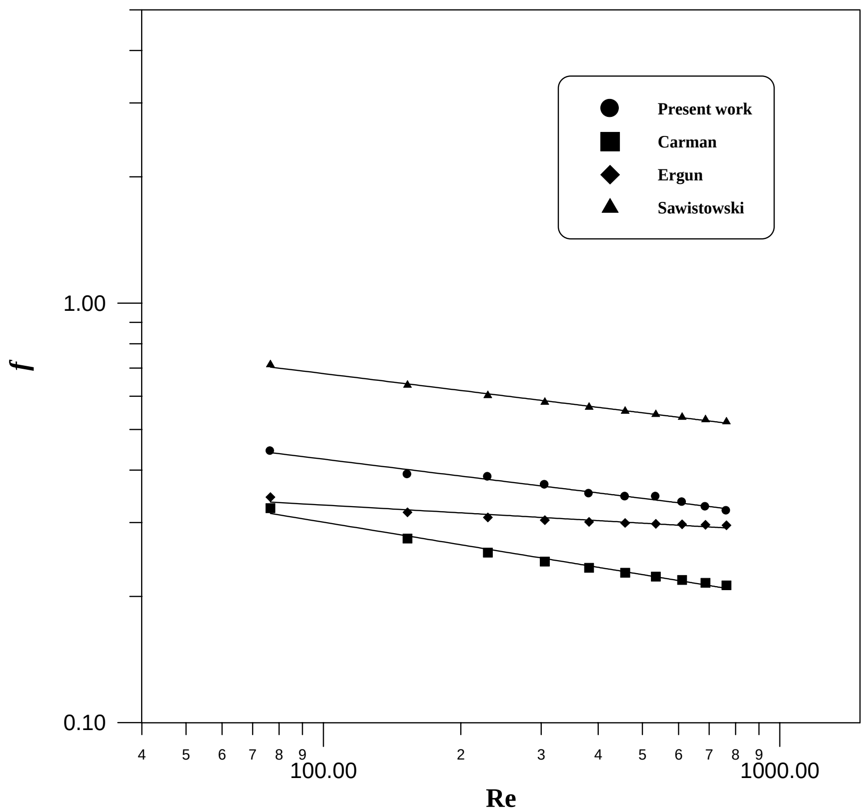

Figure 4.43 Friction factor versus Reynolds numbers for bed with particles diameters of 0.42, 0.51 and 1.01cm and porosity of 0.3562 (Appendix B.18)

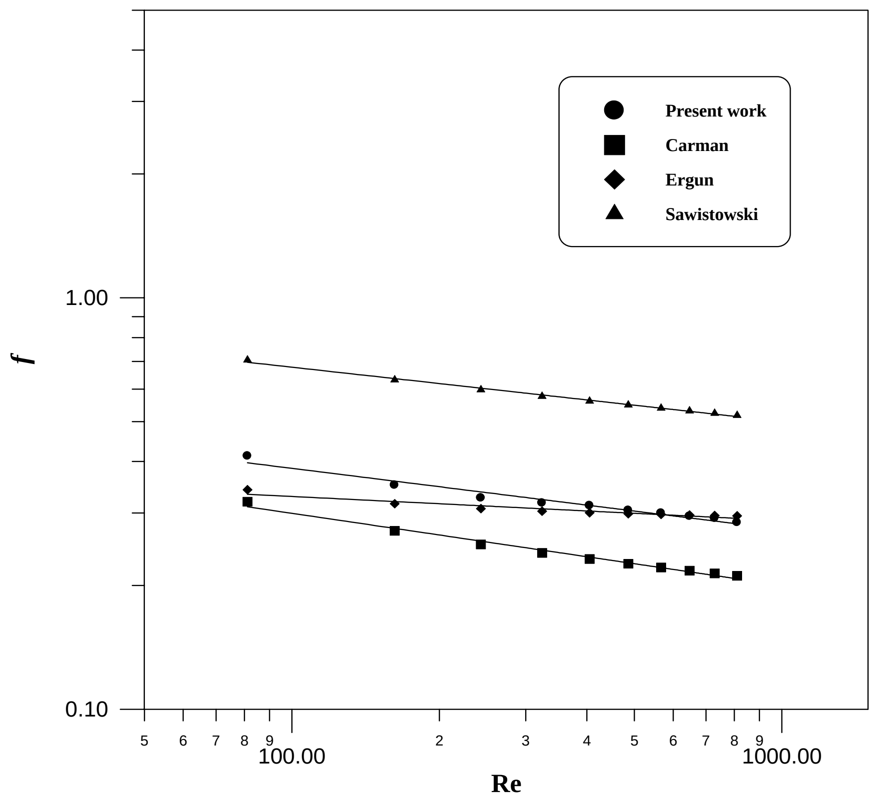

Figure 4.44 Friction factor versus Reynolds numbers for bed with particles diameters of 0.42, 0.61 and 0.79cm and porosity of 0.3695 (Appendix B.19)

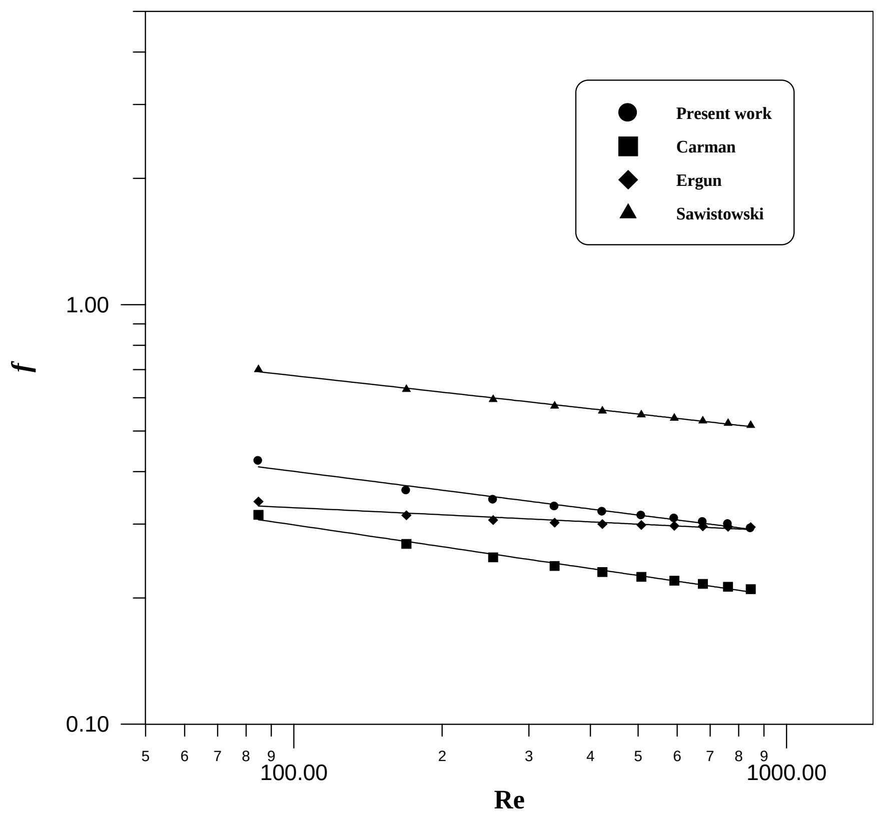

Figure 4.45 Friction factor versus Reynolds numbers for bed with particles diameters of 0.42, 0.61 and 1.01cm and porosity of 0.3665 (Appendix B.20)

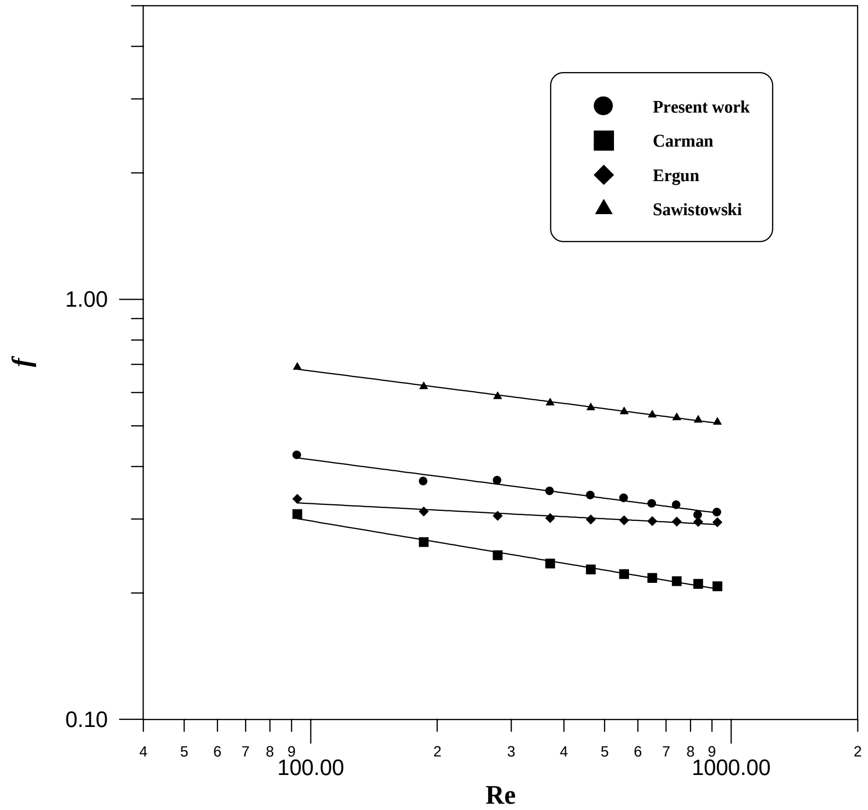

Figure 4.46 Friction factor versus Reynolds numbers for bed with particles diameters of 0.42, 0.79 and 1.01 cm and porosity of 0.3712 (Appendix B.21)

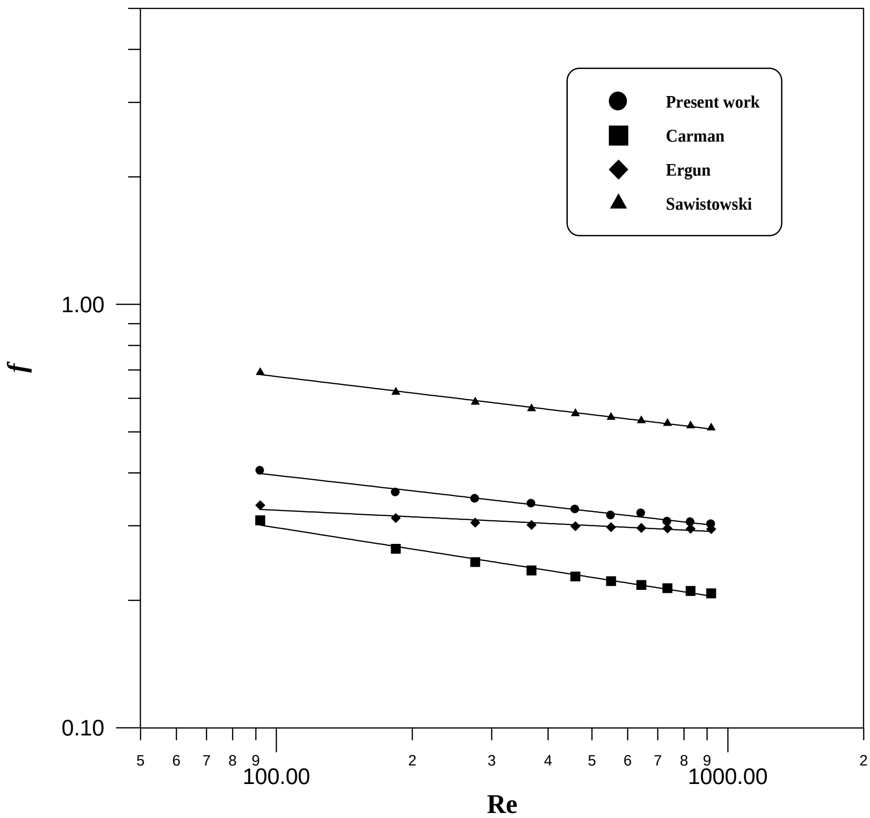

Figure 4.47 Friction factor versus Reynolds numbers for bed with particles diameters of 0.51, 0.61 and 0.79cm and porosity of 0.3854 (Appendix B.22)

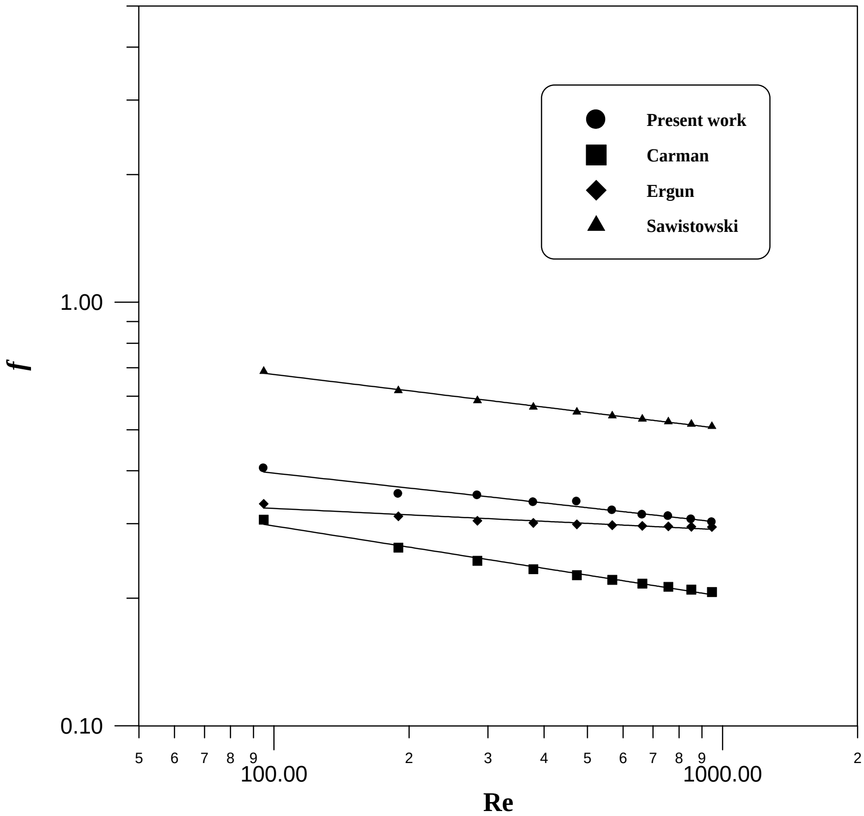

Figure 4.48 Friction factor versus Reynolds numbers for bed with particles diameters of 0.51, 0.61 and 1.01cm and porosity of 0.3771 (Appendix B.23)

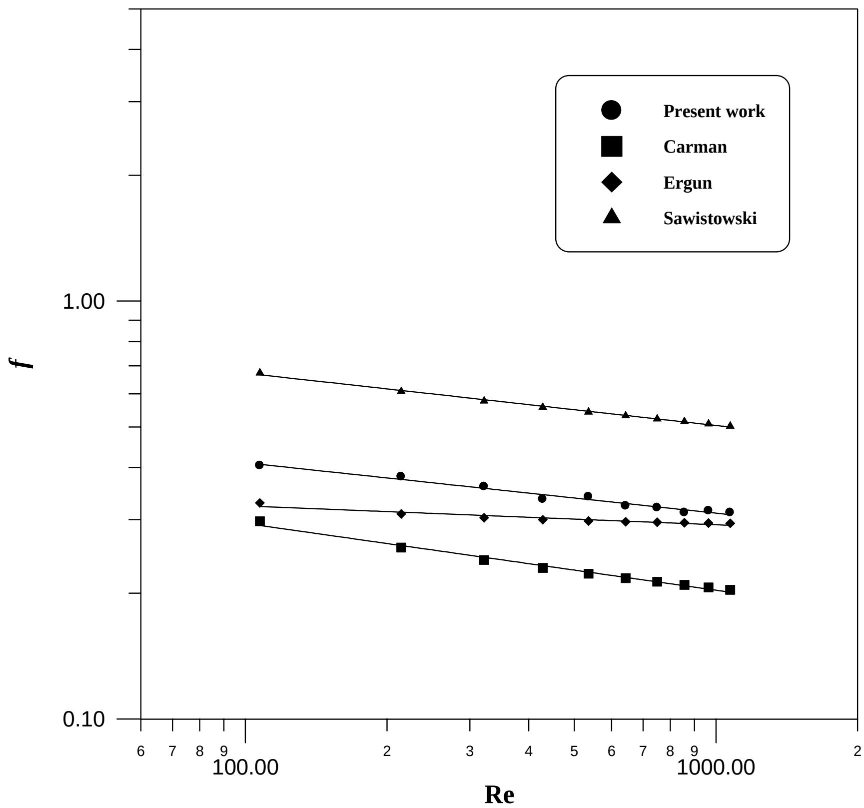

Figure 4.49 Friction factor versus Reynolds numbers for bed with particles diameters of 0.51, 0.79 and 1.01cm and porosity of 0.3895 (Appendix B.24)

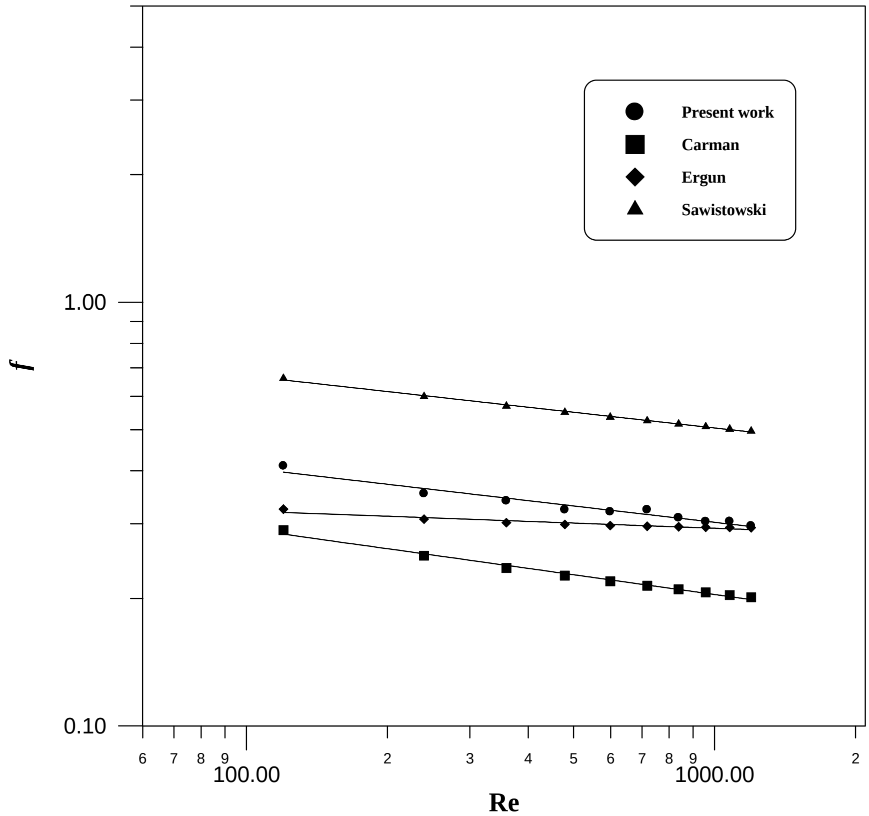

Figure 4.50 Friction factor versus Reynolds numbers for bed with particles diameters of 0.61, 0.79 and 1.01cm and porosity of 0.3962 (Appendix B.25)

It can be noticed that the porosity of ternary size packings are generally close to each other, since the voids could be filled with different sizes of particles [14].

It can be noticed that the pressure drop of tables B.19 and B.20 have the same values (the pressure drop of table B.19 range from 0.77 to 52.67kPa, and those of table B.20 range from 0.77 to 52.79kPa), because they have approximately close values of bed porosities and mean particles diameter.

The best fitting of the experimental results for water flow through beds of ternary-sizes particles is represented by the following equation.

$$f = 3.63\mathrm{Re}_1^{-1} + 0.58\mathrm{Re}_1^{-0.1} \qquad \text{... (4.6)}$$

With the correlation coefficient is 0.9015 and percentage of average errors is 4.08%.

4.4 Packing of quaternary sizes particles

4.4.1 Air flow

The values of air flow friction factors through beds of quaternary sizes particles are plotted versus Reynolds numbers as shown in Figs. 4.51 to 4.55.

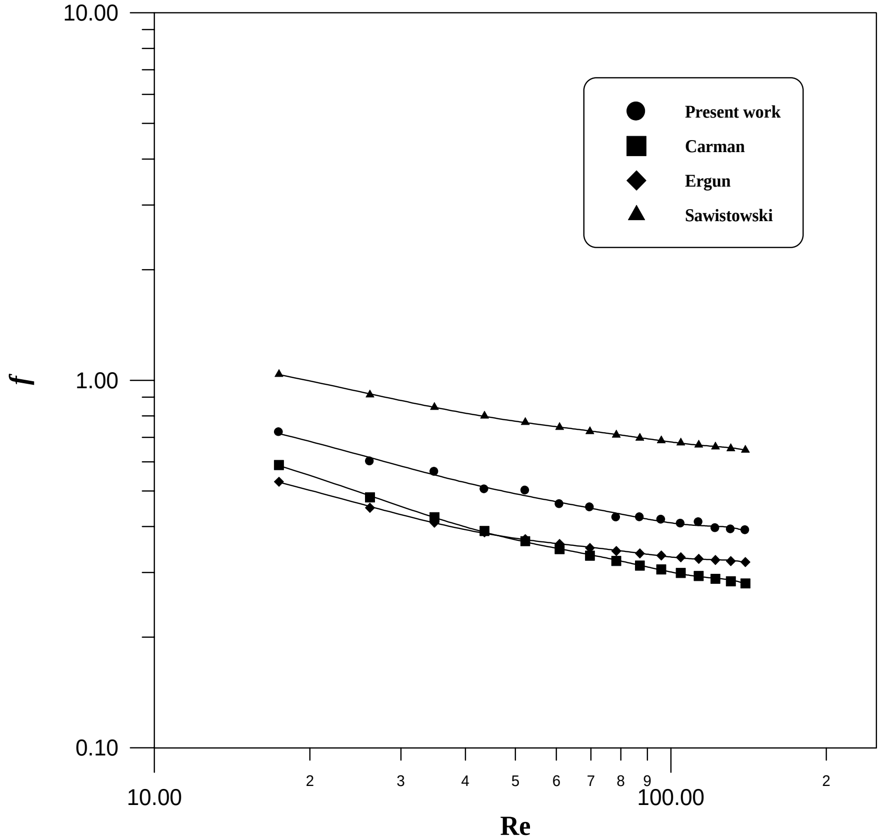

Figure 4.51 Friction factor versus Reynolds numbers for bed with particles diameters of 0.42, 0.51, 0.61 and 0.79cm and porosity of 0.3713 (App. A.26)

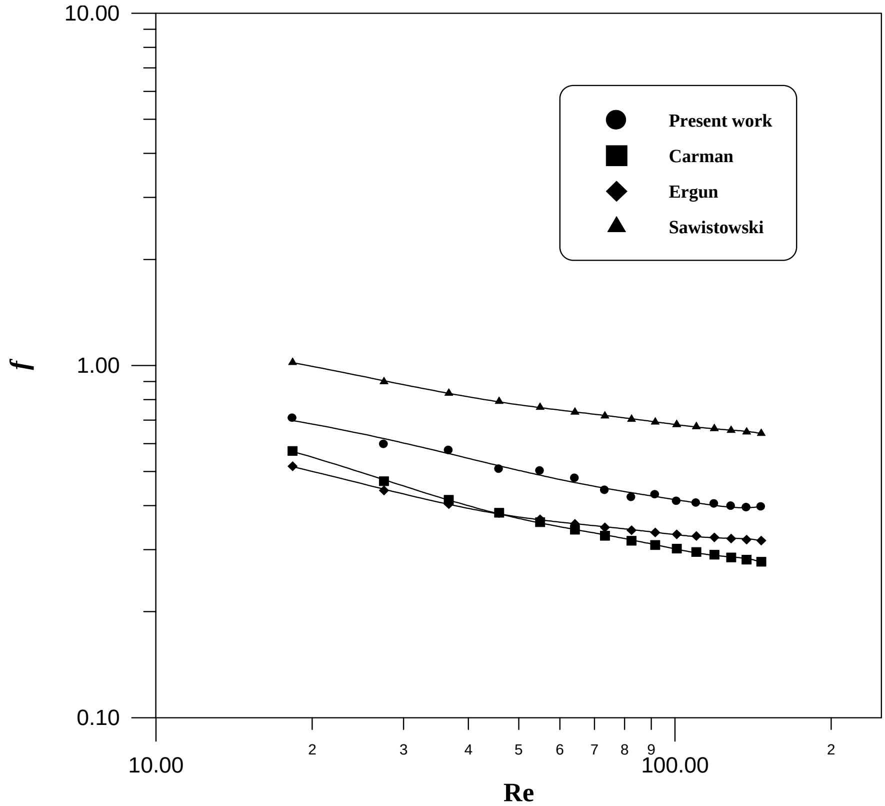

Figure 4.52 Friction factor versus Reynolds numbers for bed with particles diameters of 0.42, 0.51, 0.61 and 1.01cm and porosity of 0.3754 (App. A.27)

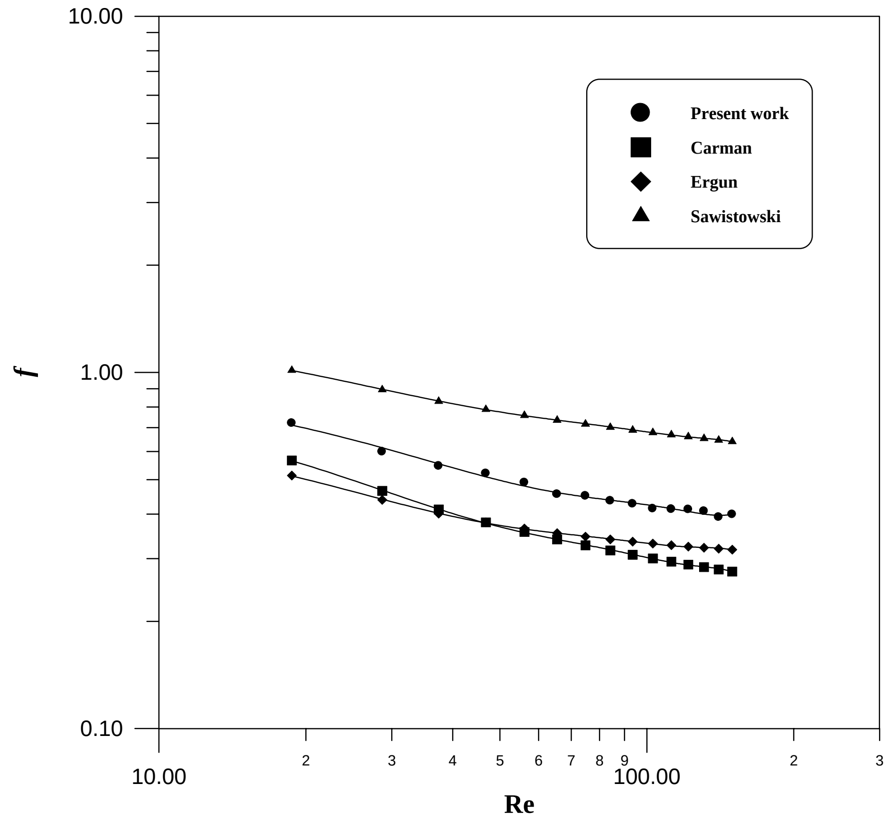

Figure 4.53 Friction factor versus Reynolds numbers for bed with particles diameters of 0.42, 0.51, 0.79 and 1.01cm and porosity of 0.3647 (App. A.28)

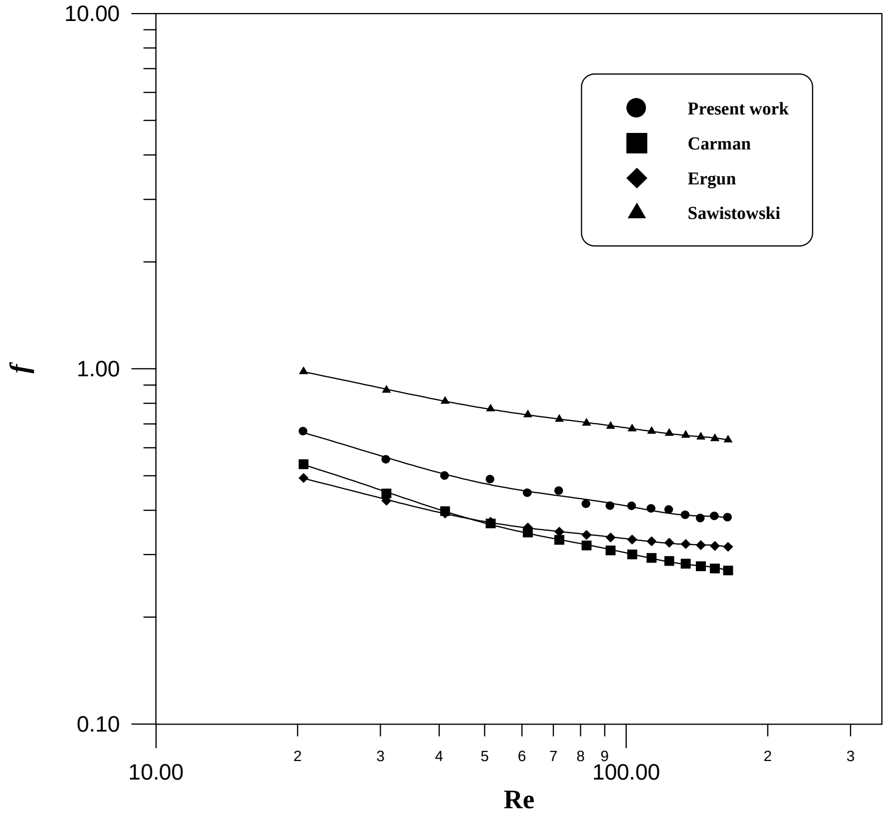

Figure 4.54 Friction factor versus Reynolds numbers for bed with particles diameters of 0.42, 0.61, 0.79 and 1.01cm and porosity of 0.3772 (App. A.29)

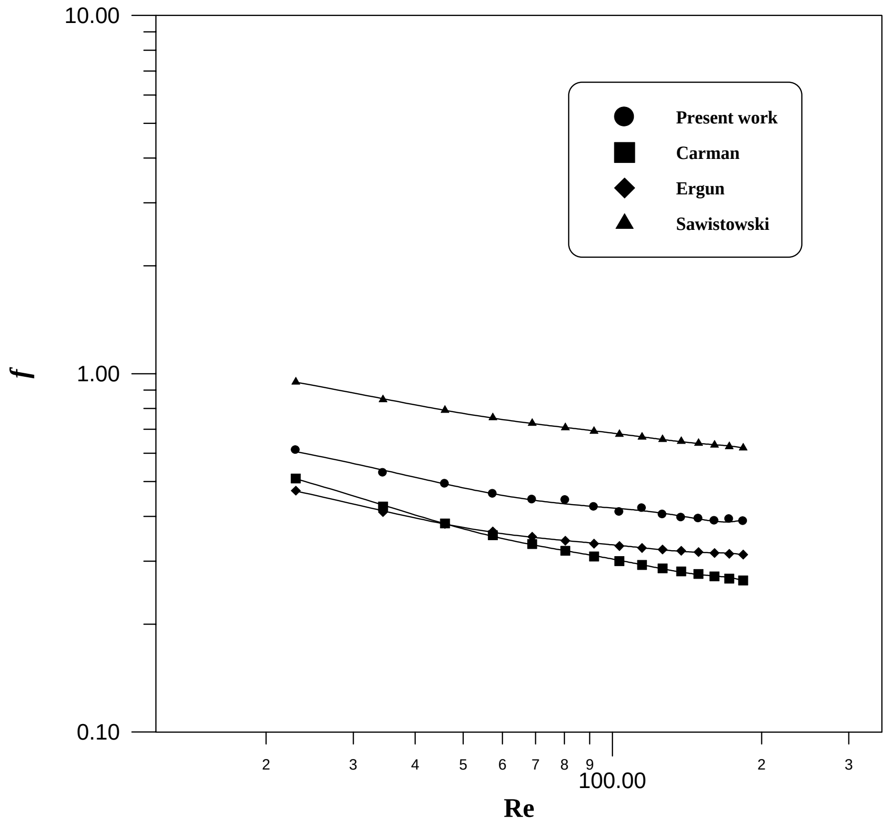

Figure 4.55 Friction factor versus Reynolds numbers for bed with particles diameters of 0.51, 0.61, 0.79 and 1.01cm and porosity of 0.3915 (App. A.30)

The values of friction factor of Figs. 4.51, 4.52 and 4.53 were approximately close to each other (range from 0.721-0.391, 0.708-0.396 and 0.720-0.399 respectively) since they have close values of Reynolds numbers (range from 17.4-139.4, 18.3-146.7 and 18.7-149.7 respectively) and porosities (0.3713, 0.3754 and 0.3647 respectively) in spite of different diameters of particles. Figs. 4.54 and 4.55 show that the values of friction factor (range 0.665-0.381and 0.612-0.387) are less than those of Figs. 4.51, 4.52 and 4.53, because of the increase in the values of porosities (0.3772 and 0.3915) and Reynolds numbers (20.6-164.8 and 22.9-183.7).

The best fitting of the experimental results for air flow through beds of quaternary-sizes particles is represented by the following equation.

$$f = 4.86\,\mathrm{Re}_1^{-1} + 0.58\,\mathrm{Re}_1^{-0.1} \qquad \text{... (4.7)}$$

With the correlation coefficient is 0.9907 and percentage of average errors is 1.84%.

4.4.2 Water flow

The values of water flow friction factors are plotted versus Reynolds numbers as shown in Figs 4.56 to 4.60.

These Figs. show that the friction factor decreases as Reynolds number increases.

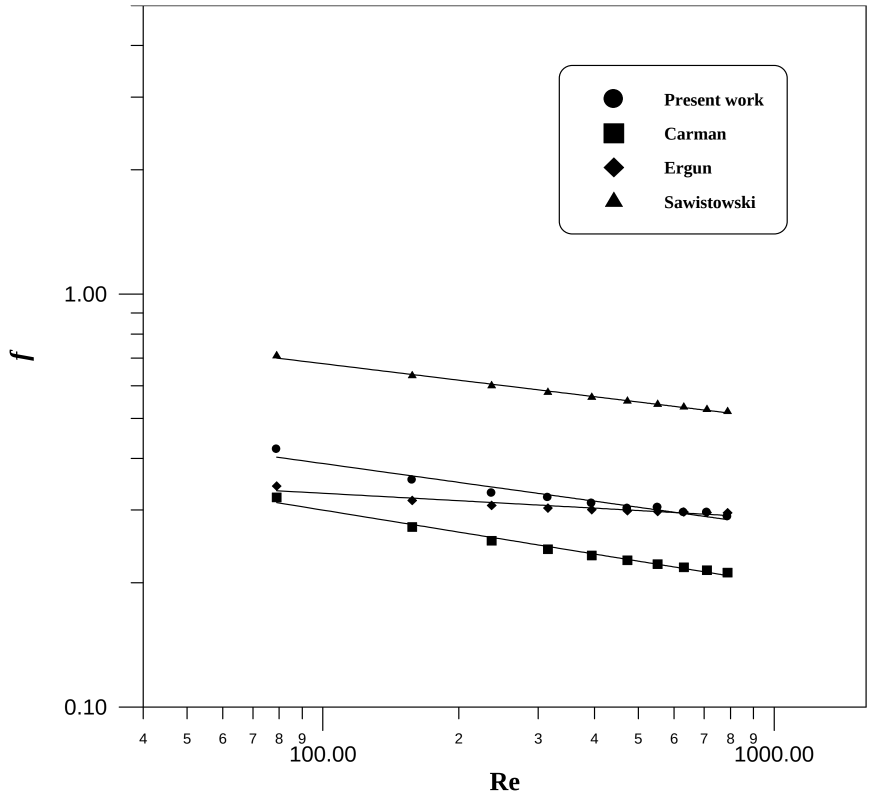

Figure 4.56 Friction factor versus Reynolds numbers for bed with particles diameters of 0.42, 0.51, 0.61 and 0.79cm and porosity of 0.3714 (App. B.26)

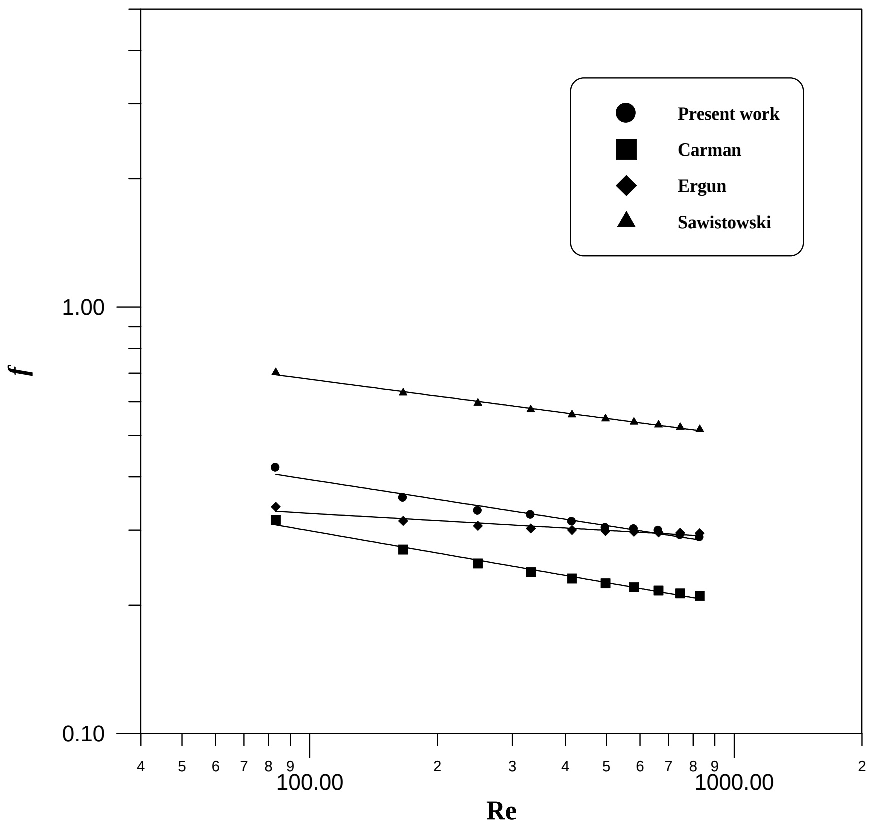

Figure 4.57 Friction factor versus Reynolds numbers for bed with particles diameters of 0.42, 0.51, 0.61 and 1.01cm and porosity of 0.3754 (App. B.27)

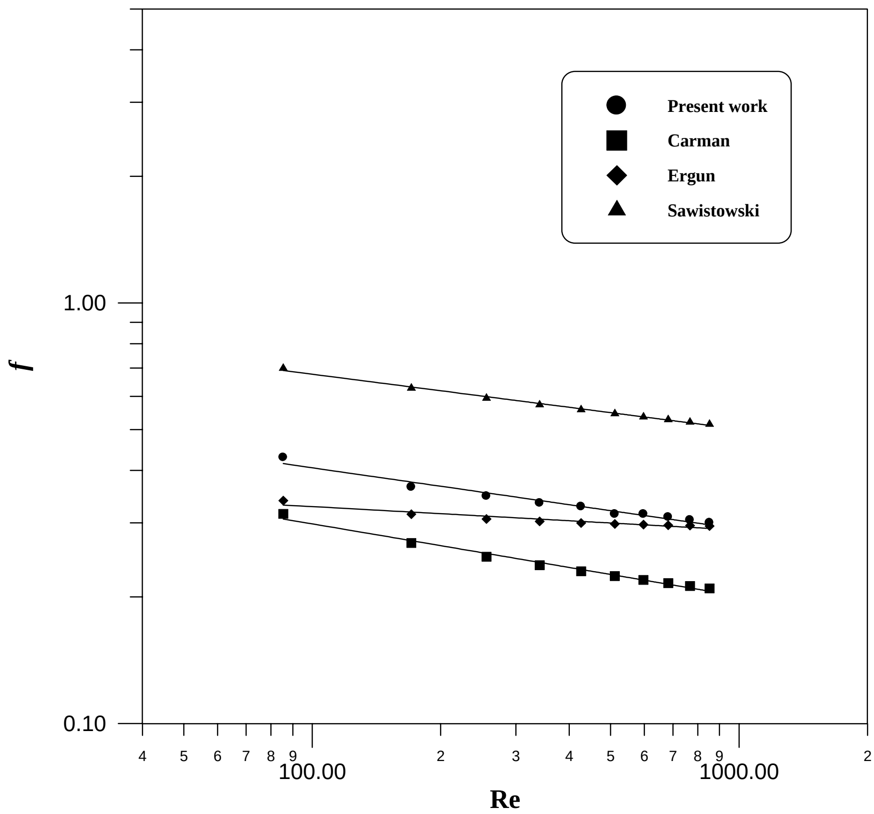

Figure 4.58 Friction factor versus Reynolds numbers for bed with particles diameters of 0.42, 0.51, 0.79 and 1.01cm and porosity of 0.3671 (App. B.28)

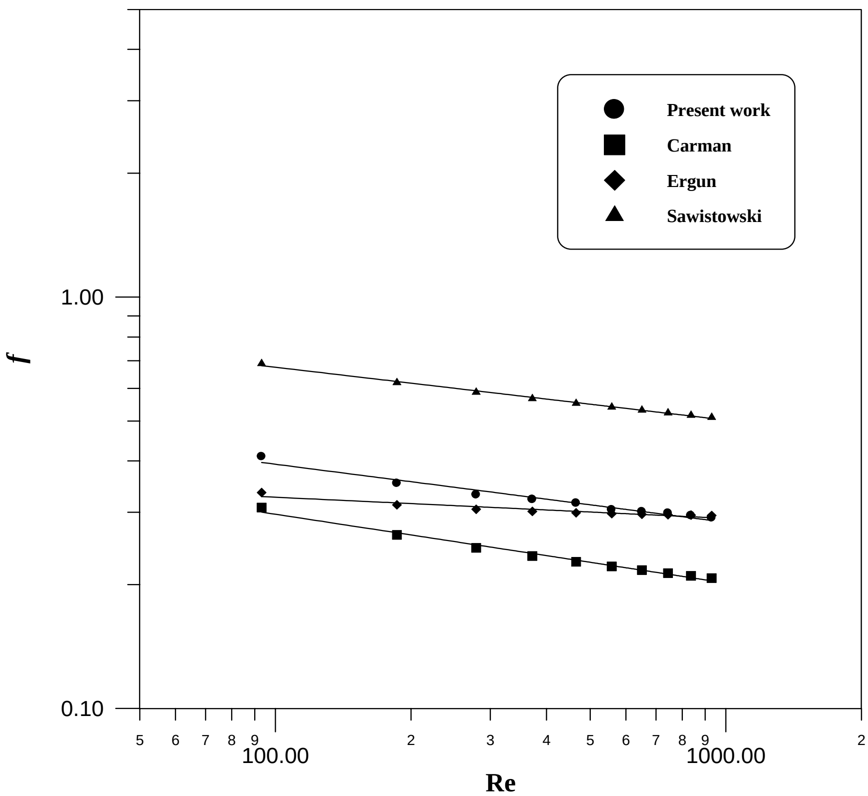

Figure 4.59 Friction factor versus Reynolds numbers for bed with particles diameters of 0.42, 0.61, 0.79 and 1.01cm and porosity of 0.3767 (App. B.29)

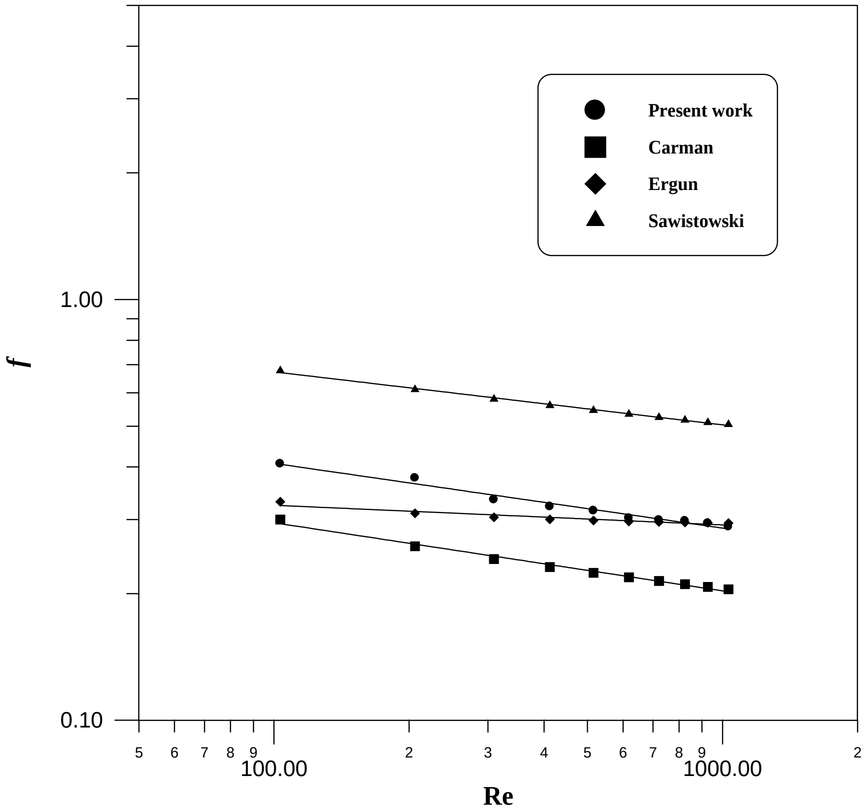

Figure 4.60 Friction factor versus Reynolds numbers for bed with particles diameters of 0.51, 0.61, 0.79 and 1.01cm and porosity of 0.3891 (App. B.30)

The curves representing the experimental results of friction factor for water flow are straighter than those of air flow where the curvatures of the curves indicate that the air flow was intermediate between the turbulent and laminar regions while water flow was at the turbulent region (at the turbulent region the Reynolds number have insignificant effect on the friction factor values) [8].

Examining the experimental results it can be seen that the pressure drop in the bed is inversely proportional to bed porosity for the same velocity of the fluid entering the bed [55].

The best fitting of the experimental results for water flow through beds of quaternary-sizes particles is represented by the following equation.

$$f = 4.93\,\mathrm{Re}_1^{\,-1} + 0.56\,\mathrm{Re}_1^{\,-0.1} \qquad \text{... (4.8)}$$

With the correlation coefficient is 0.9797 and percentage of average errors is 1.79%.

4.5 Packing of quinary sizes particles

4.5.1 Air flow

The values of air flow friction factors through beds of quinary sizes particles are plotted versus Reynolds numbers as shown in Fig. 4.61.

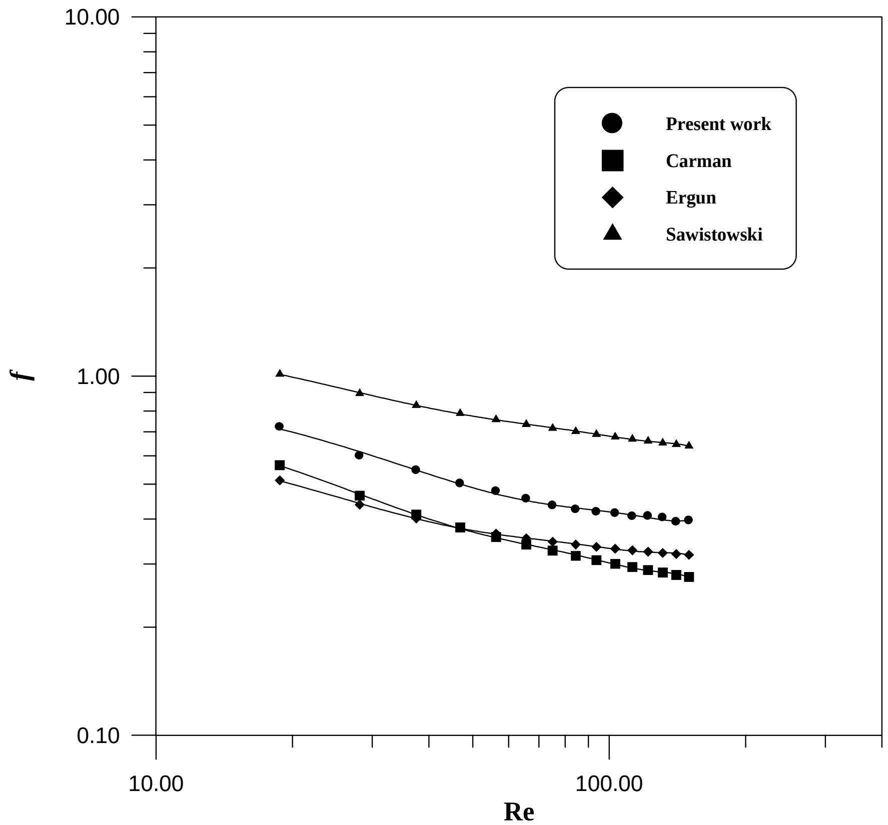

Figure 4.61 Friction factor versus Reynolds numbers for bed with particles diameters of 0.42, 0.51, 0.61, 0.79 and 1.01cm and porosity of 0.3646 (App. A.31)

The values of friction factor of Fig. 4.61 (range from 0.721 to 0.396) are close to those of Fig. 4.53 (range from 0.720 to 0.399) because they have close values of Reynolds numbers (Reynolds numbers of Fig. 4.56 range from

18.8 to 150.1 and those of Fig.4.53 range from 18.7 to 149.7) and bed porosities (the porosity of Fig. 4.60 equal to 0.3646 and of Fig.5.53 equal to 0.3647).

The best fitting of the experimental results for air flow through beds of quinary sizes particles is represented by the following equation.

$$f = 5.35\,\mathrm{Re}_1^{-1} + 0.58\,\mathrm{Re}_1^{-0.1} \qquad \text{... (4.9)}$$

With the correlation coefficient is 0.9977 and percentage of average errors is 1.15%.

The experimental results of friction factor-Reynolds number curves lie among the results of Sawistowski, Carman and Ergun (above the results of Carman and Ergun, and below those of Sawistowski); this is due to the differences in beds dimensions, packings shapes and sizes.

Ergun and Sawistowski used hollow packings which have certain values of sphericity and porosity (the lower the particle sphericity the more open is the bed) while Carman used sphere packing [4, 8].

4.5.2 Water flow

The values of water flow friction factors through beds of quinary sizes particles are plotted versus Reynolds numbers as shown in Fig. 4.62.

The friction factor values for water flow decrease slightly with increasing Reynolds number, because the water flow is at the turbulent region where the high rate velocity of fluid behaves as a slip velocity and has insignificant effect on the friction values [5].

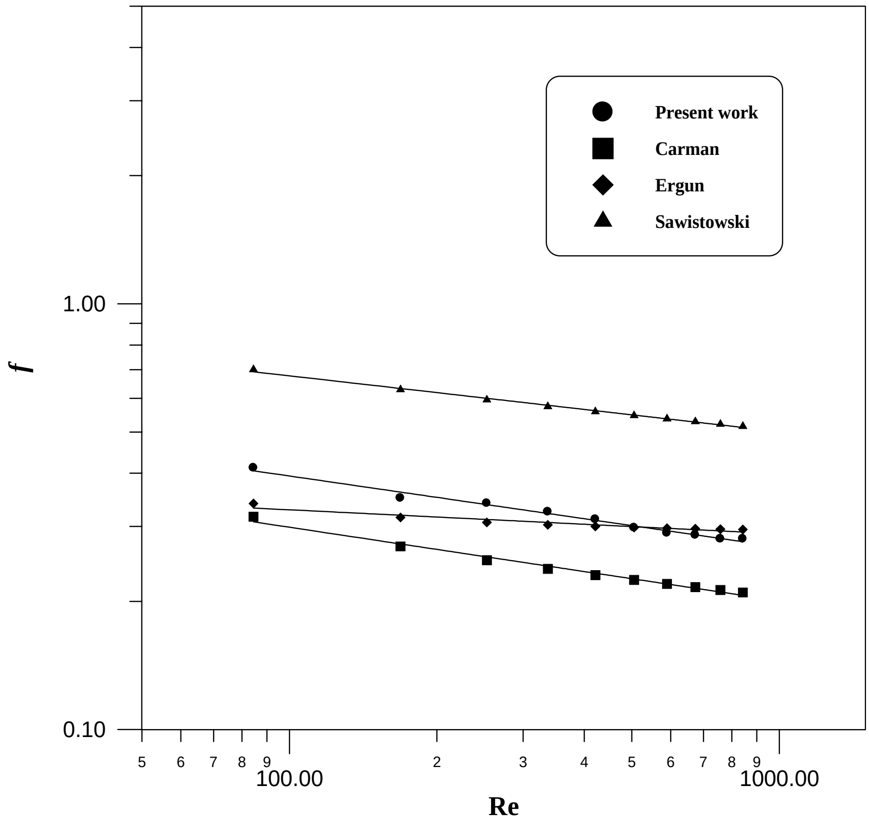

Figure 4.62 Friction factor versus Reynolds numbers for bed with particles diameters of 0.42, 0.51, 0.61, 0.79 and 1.01cm and porosity of 0.3624 (App. B.31)

The best fitting of the experimental results for water flow through beds of quinary sizes particles is represented by the following equation.

$$f = 5.67\,\mathrm{Re}_1^{-1} + 0.54\,\mathrm{Re}_1^{-0.1} \qquad \text{... (4.10)}$$

With the correlation coefficient is 0.9926 and percentage of average errors is 1.10%.

It can be noticed from the experimental results that the values of Reynolds number are different from system to system in spite of the same flow rate; this is due to the change in porosity and specific surface area of the particles.

A generalized equation for friction factor as a function of Reynolds number for a bed of multi sizes spherical particles was found as:

a. For air flow

$$f = 4.72\,\mathrm{Re_1}^{-1} + 0.59\,\mathrm{Re_1}^{-0.1} \qquad \text{... (4.11)}$$

The correlation coefficient was 0.9662 and percentage of average errors was 3.79%.

b. For water flow

$$f = 3.73\,\mathrm{Re_1}^{-1} + 0.56\,\mathrm{Re_1}^{-0.1} \qquad \text{... (4.12)}$$

The correlation coefficient was 0.8994 and percentage of average errors was 4.16%.

Table 4.1 summarized the correction factors values and percentage of errors for air and water flow through beds of mono- multi sizes particles.

Table 4.1 The correction factors and percentage of errors for air and water flow through beds of mono- multi sizes particles.

System	Correction Factor		Error%	
	Air flow	Water flow	Air flow	Water flow
Mono	0.9742	0.9741	4.66	2.44
Binary	0.9710	0.9351	3.89	3.46
Ternary	0.9898	0.9015	2.30	4.08
Quaternary	0.9907	0.9797	1.84	1.79
Quinary	0.9977	0.9926	1.15	1.10
Multi	0.9662	0.8994	3.79	4.16

Chapter Five

Conclusions and Recommendations for future work

5.1 Conclusions

1. The experimental results of friction factor for water flow show more linear behavior than those of air flow; because the range of Reynolds number of water flow is at the turbulent region while for air flow it is at the laminar, transition the onset of turbulent region.
2. The friction factor values for water flow decrease slightly with increasing Reynolds number values, because the water flow is at the turbulent region where the high rate velocity of fluid behaves as a slip velocity and has insignificant effect on the friction values.
3. Comparing the experimental results of the present work with those of Sawistowski, Carman and Ergun, it can be noticed that the curves of the present work lie among the results of Sawistowski, Carman and Ergun; this is due to the differences of beds dimensions, packings shapes and sizes.
4. The particle size and size distribution highly affected the bed porosity. For mono size packing, the lower the particle size, the lower is the bed porosity. The porosity of multi- size systems are generally less than those of mono size systems, because the particles of smaller sizes tend to fill the void spaces between the larger sizes particles.
5. The bed porosity is greatly influences the pressure drop which also depends on several parameters as bed height, fluid velocity, mean particles diameter and the physical properties of fluid. Water flow shows high values of pressure drop compared with air flow for close values of bed porosities and at same volumetric flow rates.

6. Increasing the Reynolds number values lead to decrease in the friction factor values for all size distributions.

   For close values of Reynolds number the air and water flow show close values of friction factor.

5.2 Recommendations for further work

The following suggestions are to be considered in greater detail for further work.

1. Study the effect of the shape and material of packing on the pressure drop and friction factor through packed bed.
2. Study the possibility of developing a large scale of packed bed.
3. Study the flow of two phases through the packed bed.

References

1. Fluid flow in packed bed. Article given on the internet at the web site http://www.chee.nus.edu.sg/pdf/ExpF7.pdf
2. R. Shankar Subramanian, "Flow through packed beds and fluidized beds". http://www.clarkson.edu/subramanian/ch301/notes/packfluidbed.pdf
3. Christie J. Geankoplis," Transport Processes and Unit perations", Third Edition., Prentice Hall, New Jersey, 1993.
4. A. S. Foust, L. A. Wenzel, C. W. Clump, L. Maus, and L. B. Andersen, "Principles of Unit Operations", Second Edition, John Wiley and Sons, New York, 1980.
5. M. R. Al-Ubaidi, M. Sc. Thesis, pressure drop and flow distribution in a bed of uniform particles, 1973.
6. L. oger, J.P. Troadec, D. Bideau, powder technology,46 (1986) 121.
7. Hydraulics of packed column. Article given on the internet at the web site http://www.unb.ca/che/undergrad/lab/hydraulics .pdf
8. J. M. Coulson and J.F. Richardson, "Chemical Engineering", volume II, Third Edition, Pergamon Press, London, 1985.
9. J. M. Coulson, Inst. Chem. Eng, 13 (1949) 237.
10. J. Kozeny, Ber, Wien Akad, 136 (1927) 271.
11. P. C. Carman, Soc. Chem. Ind, 27 (1938) 1403.
12. F. C. Blank, Trans. Amer. Inst. Chem, 14 (1962) 415.
13. J. Green and Ampt, J. Agric. Sci, 13 (1962) 5.
14. Fluid flow through packed and fluidized systems. Article given on the internet at the web site

http://www.fischer-tropsch.org/Bureau_of_Mines/bulletins/bultn_504/bulletin_504_bureau_of_mines-A.pdf

15. S. Back, A. Beaber, E. Boudreaux, and K. Paavola, "Pressure drop for flow in packed beds: An analysis using Ergun's equation". http://rothfus.cheme.cmu.edu/tlab/pbeds/projects/t10_s02/t10_s02.pdf (2004)
16. W. L. McCabe, J. C. Smith, and Peter Harriott, "Unit Operation of Chemical Engineering", Sixth Edition, McGraw-Hill, new York, 2001.
17. Flow through porous, packed, and fluidized beds. Article given on the internet at the web site http://www.che.lsu.edu/courses/3101/summer00/ln7.pdf
18. A. Marmur, powder technology, 44 (1985) 249.
19. R. E. Treybal, "Mass Transfer Operations", Second Edition, McGraw-Hill, New York, 1980.
20. D. B. shukla, P. M. 03a and V.P. Pandya, powder technology, 47 (1986) 233.
21. W. A. Gary, "The packing of solid particles", Chapman and Hall, First published, London, 1968.
22. C. C. Furnas, Ind. Eng. Chem, 23 (1931) 1052.
23. A. E. Westman and M. R. Hugill, J. Am. Ceram. Soc, 13 (1930) 767.
24. C. E. Schwartz and J. M. Smith, Ind. Eng. Chem, 45 (1953) 1209.
25. L. C. Graton and H. J. Fraser, J. Geol, 43 (1985) 785.
26. A. B. Yu and N. Standish, powder technology, 55 (1989) 171.
27. L. C. Graton and H. J. Fraser, Geol, 43 (1967) 785.
28. C. S. Slichter, 19^{th} Ann. Rep. U.S.G. Geol, Survey, 2 (1987) 305.
29. M. X. Max Leva, Chem. Eng, 13 (1949) 115.
30. N. Y. Saied, M. SC. Thesis, "The effect of particle surface roughness on hydraulic flow through granular media", Bradford University, 1977.

31. R. B. Bird, W. E. Stewart, and E. N. Lightfoot, "Transport phenomena", John Wiley and sons, 1960.
32. B. O. Al-Dulami, M. SC. Thesis, "Porosity of particle mixture using RRSB size distribution", Al-Nahrain University, 1998.
33. C. Pierce, J. Williams, P. Beauchemin, and R. Milloy, "Study of pressure drop versus flow rate in packed beds". http://rothfus.cheme.cmu.edu/tlab/pbeds/projects/t5_s02/t5_s02.pdf (2002)
34. V. M. H. Govindarao, and G. F. Froment, Chem. Eng. Sci, 43 (1988), 1403.
35. L. C. Graton, and H. J. Fraser, Chem. Eng, 45 (1953) 1209.
36. P. C. Carman, Trans. Inst. Chem. Eng, 15 (1937) 153.
37. J. M. Coulson, Trans. Inst. Chem. Eng, 27 (1949) 237.
38. K. J. Ives, "The scientific basis of filtration", London, 1975.
39. Porosity, Storage, Permeability, and Hydraulic Conductivity. Article given on the internet at the web site http://www.geography.uoregon.edu/amarcus/oldxyz/gog42502/Handout-aquifers.htm
40. K. Taylor, A. G. Smith, S. Ross, and M. Smith, "The prediction of pressure drop and flow distribution in packed bed filters". http://www.cfd.com.au/cfd_conf99/papers/071TAYL.PDF (1999)
41. R. F. Benenati, and C. B. Brosilow, A. I. Ch. E, 8 (1962) 35.
42. M. J. Matteson, and C. Orr, "Filtration", Second Edition, New York and Basel, 1987.
43. P. C. Carman, Trans. Inst. Chem. Eng, 15 (1937) 166.
44. R. E. Acosta, A. I. Ch. E. J, 31 (1985) 478.
45. A. A. Orning, Ind. Eng. Chem, 41 (1949) 1179.
46. W. K. Lewis and W. C. Bauer, Ind. Chem. Eng, 42 (1949) 1111.

47. P. Chung, R. Koontz, and B. Newton, "Packed beds: Pressure drop versus fluid velocity and the Ergun equation". http://rothfus.cheme.cmu.edu/tlab/pbeds/projects/t10_s02/t10_s02.pdf (2002)
48. Fluid flow through packed and fluid beds. given on the internet at the web site http://www.uic.edu/depts/chme/UnitOps/PackedBeds.pdf (2005)
49. N. Standish, and A. B. Yu, Powder Technology, 49 (1987) 249.
50. J. M. Coulson," Chemical Engineering" Vol. I, First Published, Pergamon Press, London, 1998.
51. H. Sawistowski, Chem. Eng. Sci, 6 (1957) 138.
52. S. Ergun, Chem. Eng. Prog, 48 (1952) 89.
53. R. H. Perry, D. W. Green, and J. O. Maloney, "Perry's Chemical Engineers Handbook", Seventh Edition, McGraw-Hill, New York, 1997.
54. N. Standish, and D. G. Mellor, Powder technology, 27 (1980) 61.
55. G. Meyer, and Lincolnt, A. I. Ch. E. J, 13 (1936) 11.

Appendix A

Air flow through packed bed

A.1 packing of mono sizes particles

Table A.1 For spherical particles diameter of 0.42 cm and bed porosity of 0.3746

Q (m^3/hr)	**u (m /s)**	**Re**	**ΔP (Pa)**	*f*
2	0.1218	8.423	39.289	0.992
3	0.1827	12.635	68.363	0.767
4	0.2436	16.846	102.152	0.645
5	0.3046	21.065	149.298	0.603
6	0.3655	25.277	196.445	0.551
7	0.4264	29.488	251.450	0.518
8	0.4873	33.700	314.312	0.496
9	0.5482	37.911	377.175	0.470
10	0.6091	42.123	471.469	0.476
11	0.6700	46.335	550.047	0.459
12	0.7309	50.546	636.483	0.446
13	0.7918	54.758	715.061	0.427
14	0.8528	58.976	832.928	0.429
15	0.9137	63.188	935.079	0.419
16	0.9746	67.399	1045.089	0.412

Table A.2 For spherical particles diameter of 0.51 cm and bed porosity of 0.3999

Q (m^3/hr)	**u (m /s)**	**Re**	**ΔP (Pa)**	*f*
2	0.1218	10.448	23.573	0.885
3	0.1827	15.673	41.646	0.695
4	0.2436	20.897	63.648	0.597
5	0.3046	26.130	92.722	0.557
6	0.3655	31.354	121.796	0.508
7	0.4264	36.578	157.156	0.481
8	0.4873	41.803	196.445	0.461
9	0.5482	47.027	243.592	0.451
10	0.6091	52.251	298.597	0.448
11	0.6700	57.475	353.602	0.439
12	0.7309	62.700	408.606	0.426
13	0.7918	67.924	471.469	0.419
14	0.8528	73.157	534.331	0.409
15	0.9137	78.381	612.909	0.409
16	0.9746	83.605	683.630	0.401

Table A.3 For spherical particles diameter of 0.61 cm and bed porosity of 0.4112

Q (m^3/hr)	**u (m /s)**	**Re**	**ΔP (Pa)**	*f*
2	0.1218	12.999	15.716	0.781
3	0.1827	19.499	28.288	0.625
4	0.2436	25.999	44.004	0.547
5	0.3046	32.509	62.862	0.500
6	0.3655	39.009	86.436	0.477
7	0.4264	45.509	110.009	0.446
8	0.4873	52.008	141.441	0.439
9	0.5482	58.508	168.943	0.414
10	0.6091	65.008	204.303	0.406
11	0.6700	71.507	243.592	0.400
12	0.7309	78.007	282.881	0.390
13	0.7918	84.507	322.170	0.379
14	0.8528	91.017	377.175	0.382
15	0.9137	97.517	424.322	0.375
16	0.9746	104.017	479.326	0.372

Table A.4 For spherical particles diameter of 0.79 cm and bed porosity of 0.4225

Q (m^3/hr)	**u (m /s)**	**Re**	**ΔP (Pa)**	*f*
2	0.1218	17.154	10.215	0.711
3	0.1827	25.731	18.859	0.584
4	0.2436	34.308	29.074	0.506
5	0.3046	42.899	42.432	0.473
6	0.3655	51.476	58.934	0.456
7	0.4264	60.053	77.007	0.438
8	0.4873	68.629	94.294	0.410
9	0.5482	77.206	117.867	0.405
10	0.6091	85.783	145.370	0.405
11	0.6700	94.360	172.872	0.398
12	0.7309	102.937	204.303	0.395
13	0.7918	111.514	235.734	0.389
14	0.8528	120.105	267.166	0.380
15	0.9137	128.682	306.455	0.379
16	0.9746	137.259	345.744	0.376

Table A.5 For spherical particles diameter of 1.01 cm and bed porosity of 0.4359

Q (m^3/hr)	u (m /s)	Re	ΔP (Pa)	*f*
2	0.1218	22.030	7.072	0.659
3	0.1827	33.045	13.358	0.553
4	0.2436	44.059	21.216	0.494
5	0.3046	55.092	31.431	0.468
6	0.3655	66.107	44.004	0.447
7	0.4264	77.122	56.576	0.430
8	0.4873	88.137	71.506	0.416
9	0.5482	99.152	86.436	0.397
10	0.6091	110.167	106.080	0.395
11	0.6700	121.181	125.725	0.387
12	0.7309	132.196	149.298	0.386
13	0.7918	143.211	172.872	0.381
14	0.8528	154.244	196.445	0.373
15	0.9137	165.259	220.019	0.364
16	0.9746	176.274	251.450	0.366

A.2 packing of binary sizes particles

Table A.6 For spherical particles with diameters of 0.42 and 0.51 cm and bed porosity of 0.3577

Q (m^3/hr)	u (m /s)	Re	ΔP (Pa)	*f*
2	0.1218	13.878	38.503	0.800
3	0.1827	20.817	70.721	0.653
4	0.2436	27.757	110.009	0.571
5	0.3046	34.707	157.156	0.522
6	0.3655	41.646	212.161	0.490
7	0.4264	48.585	275.023	0.466
8	0.4873	55.524	345.744	0.449
9	0.5482	62.464	416.464	0.427
10	0.6091	69.403	510.758	0.424
11	0.6700	76.342	597.194	0.410
12	0.7309	83.281	699.345	0.404
13	0.7918	90.220	809.354	0.398
14	0.8528	97.171	919.364	0.390
15	0.9137	104.110	1052.947	0.389
16	0.9746	111.049	1178.672	0.383

Table A.7 For spherical particles with diameters of 0.42 and 0.61 cm and bed porosity of 0.3622

Q (m^3/hr)	u (m /s)	Re	ΔP (Pa)	*f*
2	0.1218	15.341	33.003	0.780
3	0.1827	23.012	59.719	0.628
4	0.2436	30.682	94.294	0.557
5	0.3046	38.366	137.512	0.520
6	0.3655	46.036	184.659	0.485
7	0.4264	53.707	243.592	0.470
8	0.4873	61.377	306.455	0.453
9	0.5482	69.048	373.246	0.436
10	0.6091	76.719	447.895	0.423
11	0.6700	84.389	534.331	0.418
12	0.7309	92.060	628.625	0.413
13	0.7918	99.731	730.776	0.409
14	0.8528	107.414	832.928	0.402
15	0.9137	115.084	950.795	0.399
16	0.9746	122.755	1076.520	0.398

Table A.8 For spherical particles with diameters of 0.42 and 0.79 cm and bed porosity of 0.3589

Q (m^3/hr)	u (m /s)	Re	ΔP (Pa)	*f*
2	0.1218	16.735	31.431	0.792
3	0.1827	25.102	58.934	0.660
4	0.2436	33.470	94.294	0.594
5	0.3046	41.851	137.512	0.554
6	0.3655	50.218	188.587	0.528
7	0.4264	58.586	243.592	0.501
8	0.4873	66.953	306.455	0.482
9	0.5482	75.320	373.246	0.464
10	0.6091	83.688	447.895	0.451
11	0.6700	92.055	534.331	0.445
12	0.7309	100.423	620.767	0.434
13	0.7918	108.790	722.919	0.431
14	0.8528	117.717	817.212	0.420
15	0.9137	125.538	927.222	0.415
16	0.9746	133.906	1045.089	0.411

Table A.9 For spherical particles with diameters of 0.42 and 1.01 cm and bed porosity of 0.3455

Q (m^3/hr)	**u (m /s)**	**Re**	**ΔP (Pa)**	*f*
2	0.1218	17.342	33.809	0.808
3	0.1827	26.014	63.642	0.676
4	0.2436	34.685	102.096	0.610
5	0.3046	43.370	150.209	0.574
6	0.3655	52.041	202.712	0.538
7	0.4264	60.713	262.559	0.512
8	0.4873	69.384	330.189	0.493
9	0.5482	78.055	397.534	0.469
10	0.6091	86.726	487.625	0.466
11	0.6700	95.397	571.017	0.451
12	0.7309	104.068	668.993	0.444
13	0.7918	112.740	772.743	0.437
14	0.8528	121.425	886.137	0.432
15	0.9137	130.096	1012.508	0.430
16	0.9746	138.767	1131.546	0.422

Table A.10 For spherical particles with diameters of 0.51 and 0.61 cm and bed porosity of 0.3709

Q (m^3/hr)	**u (m /s)**	**Re**	**ΔP (Pa)**	*f*
2	0.1218	17.418	26.717	0.770
3	0.1827	26.126	48.718	0.624
4	0.2436	34.835	78.578	0.566
5	0.3046	43.558	110.009	0.507
6	0.3655	52.267	149.298	0.478
7	0.4264	60.976	196.445	0.462
8	0.4873	69.685	251.450	0.453
9	0.5482	78.394	298.597	0.425
10	0.6091	87.102	361.459	0.417
11	0.6700	95.811	440.037	0.419
12	0.7309	104.520	510.758	0.409
13	0.7918	113.229	597.194	0.407
14	0.8528	121.952	675.772	0.397
15	0.9137	130.661	777.923	0.398
16	0.9746	139.370	872.217	0.393

Table A.11 For spherical particles with diameters of 0.51 and 0.79 cm and bed porosity of 0.3879

Q (m^3/hr)	u (m /s)	Re	ΔP (Pa)	*f*
2	0.1218	20.497	18.091	0.684
3	0.1827	30.746	34.609	0.582
4	0.2436	40.994	55.060	0.520
5	0.3046	51.259	78.657	0.476
6	0.3655	61.508	110.119	0.462
7	0.4264	71.757	146.301	0.451
8	0.4873	82.005	184.843	0.437
9	0.5482	92.254	220.238	0.411
10	0.6091	102.502	267.432	0.404
11	0.6700	112.751	322.492	0.403
12	0.7309	122.999	385.417	0.405
13	0.7918	133.248	440.477	0.394
14	0.8528	143.513	503.402	0.388
15	0.9137	153.762	582.059	0.391
16	0.9746	164.010	652.850	0.386

Table A.12 For spherical particles with diameters of 0.51 and 1.01 cm and bed porosity of 0.3733

Q (m^3/hr)	u (m /s)	Re	ΔP (Pa)	*f*
2	0.1218	21.318	19.645	0.707
3	0.1827	31.977	36.932	0.590
4	0.2436	42.636	60.505	0.544
5	0.3046	53.312	86.436	0.497
6	0.3655	63.971	119.439	0.477
7	0.4264	74.630	157.156	0.461
8	0.4873	85.289	196.445	0.441
9	0.5482	95.948	239.663	0.426
10	0.6091	106.607	290.739	0.418
11	0.6700	117.266	349.673	0.416
12	0.7309	127.925	408.606	0.408
13	0.7918	138.584	471.469	0.401
14	0.8528	149.260	542.189	0.398
15	0.9137	159.919	612.909	0.392
16	0.9746	170.578	699.345	0.393

Table A.13 For spherical particles with diameters of 0.61 and 0.79 cm and bed porosity of 0.4042

Q (m^3/hr)	u (m /s)	Re	ΔP (Pa)	*f*
2	0.1218	24.328	12.573	0.619
3	0.1827	36.491	25.145	0.550
4	0.2436	48.655	40.861	0.503
5	0.3046	60.839	59.719	0.470
6	0.3655	73.003	83.293	0.455
7	0.4264	85.167	111.581	0.448
8	0.4873	97.330	141.441	0.435
9	0.5482	109.494	168.943	0.411
10	0.6091	121.658	204.303	0.402
11	0.6700	133.822	243.592	0.396
12	0.7309	145.986	290.739	0.397
13	0.7918	158.150	337.886	0.394
14	0.8528	170.333	385.033	0.387
15	0.9137	182.497	432.180	0.378
16	0.9746	194.661	495.042	0.381

Table A.14 For spherical particles with diameters of 0.61 and 1.01 cm and bed porosity of 0.3901

Q (m^3/hr)	u (m /s)	Re	ΔP (Pa)	*f*
2	0.1218	25.599	14.144	0.677
3	0.1827	38.398	27.502	0.585
4	0.2436	51.197	44.004	0.527
5	0.3046	64.018	66.006	0.505
6	0.3655	76.817	90.365	0.481
7	0.4264	89.617	117.867	0.461
8	0.4873	102.416	149.298	0.447
9	0.5482	115.215	180.730	0.427
10	0.6091	128.015	220.019	0.421
11	0.6700	140.814	267.166	0.423
12	0.7309	153.613	314.312	0.418
13	0.7918	166.413	361.459	0.410
14	0.8528	179.233	416.464	0.407
15	0.9137	192.033	471.469	0.401
16	0.9746	204.832	526.473	0.394

Table A.15 For spherical particles with diameters of 0.79 and 1.01cm and bed porosity of 0.4220

Q (m^3/hr)	u (m /s)	Re	ΔP (Pa)	*f*
2	0.1218	33.197	7.858	0.585
3	0.1827	49.796	15.716	0.520
4	0.2436	66.394	25.931	0.482
5	0.3046	83.02	39.289	0.467
6	0.3655	99.619	53.433	0.441
7	0.4264	116.218	70.720	0.429
8	0.4873	132.816	86.436	0.402
9	0.5482	149.415	108.438	0.398
10	0.6091	166.013	133.583	0.397
11	0.6700	182.612	157.156	0.386
12	0.7309	199.211	188.587	0.390
13	0.7918	215.809	212.161	0.373
14	0.8528	232.435	251.450	0.382
15	0.9137	249.034	282.881	0.374
16	0.9746	265.632	322.170	0.374

A.3 packing of ternary sizes particles

Table A.16 For spherical particles with diameters of 0.42, 0.51 and 0.61cm and bed porosity of 0.3598

Q (m^3/hr)	u (m /s)	Re	ΔP (Pa)	*f*
2	0.1218	15.250	33.003	0.767
3	0.1827	22.876	61.291	0.633
4	0.2436	30.501	102.152	0.593
5	0.3046	38.138	141.441	0.526
6	0.3655	45.764	196.445	0.507
7	0.4264	53.389	251.450	0.477
8	0.4873	61.040	322.170	0.468
9	0.5482	68.639	385.033	0.442
10	0.6091	76.264	463.611	0.431
11	0.6700	83.889	557.905	0.428
12	0.7309	91.515	660.056	0.426
13	0.7918	99.140	754.350	0.415
14	0.8528	106.777	864.359	0.410
15	0.9137	114.403	982.226	0.406
16	0.9746	122.028	1100.093	0.399

Table A.17 For spherical particles with diameters of 0.42, 0.51 and 0.79 cm and bed porosity of 0.3620

Q (m^3/hr)	**u (m /s)**	**Re**	**ΔP (Pa)**	***f***
2	0.1218	16.369	29.860	0.755
3	0.1827	24.553	56.576	0.636
4	0.2436	32.737	86.436	0.547
5	0.3046	40.935	125.725	0.508
6	0.3655	49.120	172.872	0.486
7	0.4264	57.304	227.877	0.470
8	0.4873	65.448	282.881	0.447
9	0.5482	73.673	345.744	0.432
10	0.6091	81.857	416.464	0.421
11	0.6700	90.041	495.042	0.414
12	0.7309	98.226	557.905	0.392
13	0.7918	106.410	667.914	0.400
14	0.8528	114.608	762.208	0.393
15	0.9137	122.792	856.501	0.385
16	0.9746	130.977	974.368	0.385

Table A.18 For spherical particles with diameters of 0.42, 0.51 and 1.01 cm and bed porosity of 0.3561

Q (m^3/hr)	**u (m /s)**	**Re**	**ΔP (Pa)**	***f***
2	0.1218	16.878	30.645	0.770
3	0.1827	25.317	58.148	0.650
4	0.2436	33.757	90.365	0.568
5	0.3046	42.210	133.583	0.537
6	0.3655	50.649	180.730	0.505
7	0.4264	59.088	235.734	0.484
8	0.4873	67.527	298.597	0.469
9	0.5482	75.966	361.459	0.449
10	0.6091	84.405	440.037	0.442
11	0.6700	92.844	526.473	0.437
12	0.7309	101.284	620.767	0.433
13	0.7918	109.723	691.487	0.411
14	0.8528	118.176	801.497	0.411
15	0.9137	126.615	911.506	0.407
16	0.9746	135.054	1021.515	0.401

Table A.19 For spherical particles with diameters of 0.42, 0.61 and 0.79 cm and bed porosity of 0.3668

Q (m^3/hr)	**u (m /s)**	**Re**	**ΔP (Pa)**	***f***
2	0.1218	17.755	25.931	0.734
3	0.1827	26.632	48.718	0.613
4	0.2436	35.510	75.435	0.534
5	0.3046	44.402	110.009	0.498
6	0.3655	53.279	149.298	0.469
7	0.4264	62.157	188.587	0.435
8	0.4873	71.034	243.592	0.431
9	0.5482	79.912	298.597	0.417
10	0.6091	88.789	361.459	0.409
11	0.6700	97.667	432.180	0.404
12	0.7309	106.544	510.758	0.401
13	0.7918	115.422	589.336	0.395
14	0.8528	124.314	660.056	0.381
15	0.9137	133.191	762.208	0.383
16	0.9746	142.069	856.501	0.379

Table A.20 For spherical particles with diameters of 0.42, 0.61 and 1.01 cm and bed porosity of 0.3636

Q (m^3/hr)	**u (m /s)**	**Re**	**ΔP (Pa)**	***f***
2	0.1218	18.524	25.931	0.752
3	0.1827	27.787	48.718	0.628
4	0.2436	37.049	74.649	0.541
5	0.3046	46.326	110.009	0.510
6	0.3655	55.589	149.298	0.481
7	0.4264	64.851	196.445	0.465
8	0.4873	74.113	243.592	0.441
9	0.5482	83.375	298.597	0.428
10	0.6091	92.638	361.459	0.419
11	0.6700	101.900	432.180	0.414
12	0.7309	111.162	495.042	0.399
13	0.7918	120.424	581.478	0.399
14	0.8528	129.702	660.056	0.391
15	0.9137	138.964	754.350	0.389
16	0.9746	148.226	848.644	0.384

Table A.21 For spherical particles with diameters of 0.42, 0.79 and 1.01 cm and bed porosity of 0.3682

Q (m^3/hr)	**u (m /s)**	**Re**	**ΔP (Pa)**	*f*
2	0.1218	20.303	22.002	0.720
3	0.1827	30.455	40.861	0.594
4	0.2436	40.607	66.791	0.547
5	0.3046	50.775	98.223	0.514
6	0.3655	60.927	133.583	0.486
7	0.4264	71.079	172.872	0.462
8	0.4873	81.231	220.019	0.450
9	0.5482	91.382	267.166	0.432
10	0.6091	101.534	330.028	0.432
11	0.6700	111.686	377.175	0.408
12	0.7309	121.838	447.895	0.407
13	0.7918	131.989	518.616	0.402
14	0.8528	142.158	589.336	0.394
15	0.9137	152.309	675.772	0.393
16	0.9746	162.461	762.208	0.390

Table A.22 For spherical particles with diameters of 0.51, 0.61 and 0.79 cm and bed porosity of 0.3827

Q (m^3/hr)	**u (m /s)**	**Re**	**ΔP (Pa)**	*f*
2	0.1218	20.131	19.645	0.704
3	0.1827	30.196	36.932	0.588
4	0.2436	40.262	58.148	0.521
5	0.3046	50.344	86.4359	0.495
6	0.3655	60.409	117.867	0.469
7	0.4264	70.474	157.156	0.460
8	0.4873	80.540	196.445	0.440
9	0.5482	90.605	235.734	0.417
10	0.6091	100.671	290.739	0.417
11	0.6700	110.736	353.602	0.419
12	0.7309	120.801	408.606	0.407
13	0.7918	130.867	471.469	0.400
14	0.8528	140.949	542.189	0.396
15	0.9137	151.014	605.051	0.385
16	0.9746	161.080	691.487	0.387

Table A.23 For spherical particles with diameters of 0.51, 0.61 and 1.01 cm and bed porosity of 0.3746

Q (m^3/hr)	**u (m /s)**	**Re**	**ΔP (Pa)**	*f*
2	0.1218	20.757	20.430	0.720
3	0.1827	31.135	37.717	0.591
4	0.2436	41.514	62.862	0.554
5	0.3046	51.910	91.151	0.514
6	0.3655	62.288	121.796	0.477
7	0.4264	72.667	165.014	0.475
8	0.4873	83.045	196.445	0.433
9	0.5482	93.424	235.734	0.410
10	0.6091	103.802	298.597	0.421
11	0.6700	114.180	353.602	0.412
12	0.7309	124.559	416.464	0.408
13	0.7918	134.938	471.469	0.393
14	0.8528	145.333	550.047	0.395
15	0.9137	155.712	620.767	0.389
16	0.9746	166.090	707.203	0.389

Table A.24 For spherical particles with diameters of 0.51, 0.79 and 1.01 cm and bed porosity of 0.3868

Q (m^3/hr)	**u (m /s)**	**Re**	**ΔP (Pa)**	*f*
2	0.1218	23.478	15.716	0.676
3	0.1827	35.218	29.860	0.571
4	0.2436	46.957	48.718	0.524
5	0.3046	58.715	72.292	0.497
6	0.3655	70.455	100.580	0.480
7	0.4264	82.194	125.725	0.441
8	0.4873	93.933	157.156	0.422
9	0.5482	105.672	196.445	0.417
10	0.6091	117.412	243.592	0.419
11	0.6700	129.151	282.881	0.402
12	0.7309	140.890	337.886	0.403
13	0.7918	152.629	385.033	0.392
14	0.8528	164.388	440.037	0.386
15	0.9137	176.127	518.616	0.396
16	0.9746	187.866	565.762	0.380

Table A.25 For spherical particles with diameters of 0.61, 0.79 and 1.01cm and bed porosity of 0.3935

Q (m^3/hr)	**u (m /s)**	**Re**	**ΔP (Pa)**	***f***
2	0.1218	26.226	12.573	0.628
3	0.1827	39.338	23.573	0.523
4	0.2436	52.451	40.861	0.510
5	0.3046	65.585	59.719	0.477
6	0.3655	78.698	78.578	0.436
7	0.4264	91.811	106.080	0.432
8	0.4873	104.924	133.583	0.417
9	0.5482	118.037	166.586	0.411
10	0.6091	131.149	204.303	0.408
11	0.6700	144.262	243.592	0.402
12	0.7309	157.375	284.453	0.395
13	0.7918	170.488	330.028	0.3901
14	0.8528	183.622	369.317	0.376
15	0.9137	196.735	432.180	0.384
16	0.9746	209.848	487.184	0.380

A.4 packing of quaternary sizes particles

Table A.26 For spherical particles with diameters of 0.42, 0.51, 0.61 and 0.79cm and bed porosity of 0.3713

Q (m^3/hr)	**u (m /s)**	**Re**	**ΔP (Pa)**	***f***
2	0.1218	17.421	25.145	0.721
3	0.1827	26.131	47.147	0.601
4	0.2436	34.841	78.578	0.563
5	0.3046	43.566	110.009	0.505
6	0.3655	52.276	157.156	0.501
7	0.4264	60.896	196.445	0.460
8	0.4873	69.697	251.450	0.451
9	0.5482	78.407	298.597	0.423
10	0.6091	87.117	369.317	0.424
11	0.6700	95.828	440.037	0.417
12	0.7309	104.538	510.758	0.407
13	0.7918	113.248	605.051	0.411
14	0.8528	121.973	675.772	0.395
15	0.9137	130.683	770.065	0.393
16	0.9746	139.393	872.217	0.391

Table A.27 For spherical particles with diameters of 0.42, 0.51, 0.61 and 1.01 cm and bed porosity of 0.3754

Q (m^3/hr)	u (m /s)	Re	ΔP (Pa)	*f*
2	0.1218	18.330	22.788	0.708
3	0.1827	27.496	43.218	0.597
4	0.2436	36.661	73.863	0.574
5	0.3046	45.841	102.152	0.507
6	0.3655	55.006	145.370	0.501
7	0.4264	64.171	188.587	0.478
8	0.4873	73.336	227.877	0.442
9	0.5482	82.502	275.023	0.422
10	0.6091	91.667	345.744	0.429
11	0.6700	100.832	400.748	0.411
12	0.7309	109.997	471.469	0.407
13	0.7918	119.162	550.047	0.404
14	0.8528	128.342	628.625	0.398
15	0.9137	137.508	715.061	0.395
16	0.9746	146.673	817.212	0.396

Table A.28 For spherical particles with diameters of 0.42, 0.51, 0.79 and 1.01 cm and bed porosity of 0.3647

Q (m^3/hr)	u (m /s)	Re	ΔP (Pa)	*f*
2	0.1218	18.712	24.359	0.720
3	0.1827	28.680	45.575	0.599
4	0.2436	37.424	73.863	0.546
5	0.3046	46.795	110.009	0.520
6	0.3655	56.151	149.298	0.490
7	0.4264	65.507	188.587	0.455
8	0.4873	74.862	243.592	0.450
9	0.5482	84.218	298.597	0.436
10	0.6091	93.574	361.459	0.427
11	0.6700	102.930	424.322	0.415
12	0.7309	112.286	502.900	0.413
13	0.7918	121.642	589.336	0.412
14	0.8528	131.013	675.772	0.408
15	0.9137	140.369	746.492	0.392
16	0.9746	149.725	864.359	0.399

Table A.29 For spherical particles with diameters of 0.42, 0.61, 0.79 and 1.01 cm and bed porosity of 0.3772

Q (m^3/hr)	u (m /s)	Re	ΔP (Pa)	*f*
2	0.1218	20.591	18.859	0.665
3	0.1827	30.887	35.360	0.554
4	0.2436	41.183	56.576	0.499
5	0.3046	51.496	86.436	0.487
6	0.3655	61.791	113.938	0.446
7	0.4264	72.087	157.156	0.452
8	0.4873	82.383	188.587	0.415
9	0.5482	92.679	235.734	0.410
10	0.6091	102.974	290.739	0.410
11	0.6700	113.270	345.744	0.403
12	0.7309	123.566	408.606	0.400
13	0.7918	133.862	463.611	0.387
14	0.8528	144.174	526.473	0.379
15	0.9137	154.470	612.909	0.384
16	0.9746	164.766	691.487	0.381

Table A.30 For spherical particles with diameters of 0.51, 0.61, 0.79 and 1.01cm and bed porosity of 0.3915

Q (m^3/hr)	u (m /s)	Re	ΔP (Pa)	*f*
2	0.1218	22.962	14.144	0.612
3	0.1827	34.443	27.502	0.529
4	0.2436	45.924	45.575	0.493
5	0.3046	57.424	66.791	0.462
6	0.3655	68.905	92.722	0.445
7	0.4264	80.386	125.725	0.444
8	0.4873	91.867	157.156	0.425
9	0.5482	103.348	192.516	0.411
10	0.6091	114.829	243.592	0.421
11	0.6700	126.310	282.881	0.404
12	0.7309	137.791	330.028	0.396
13	0.7918	149.272	385.033	0.394
14	0.8528	160.771	440.037	0.388
15	0.9137	172.252	510.758	0.392
16	0.9746	183.733	573.620	0.387

A.5 packing of quinary sizes particles

Table A.31 For spherical particles with diameters of 0.42, 0.51, 0.61, 0.79 and 1.01cm and bed porosity of 0.3646

Q (m^3/hr)	u (m /s)	Re	ΔP (Pa)	*f*
2	0.1218	18.756	24.359	0.721
3	0.1827	28.134	45.575	0.600
4	0.2436	37.512	73.863	0.545
5	0.3046	46.905	106.080	0.502
6	0.3655	56.283	145.370	0.478
7	0.4264	65.661	188.587	0.456
8	0.4873	75.039	235.734	0.436
9	0.5482	84.417	290.739	0.425
10	0.6091	93.794	353.602	0.419
11	0.6700	103.172	424.322	0.415
12	0.7309	112.550	495.042	0.407
13	0.7918	121.928	581.478	0.407
14	0.8528	131.321	667.914	0.403
15	0.9137	140.699	746.492	0.393
16	0.9746	150.077	856.501	0.396

Appendix B

Water flow through packed bed

B.1 packing of mono sizes particles

Table B.1 For spherical particles diameter of 0.42 cm and bed porosity of 0.3793

Q (m^3/hr)	u (m /s)	Re	ΔP (kPa)	*f*
0.5	0.0305	38.467	0.940	0.456
1	0.0609	76.807	3.091	0.376
1.5	0.0914	115.273	6.429	0.348
2	0.1218	153.614	10.633	0.324
2.5	0.1523	192.080	16.567	0.323
3	0.1827	230.421	22.872	0.309
3.5	0.2132	268.887	30.291	0.301
4	0.2436	307.228	38.698	0.295
4.5	0.2741	345.694	48.465	0.291
5	0.3046	384.161	59.097	0.288

Table B.2 For spherical particles diameter of 0.51 cm and bed porosity of 0.4051

Q (m^3/hr)	u (m /s)	Re	ΔP (kPa)	*f*
0.5	0.0305	47.771	0.606	0.445
1	0.0609	95.385	1.978	0.364
1.5	0.0914	143.156	4.204	0.344
2	0.1218	190.770	7.047	0.325
2.5	0.1523	238.541	10.633	0.313
3	0.1827	286.155	14.836	0.304
3.5	0.2132	333.926	19.905	0.299
4	0.2436	381.540	25.469	0.293
4.5	0.2741	429.311	31.774	0.289
5	0.3046	477.082	38.945	0.287

Table B.3 For spherical particles diameter of 0.61 cm and bed porosity of 0.4156

Q (m^3/hr)	**u (m /s)**	**Re**	**ΔP (kPa)**	***f***
0.5	0.0305	59.362	0.433	0.414
1	0.0609	118.530	1.484	0.356
1.5	0.0914	177.892	3.091	0.330
2	0.1218	237.060	5.316	0.319
2.5	0.1523	296.422	8.036	0.309
3	0.1827	355.590	11.374	0.304
3.5	0.2132	414.952	15.331	0.298
4	0.2436	474.120	19.534	0.293
4.5	0.2741	533.482	24.356	0.289
5	0.3046	592.845	29.672	0.285

Table B.4 For spherical particles diameter of 0.79 cm and bed porosity of 0.4265

Q (m^3/hr)	**u (m /s)**	**Re**	**ΔP (kPa)**	***f***
0.5	0.0305	78.291	0.297	0.394
1	0.0609	156.325	1.051	0.350
1.5	0.0914	234.615	2.176	0.322
2	0.1218	312.649	3.833	0.319
2.5	0.1523	390.940	5.811	0.309
3	0.1827	468.974	8.160	0.302
3.5	0.2132	547.264	10.880	0.296
4	0.2436	625.298	13.971	0.291
4.5	0.2741	703.589	17.556	0.289
5	0.3046	781.879	21.389	0.285

Table B.5 For spherical particles diameter of 1.01 cm and bed porosity of 0.4321

Q (m^3/hr)	u (m /s)	Re	ΔP (kPa)	*f*
0.5	0.0305	100.533	0.223	0.394
1	0.0609	200.737	0.754	0.335
1.5	0.0914	301.27	1.607	0.317
2	0.1218	401.474	2.782	0.309
2.5	0.1523	502.008	4.204	0.299
3	0.1827	602.212	5.811	0.287
3.5	0.2132	702.745	7.913	0.287
4	0.2436	802.949	10.262	0.285
4.5	0.2741	903.482	12.982	0.285
5	0.3046	1004.016	15.702	0.279

B.2 packing of binary sizes particles

Table B.6 For spherical particles with diameters of 0.42 and 0.51 cm and bed porosity of 0.3551

Q (m^3/hr)	u (m /s)	Re	ΔP (kPa)	*f*
0.5	0.0305	62.39594	1.137	0.427
1	0.0609	124.5873	3.709	0.349
1.5	0.0914	186.9832	7.789	0.325
2	0.1218	249.1746	12.982	0.305
2.5	0.1523	311.5706	19.411	0.292
3	0.1827	373.7619	27.447	0.287
3.5	0.2132	436.1579	36.349	0.279
4	0.2436	498.3492	46.363	0.273
4.5	0.2741	560.7452	57.861	0.269
5	0.3046	623.1411	70.225	0.264

Table B.7 For spherical particles with diameters of 0.42 and 0.61 cm and bed porosity of 0.3650

Q (m^3/hr)	**u (m /s)**	**Re**	**ΔP (kPa)**	***f***
0.5	0.0305	70.147	0.964	0.434
1	0.0609	140.065	3.276	0.370
1.5	0.0914	210.212	6.924	0.347
2	0.1218	280.130	11.622	0.328
2.5	0.1523	350.277	17.680	0.319
3	0.1827	420.194	24.851	0.312
3.5	0.2132	490.342	33.010	0.304
4	0.2436	560.259	42.036	0.297
4.5	0.2741	630.407	53.287	0.297
5	0.3046	700.554	64.785	0.293

Table B.8 For spherical particles with diameters of 0.42 and 0.79 cm and bed porosity of 0.3590

Q (m^3/hr)	**u (m /s)**	**Re**	**ΔP (kPa)**	***f***
0.5	0.0305	75.873	0.989	0.462
1	0.0609	151.497	3.338	0.391
1.5	0.0914	227.369	6.924	0.360
2	0.1218	302.993	11.745	0.344
2.5	0.1523	378.866	17.433	0.327
3	0.1827	454.490	24.727	0.322
3.5	0.2132	530.363	33.010	0.316
4	0.2436	605.987	42.159	0.309
4.5	0.2741	681.859	52.421	0.303
5	0.3046	757.732	63.672	0.298

Table B.9 For spherical particles with diameters of 0.42 and 1.01 cm and bed porosity of 0.3484

Q (m^3/hr)	**u (m /s)**	**Re**	**ΔP (kPa)**	*f*
0.5	0.0305	79.304	1.014	0.462
1	0.0609	158.348	3.338	0.382
1.5	0.0914	237.652	7.171	0.364
2	0.1218	316.696	11.993	0.343
2.5	0.1523	396.000	17.927	0.328
3	0.1827	475.044	25.469	0.324
3.5	0.2132	554.349	33.876	0.316
4	0.2436	633.393	43.272	0.309
4.5	0.2741	712.697	53.905	0.304
5	0.3046	792.001	65.279	0.298

Table B.10 For spherical particles with diameters of 0.51 and 0.61 cm and bed porosity of 0.3681

Q (m^3/hr)	**u (m /s)**	**Re**	**ΔP (kPa)**	*f*
0.5	0.0305	78.246	0.816	0.424
1	0.0609	156.235	2.720	0.354
1.5	0.0914	234.481	5.811	0.336
2	0.1218	312.470	9.767	0.318
2.5	0.1523	390.716	14.960	0.312
3	0.1827	468.705	21.018	0.304
3.5	0.2132	546.951	28.065	0.298
4	0.2436	624.941	35.978	0.293
4.5	0.2741	703.186	44.879	0.289
5	0.3046	781.432	55.265	0.288

Table B.11 For spherical particles with diameters of 0.51 and 0.79 cm and bed porosity of 0.3882

Q (m^3/hr)	**u (m /s)**	**Re**	**ΔP (kPa)**	*f*
0.5	0.0305	92.992	0.581	0.407
1	0.0609	185.680	1.978	0.348
1.5	0.0914	278.672	4.204	0.328
2	0.1218	371.360	7.047	0.310
2.5	0.1523	464.352	10.880	0.306
3	0.1827	557.040	15.207	0.297
3.5	0.2132	650.032	20.523	0.294
4	0.2436	742.720	26.334	0.289
4.5	0.2741	835.712	33.134	0.287
5	0.3046	928.705	40.429	0.284

Table B.12 For spherical particles with diameters of 0.51 and 1.01 cm and bed porosity of 0.3730

Q (m^3/hr)	**u (m /s)**	**Re**	**ΔP (kPa)**	*f*
0.5	0.0305	96.529	0.643	0.427
1	0.0609	192.742	2.225	0.371
1.5	0.0914	289.271	4.451	0.329
2	0.1218	385.484	7.789	0.324
2.5	0.1523	482.013	11.622	0.310
3	0.1827	578.225	16.567	0.307
3.5	0.2132	674.754	22.131	0.301
4	0.2436	770.967	28.312	0.295
4.5	0.2741	867.496	35.607	0.293
5	0.3046	964.025	43.149	0.287

Table B.13 For spherical particles with diameters of 0.61 and 0.79 cm and bed porosity of 0.4019

Q (m^3/hr)	**u (m /s)**	**Re**	**ΔP (kPa)**	***f***
0.5	0.0305	109.416	0.457	0.409
1	0.0609	218.474	1.545	0.346
1.5	0.0914	327.891	3.276	0.326
2	0.1218	436.948	5.687	0.318
2.5	0.1523	546.365	8.654	0.310
3	0.1827	655.422	11.993	0.298
3.5	0.2132	764.839	16.320	0.298
4	0.2436	873.896	20.894	0.293
4.5	0.2741	983.313	26.334	0.291
5	0.3046	1092.729	31.898	0.286

Table B.14 For spherical particles with diameters of 0.61 and 1.01 cm and bed porosity of 0.3904

Q (m^3/hr)	**u (m /s)**	**Re**	**ΔP (kPa)**	***f***
0.5	0.0305	116.138	0.457	0.407
1	0.0609	231.896	1.607	0.359
1.5	0.0914	348.034	3.338	0.331
2	0.1218	463.791	5.811	0.324
2.5	0.1523	579.930	8.531	0.305
3	0.1827	695.687	12.116	0.301
3.5	0.2132	811.825	16.443	0.300
4	0.2436	927.583	21.018	0.293
4.5	0.2741	1043.721	26.458	0.292
5	0.3046	1159.859	32.021	0.286

Table B.15 For spherical particles with diameters of 0.61 and 1.01 cm and bed porosity of 0.3904

Q (m^3/hr)	**u (m /s)**	**Re**	**ΔP (kPa)**	*f*
0.5	0.0305	150.620	0.284	0.393
1	0.0609	300.746	0.989	0.343
1.5	0.0914	451.366	2.102	0.324
2	0.1218	601.492	3.709	0.322
2.5	0.1523	752.112	5.440	0.302
3	0.1827	902.238	7.789	0.300
3.5	0.2132	1052.858	10.509	0.297
4	0.2436	1202.984	13.353	0.289
4.5	0.2741	1353.604	16.938	0.290
5	0.3046	1504.224	20.523	0.284

B.3 packing of ternary sizes particles

Table B.16 For spherical particles with diameters of 0.42, 0.51 and 0.61cm and bed porosity of 0.3600

Q (m^3/hr)	**u (m /s)**	**Re**	**ΔP (kPa)**	*f*
0.5	0.0305	69.164	1.014	0.437
1	0.0609	138.101	3.338	0.361
1.5	0.0914	207.265	7.047	0.339
2	0.1218	276.203	11.745	0.318
2.5	0.1523	345.367	17.680	0.306
3	0.1827	414.304	24.480	0.294
3.5	0.2132	483.468	32.269	0.285
4	0.2436	552.406	41.665	0.282
4.5	0.2741	621.570	52.050	0.278
5	0.3046	690.734	62.807	0.272

Table B.17 For spherical particles with diameters of 0.42, 0.51 and 0.79 cm and bed porosity of 0.3648

Q (m^3/hr)	**u (m /s)**	**Re**	**ΔP (kPa)**	***f***
0.5	0.0305	74.845	0.890	0.429
1	0.0609	149.445	2.967	0.359
1.5	0.0914	224.291	6.429	0.345
2	0.1218	298.891	11.003	0.332
2.5	0.1523	373.736	16.443	0.318
3	0.1827	448.336	23.120	0.310
3.5	0.2132	523.181	30.909	0.305
4	0.2436	597.781	39.687	0.300
4.5	0.2741	672.627	50.319	0.300
5	0.3046	747.472	61.076	0.295

Table B.18 For spherical particles with diameters of 0.42, 0.51 and 1.01 cm and bed porosity of 0.3562

Q (m^3/hr)	**u (m /s)**	**Re**	**ΔP (kPa)**	***f***
0.5	0.0305	76.523	0.952	0.444
1	0.0609	152.795	3.338	0.390
1.5	0.0914	229.319	7.418	0.385
2	0.1218	305.591	12.611	0.369
2.5	0.1523	382.114	18.792	0.351
3	0.1827	458.386	26.581	0.345
3.5	0.2132	534.909	36.225	0.346
4	0.2436	611.181	45.868	0.335
4.5	0.2741	687.705	56.625	0.327
5	0.3046	764.228	68.370	0.320

Table B.19 For spherical particles with diameters of 0.42, 0.61 and 0.79 cm and bed porosity of 0.3695

Q (m^3/hr)	u (m /s)	Re	ΔP (kPa)	*f*
0.5	0.0305	81.163	0.767	0.413
1	0.0609	162.061	2.596	0.351
1.5	0.0914	243.224	5.440	0.326
2	0.1218	324.121	9.396	0.317
2.5	0.1523	405.285	14.466	0.312
3	0.1827	486.182	20.276	0.304
3.5	0.2132	567.346	27.200	0.300
4	0.2436	648.243	34.865	0.294
4.5	0.2741	729.406	43.643	0.291
5	0.3046	810.570	52.668	0.284

Table B.20 For spherical particles with diameters of 0.42, 0.61 and 1.01 cm and bed porosity of 0.3665

Q (m^3/hr)	u (m /s)	Re	ΔP (kPa)	*f*
0.5	0.0305	84.731	0.767	0.424
1	0.0609	169.184	2.596	0.360
1.5	0.0914	253.915	5.564	0.343
2	0.1218	338.368	9.520	0.330
2.5	0.1523	423.099	14.465	0.321
3	0.1827	507.553	20.400	0.314
3.5	0.2132	592.284	27.323	0.309
4	0.2436	676.737	34.989	0.303
4.5	0.2741	761.468	43.767	0.300
5	0.3046	846.199	52.792	0.293

Table B.21 For spherical particles with diameters of 0.42, 0.79 and 1.01 cm and bed porosity of 0.3712

Q (m^3/hr)	**u (m /s)**	**Re**	**ΔP (kPa)**	***f***
0.5	0.0305	92.904	0.680	0.425
1	0.0609	185.503	2.349	0.368
1.5	0.0914	278.407	5.316	0.370
2	0.1218	371.007	8.902	0.349
2.5	0.1523	463.911	13.600	0.341
3	0.1827	556.510	19.287	0.336
3.5	0.2132	649.414	25.469	0.326
4	0.2436	742.013	33.010	0.323
4.5	0.2741	834.917	39.563	0.306
5	0.3046	927.821	49.578	0.311

Table B.22 For spherical particles with diameters of 0.51, 0.61 and 0.79 cm and bed porosity of 0.3854

Q (m^3/hr)	**u (m /s)**	**Re**	**ΔP (kPa)**	***f***
0.5	0.0305	92.045	0.593	0.404
1	0.0609	183.788	2.102	0.359
1.5	0.0914	275.833	4.574	0.347
2	0.1218	367.575	7.913	0.338
2.5	0.1523	459.620	11.993	0.328
3	0.1827	551.363	16.691	0.317
3.5	0.2132	643.408	22.996	0.321
4	0.2436	735.151	28.683	0.306
4.5	0.2741	827.196	36.225	0.306
5	0.3046	919.240	44.261	0.302

Table B.23 For spherical particles with diameters of 0.51, 0.61 and 1.01 cm and bed porosity of 0.3771

Q (m^3/hr)	**u (m /s)**	**Re**	**ΔP (kPa)**	*f*
0.5	0.0305	94.836	0.606	0.405
1	0.0609	189.361	2.102	0.352
1.5	0.0914	284.197	4.698	0.350
2	0.1218	378.722	8.036	0.337
2.5	0.1523	473.558	12.611	0.338
3	0.1827	568.083	17.309	0.323
3.5	0.2132	662.919	22.996	0.315
4	0.2436	757.444	29.796	0.312
4.5	0.2741	852.280	37.090	0.307
5	0.3046	947.117	45.127	0.303

Table B.24 For spherical particles with diameters of 0.51, 0.79 and 1.01 cm and bed porosity of 0.3895

Q (m^3/hr)	**u (m /s)**	**Re**	**ΔP (kPa)**	*f*
0.5	0.0305	107.358	0.495	0.404
1	0.0609	214.364	1.855	0.380
1.5	0.0914	321.721	3.956	0.360
2	0.1218	428.727	6.553	0.336
2.5	0.1523	536.085	10.385	0.340
3	0.1827	643.091	14.218	0.324
3.5	0.2132	750.448	19.163	0.320
4	0.2436	857.454	24.356	0.312
4.5	0.2741	964.812	31.156	0.315
5	0.3046	1072.170	38.080	0.312

Table B.25 For spherical particles with diameters of 0.61, 0.79 and 1.01cm and bed porosity of 0.3962

Q (m^3/hr)	u (m /s)	Re	ΔP (kPa)	*f*
0.5	0.0305	119.931	0.433	0.411
1	0.0609	239.468	1.484	0.353
1.5	0.0914	359.398	3.215	0.340
2	0.1218	478.936	5.440	0.324
2.5	0.1523	598.866	8.407	0.320
3	0.1827	718.403	12.240	0.324
3.5	0.2132	838.334	15.949	0.310
4	0.2436	957.871	20.400	0.304
4.5	0.2741	1077.802	25.840	0.305
5	0.3046	1197.732	31.156	0.296

B.4 packing of quaternary sizes particles

Table B.26 For spherical particles with diameters of 0.42, 0.51, 0.61 and 0.79cm and bed porosity of 0.3714

Q (m^3/hr)	u (m /s)	Re	ΔP (kPa)	*f*
0.5	0.0305	78.983	0.791	0.421
1	0.0609	157.706	2.658	0.355
1.5	0.0914	236.689	5.564	0.330
2	0.1218	315.412	9.644	0.322
2.5	0.1523	394.395	14.589	0.311
3	0.1827	473.118	20.400	0.302
3.5	0.2132	552.101	27.941	0.304
4	0.2436	630.825	35.483	0.296
4.5	0.2741	709.807	44.879	0.296
5	0.3046	788.790	54.152	0.289

Table B.27 For spherical particles with diameters of 0.42, 0.51, 0.61 and 1.01cm and bed porosity of 0.3754

Q (m^3/hr)	**u (m /s)**	**Re**	**ΔP (kPa)**	*f*
0.5	0.0305	83.081	0.729	0.420
1	0.0609	165.889	2.473	0.357
1.5	0.0914	248.970	5.193	0.333
2	0.1218	331.778	9.025	0.326
2.5	0.1523	414.859	13.600	0.314
3	0.1827	497.667	18.916	0.303
3.5	0.2132	580.748	25.592	0.301
4	0.2436	663.556	33.134	0.299
4.5	0.2741	746.637	40.923	0.292
5	0.3046	829.717	49.948	0.288

Table B.28 For spherical particles with diameters of 0.42, 0.51, 0.79 and 1.01cm and bed porosity of 0.3671

Q (m^3/hr)	**u (m /s)**	**Re**	**ΔP (kPa)**	*f*
0.5	0.0305	85.454	0.767	0.430
1	0.0609	170.628	2.596	0.365
1.5	0.0914	256.082	5.564	0.347
2	0.1218	341.255	9.520	0.335
2.5	0.1523	426.709	14.589	0.328
3	0.1827	511.883	20.152	0.315
3.5	0.2132	597.337	27.447	0.315
4	0.2436	682.511	35.236	0.310
4.5	0.2741	767.965	43.890	0.305
5	0.3046	853.419	53.410	0.300

Table B.29 For spherical particles with diameters of 0.42, 0.61, 0.79 and 1.01cm and bed porosity of 0.3767

Q (m^3/hr)	**u (m /s)**	**Re**	**ΔP (kPa)**	*f*
0.5	0.0305	93.180	0.631	0.409
1	0.0609	186.053	2.164	0.352
1.5	0.0914	279.233	4.574	0.331
2	0.1218	372.107	7.913	0.322
2.5	0.1523	465.287	12.116	0.316
3	0.1827	558.161	16.814	0.304
3.5	0.2132	651.340	22.625	0.301
4	0.2436	744.214	29.301	0.298
4.5	0.2741	837.394	36.596	0.294
5	0.3046	930.573	44.632	0.291

Table B.30 For spherical particles with diameters of 0.51, 0.61, 0.79 and 1.01cm and bed porosity of 0.3891

Q (m^3/hr)	**u (m /s)**	**Re**	**ΔP (kPa)**	*f*
0.5	0.0305	103.257	0.519	0.407
1	0.0609	206.176	1.916	0.377
1.5	0.0914	309.433	3.833	0.334
2	0.1218	412.351	6.553	0.322
2.5	0.1523	515.608	10.014	0.315
3	0.1827	618.527	13.847	0.302
3.5	0.2132	721.784	18.669	0.299
4	0.2436	824.702	24.232	0.298
4.5	0.2741	927.959	30.291	0.294
5	0.3046	1031.216	36.720	0.288

B.5 packing of quinary sizes particles

Table B.31 For spherical particles with diameters of 0.42, 0.51, 0.61, 0.79 and 1.01cm and bed porosity of 0.3624

Q (m^3/hr)	u (m /s)	Re	ΔP (kPa)	*f*
0.5	0.0305	84.423	0.767	0.412
1	0.0609	168.570	2.596	0.350
1.5	0.0914	252.994	5.687	0.340
2	0.1218	337.140	9.644	0.325
2.5	0.1523	421.564	14.465	0.312
3	0.1827	505.710	19.905	0.298
3.5	0.2132	590.134	26.334	0.290
4	0.2436	674.281	34.000	0.286
4.5	0.2741	758.704	42.159	0.280
5	0.3046	843.128	52.050	0.280

Appendix C

Calibration of Rotameters

A. for air flow

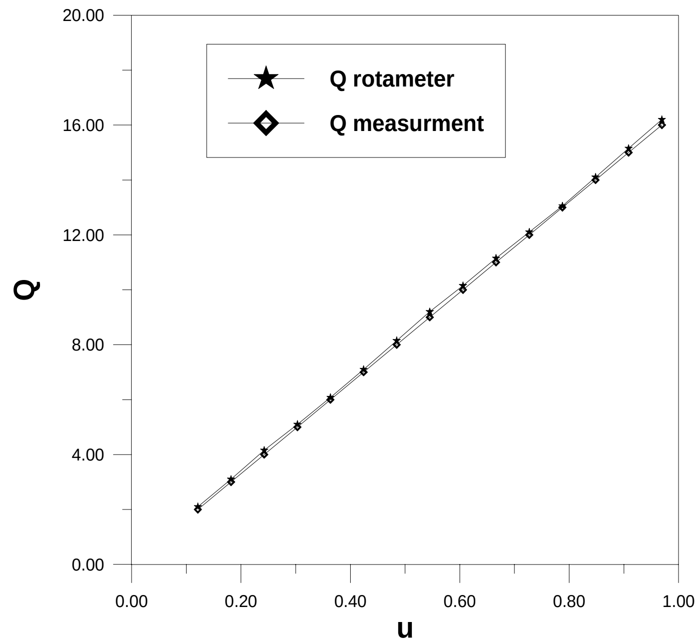

Figure C-1 show the calibration of air rotameter

B. for water flow

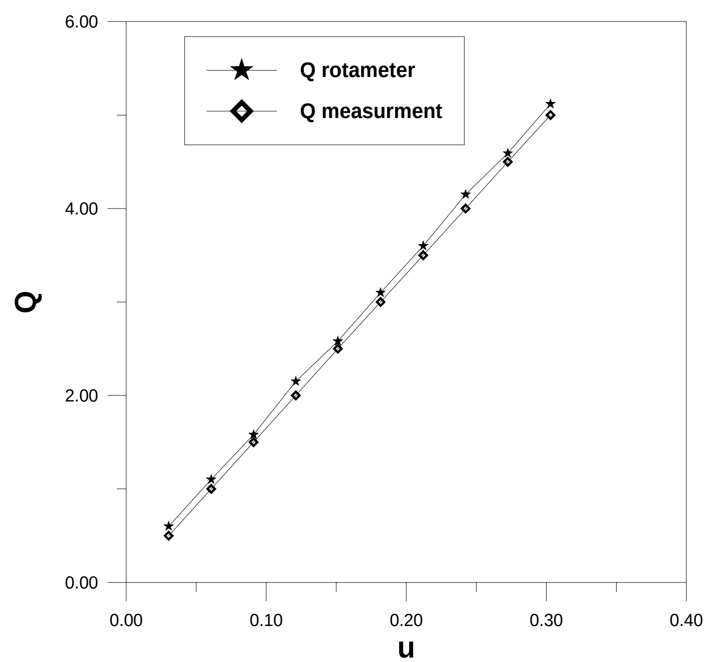

Figure C-2 show the calibration of water rotamet

الخلاصة

يتضمن هذا البحث دراسة جريان طور واحد من الموائع خلال عمود حشوي, حيث نوعان من الموائع قد تم استخدامها بشكل منفصل (هواء وماء). كان العمود المحشو يحتوي على جسيمات زجاجية كروية الحجم وموزعة بشكل عشوائي.

وقد كان قطر العمود المحشو ٧,٦٢cm و طوله ٥٧cm . وكان قطر الكريات الزجاجية ٠,٤٢, ٠,٥٠, ٠,٦١, ٠,٧٩ and ١,٠١ cm . كما استخدمت عدة سرع لمعدل الجريان للموائع الممثل بعدد رينولدز (modified Reynolds number).لقد اجريت التجارب عند درجة حرارة المختبر (٣٢°C)بالنسبة لجريان الهواء, وعند درجة حرارة ماء الحنفية (٢٥°C) بالنسبة لجريان الماء. لقد تم دراسة عدة عوامل خلال هذا العمل كنوع المائع, سرعة الجريان وتغير مسامية الحشوة (احادية, ثنائية, متعددة حجوم مختلفة) لمعرفة تاثير هذه العوامل على هبوط الضغط ومعامل الاحتكاك.

اثبتت النتائج ان هبوط الضغط خلال عمود حشوي يتأثر لدرجة كبيرة بمسامية الحشوة والتي لها تأثير ملموس على معامل الاحتكاك. حيث لوحظ انه عندما تزداد مسامية الحشوة من ٠,٣٤٥٥ الى ٠,٤٣٥٩ تقل قيم معامل الاحتكاك من٠,٨٠٨ الى ٠,٣٦٦, ويقل هبوط الضغط من ٣٣,٨ الى ٧,١ Pa .

كان عدد رينولدز لجريان الهواء يتراوح من ٨,٤٢ الى ٢٦٥,٦٣ والذي ادى الى انخفاض قيم معامل الاحتكاك من ٠,٩٩٢ الى ٠,٣٧٤. اما بالنسبة لجريان الماء فقد تراوح عدد رينولدز من ٣٨,٤٧ الى ١٥٠٤,٢٢ والذي ادى الى انخفاض قيم معامل الاحتكاك من ٠,٤٥٦ الى ٠,٢٨٤.

لقد تمت دراسة تأثير نوع المائع (هواء و ماء) على هبوط الضغط و معامل الاحتكاك خلال العمود الحشوي. حيث لوحظ انه لنفس مسامية الحشوة و سرعة جريان المائع هبوط الضغط لجريان الهواء اقل من هبوط الضغط لجريان الماء.

العلاقات تجريبية لمعامل الاحتكاك بدلالة عدد رينولدز لجريان الهواء والماء خلال حشوة مكونة من جسيمات متعددة الحجوم هي:

لجريان الهواء هي:

$$f = 4.72\,\mathrm{Re}_1^{\,-1} + 0.59\,\mathrm{Re}_1^{\,-0.1}$$

كان معامل التصحيح ٠,٩٦٦٢ و كانت نسبة الخطأ ٣,٧٩% .

لجريان الماء هي:

$$f = 3.73 \mathrm{Re}_1^{-1} + 0.56 \mathrm{Re}_1^{-0.1}$$

كان معامل التصحيح ٠,٨٩٩٤ و كانت نسبة الخطأ ٤,١٦٪ .

شكر و تقدير

اود ان اعبر عن خالص شكري وتقديري للمشرف **ا.م.د. محمد نصيف لطيف** لما قدمه لي من توجيهات ونصائح قيمة طوال فترة انجاز البحث.

اود ان اشكر **ا.د.قاسم جبار سليمان** رئيس قسم الهندسة الكيمياوية لابدائه المساعدة اللازمة اثناء هذا العمل.

اود ايضا ان اتقدم بالشكر الجزيل الى من كان جزئا مكملا بانجاز هذا المشروع وخصوصا **ا.د.عباس حميد سليمون**, **د.عمار صالح**, **د.باسم عبيد** و **ا.م.د. سيسيليا خوشابا**.

ولا انسى ان اشكر من رباني على طريق الخير والمعرفة اعز من في الوجود **ابي** و**امي** و**اخوتي**.

م. وقار عبد الواحد

حزيران ٢٠٠٧

وصف الحشوات المكونة من حبيبات كروية احادية و متعددة الحجوم

رسالة

مقدمة إلى كلية الهندسة في جامعة النهرين

وهي جزء من متطلبات نيل درجة ماجستير علوم

في الهندسة الكيمياوية

من قبل

وقار عبد الواحد عبد النبي

(بكالوريوس علوم في الهندسة الكيمياوية ٢٠٠٤)

جمادي الثاني ١٤٢٨

حزيران ٢٠٠٧